EVOLUTION AND FUNCTIONAL MORPHOLOGY OF THE GILL VENTILATORY SYSTEM OF RAY-FINNED FISHES (ACTINOPTERYGII)

A Dissertation

Presented to the Faculty of the Graduate School

of Cornell University

In Partial Fulfillment of the Requirements for the Degree of

Doctor of Philosophy

by

Stacy Christine Farina

August 2015

EVOLUTION AND FUNCTIONAL MORPHOLOGY OF THE GILL VENTILATORY SYSTEM OF RAY-FINNED FISHES (ACTINOPTERYGII)

Stacy Christine Farina, Ph. D.

Cornell University 2015

To ventilate their gills, ray-finned fishes (Actinopterygii) use pumps in their buccal and opercular chambers to alternate between positive and negative pressures, driving water over the gills in a unidirectional current. The basic mechanics are conserved across Actinopterygii, but there is considerable morphological and functional variation of the buccal and opercular pumps. I used comparative approaches to investigate the evolution of ventilatory morphology and function across actinopterygians. In the first chapter, I reconstructed the evolutionary history of restricted gill openings across 433 actinopterygian families using recently published molecular data. Restricted gill openings have evolved at least 11 times among ray-finned fishes with diverse morphology and ecology. Fishes with restricted gill openings also occupied a larger cranial morphospace than fishes with other morphologies. In the second chapter, I studied the gill ventilation of the goosefish, *Lophius americanus*, which exhibits extremely slow ventilation. I found that the inspiration phase of ventilation is greatly increased relative to that of typical fishes, and that, during this phase, the branchiostegals slowly expand. I described the specialized musculature of the gill opening, which has functional and systematic implications for *Lophius*. In the third chapter, I studied ventilation function among four sculpins and found considerable variation in buccal and gill chamber pressures. Using phylogenetically corrected generalized least squares models (PGLS), I linked variation in pressures to morphology of the ventilatory pumps, and variation in pressures correlated closely with the size of the branchiostegal

apparatus. I propose that adding a third pump to the traditional two-pump model, in which the branchiostegal rays work in parallel with the operculum, is a useful framework for comparative gill ventilatory studies. In the fourth chapter, I reconstructed the phylogeny of sculpins and close relatives (Cottoidei) using published molecular data to analyze measurements of cranial bones from a subset of 23 cottoids. Using PGLS models, I found that suction-feeding associated characters (jaws and operculum) are closely evolutionarily correlated. However, there is only weak correlation between the branchiostegals and these structures. The branchiostegal apparatus may be a source of modularity within gill ventilation that releases constraints imposed by close coupling of feeding and ventilation.

BIOGRAPHICAL SKETCH

Stacy C. Farina was born in Morristown, New Jersey, in 1988. As a child living in rural Frelinghuysen Township, she developed a love of nature through her time spent observing and interacting with wildlife around her home. She was especially fond of the fishes living in a pond nearby that was part of the Delaware River watershed. She also took an interest in writing short stories and poetry, and one of her early poems was published in the 1999 edition of *A Celebration of New Jersey's Young Poets*. Her passions for nature and writing persisted throughout her adolescence, complimented by a growing interest in computers and science.

In fall 2006, Stacy began her undergraduate studies at the University of New Hampshire (UNH). During her first year at UNH, Stacy worked in the laboratory of Dr. Jim Haney on the 3.0 edition of his online key to zooplankton of the Northeast USA. In summer 2007, she took a course at Shoals Marine Laboratory entitled Research in Marine Biology, where the mentorship of her instructors and the immersive fieldwork solidified her desire to pursue marine biology. During her second year, Stacy began working in the laboratory of Dr. Hunt Howell, assisting his former Ph.D. student, Dr. Mick Walsh, with a study of hatchery-raised winter flounder weaning onto wild diets. Under the guidance of Dr. Walsh, she received a research award and presented at The Eleventh Flatfish Biology Conference. She was also selected to join the National Oceanic and Atmospheric Administration's Hollings Undergraduate Scholars program. Stacy spent summer 2008 working in the fish collection at Harvard University's Museum of Comparative Zoology, where she developed a passion for biological collections and fish diversity.

In summer 2009, Stacy interned at the Northwest Fisheries Science Center in Seattle, WA, with her Hollings mentor Dr. Orlay Johnson. As a part of her internship, Stacy worked with

Drs. Ted Pietsch and Chris Kenaley on the innervation of the lateral line system of anglerfishes, which she later completed as her honors thesis with the assistance of Drs. Jiakun Song and Hunt Howell. During her final year, Stacy had the rare opportunity to take on the roll of a graduate teaching assistant for Dr. Howell's Vertebrate Morphology course, during which she fostered a passion for teaching and for comparative anatomy. Throughout her time at UNH, Stacy was also an active member of the UNH Fencing Club, eventually becoming captain of the épée squad. She graduated in May 2010 with a B.S. in Biology (Marine and Freshwater concentration), a minor in genetics, and *summa cum laude* honors.

In fall 2010, Stacy began her Ph.D. program at Cornell University in the Department of Ecology and Evolutionary Biology, with Dr. William E. Bemis. She began the first chapter of her dissertation while working in the fish collection at the Cornell University Museum of Vertebrates with John P. Friel, and she continued the project by traveling to three additional collections over the following year. In 2011, Stacy received a Raney Award from the American Society of Ichthyologists and Herpetologists to conduct research on *Lophius americanus* at Shoals Marine Laboratory (SML). In summer 2012, she took a course at Friday Harbor Laboratories (FHL) with Dr. Adam P. Summers, and she used her course project data as the basis for an NSF Doctoral Dissertation Improvement Grant proposal, which she was awarded in 2013. Stacy continued to travel to FHL until completing her dissertation research in 2015.

Stacy was a teaching assistant at SML from 2010 – 2013, and she returned in 2014 and 2015 as a guest lecturer. At Cornell University, she was a teaching assistant for *The Vertebrates* and *Evolutionary Biology and Diversity*. In 2012, she designed and instructed a First-Year Writing Seminar. In 2014, she was a teaching assistant for the fish course at FHL. She has greatly enjoyed mentoring undergraduate researchers from SML and FHL.

ACKNOWLEDGEMENTS

This dissertation would not have been possible without the support of many people and organizations, and I am grateful to each and every one. It is truly a privilege to pursue the study of biology with the assistance, encouragement, and camaraderie of such dedicated and remarkable people.

My doctoral committee has been an outstanding source of mentorship and support throughout my studies as a graduate student. My committee chair, William E. Bemis, opened his lab to a passionate undergraduate interested in the functional morphology of fishes, and ever since, he has enthusiastically encouraged my pursuits in everything from evolutionary morphology to robotics. Willy has been a mentor to me in both research and teaching, and we have enjoyed countless hours of working together at Cornell and at Shoals Marine Laboratory. Willy has taught me nearly everything I know about the history of ichthyology and comparative vertebrate anatomy, and he has provided invaluable training in photography and illustration that I will draw upon for the rest of my career. I asked Adam P. Summers to join my committee after I took his course in Functional Morphology and Ecology of Marine Fishes at Friday Harbor Laboratories (FHL). He has since welcomed me into his lab at FHL for numerous visits, during which he has been incredibly generous with his time and resources. He has trained me in techniques involving bioinstrumentation, biomechanics, and physical modeling, and he has provided access to critical equipment and animals in his lab. Most significantly, he has given me invaluable opportunities for professional development through candid discussions and by fostering a laboratory environment in which respect, innovation, and collaboration are valued as highly as research performance. I have truly enjoyed spending time in the Summers laboratory, and I have learned much from working with Adam and his lab group. Since the beginning of my

graduate program, Amy McCune has contributed considerably to my intellectual and professional development. Meeting with her lab group and taking her course in Macroevolution gave me critical tools for developing a refined understanding of patterns of phenotypic evolution. Amy has also been an excellent source of feedback, and working with her has greatly improved the quality and clarity of my dissertation. I also sincerely appreciate Amy's support of my teaching activities and her role in cultivating a supportive environment for graduate students within our department. Throughout my time at Cornell, Harry Greene has impressed upon me the importance of organismal biology and understanding its role in society and culture. He has also been an excellent role model for teaching and outreach, and I have greatly enjoyed learning about his strategies for engaging a wide range of audiences. Through feedback and discussions, he has helped to develop my implementation of organism-focused research, and he has encouraged me to carefully and diligently observe nature.

I have been fortunate to have opportunities to collaborate and discuss my research extensively with researchers in addition to my formal committee, which has been a significant asset to my dissertation. John P. Friel served on my committee for four years, before accepting a position as Museum Director at the Alabama Museum of Natural History, and we discussed the first three chapters of my dissertation extensively during this time. His feedback strongly influenced the planning and execution of my first chapter, and our discussions were always productive and informative. Thomas Near provided significant feedback on my first chapter, especially regarding statistical analyses and interpretation of phylogenetic patterns. He also provided the molecular data for our reconstruction of the evolutionary history of branchiostegal membrane morphology. Lara Ferry worked closely with me to design the experiment conducted in my third chapter, including training me to record from pressure transducers and interpret the

resulting data. Elizabeth Brainerd has also worked with me to interpret ventilatory pressures, and she has helped to considerably shape my understanding of vertebrate ventilation. Matthew Knope has provided insight into sculpin evolution and analyses of continuous characters in general, contributing to the third and fourth chapters both in terms of molecular data and feedback.

I have also received critical help with instrumentation and statistical analyses from other researchers. Mark Riccio conducted the CT scanning of sculpin species and provided assistance with 3D reconstruction. Pete Marchetto provided substantial guidance and assistance with bioinstrumentation challenges. Elizabeth Murray and Liam Revell provided training and insight regarding techniques in phylogenetic reconstruction and character analyses. Nick Mason, Collin Edwards, Peter C. Wainwright, and Francoise Vermeylen also provided invaluable statistical consultation.

I would also like to thank the collaborators with whom I have engaged in projects unrelated to this dissertation, as I have learned much about the research process from each one of you, especially my undergraduate collaborators. As an undergraduate myself, I worked under the guidance of Ted Pietsch, Chris Kenaley, Jiakun Song, and Hunt Howell on lateral line innervation as an honors thesis, with much support from Orlay Johnson and Jacqueline Webb. As a graduate student, I worked with undergraduate William Gough and professor Frank Fish to study locomotion of eider ducks on the surface of the water. I have also worked with undergraduate Noah Bressman and professor Alice Gibb to study locomotion of fishes on land. I have also worked with graduate students Amberle McKee and Ian MacDonald and professor Adam Summers to compare burial behavior in five flatfish species. I have worked with undergraduate Katherine Corn on three projects, including the fourth chapter of my dissertation,

a test of shark tooth cutting efficiency, and flatfish burial performance as it scales with fish size. The majority of these projects were initiated by undergraduate and graduate student research conducted at Shoals Marine Laboratory and Friday Harbor Laboratories, and many have been supported by student-awarded research grants and/or have resulted in manuscripts. I consider it a great privilege to be involved with so many excellent projects.

This dissertation would not have been possible without the assistance of the many individuals, facilities, and organizations that provided research support. The second chapter was completed at Shoals Marine Laboratory, and the excellent staff provided considerable research support, as well as a friendly and productive atmosphere, especially Phil Thompson and Hal Weeks. Research for the third and fourth chapters was largely conducted at Friday Harbor Laboratories. The FHL staff were invaluable to the success of this work, providing extensive research support and fostering a professional, respectful, and enjoyable campus environment. For access to specimens and research space at ichthyological collections, I am grateful to John P. Friel and Charles M. Dardia (Cornell University Museum of Vertebrates), John Lundberg (Academy of Natural Sciences of Drexel University), Karsten Hartel and Andrew Williston (Museum of Comparative Zoology), and Theodore W. Pietsch and Katherine Maslenikov (University of Washington). I would also like to thank Captain Jim Ford (F/V Lisa Ann II), Captain David Goethel (F/V Ellen Diane), and John Galbraith (NMFS/NEFS) for their assistance in collecting *Lophius americanus* specimens.

I would also like to thank the funding sources that supported this work, including an NSF Doctoral Dissertation Improvement Grant (DEB-1310812), two Graduate Research Awards from the Stephen and Ruth Wainwright Endowment from Friday Harbor Laboratories, an award from the Edward C. Raney Fund from the American Society of Ichthyologists and Herpetologists,

support from the Department of Ecology and Evolutionary Biology, the Cornell University Knight Institute, the Orenstein Fund, and the Tontogany Creek Fund.

My research questions and my enthusiasm for fish ventilation have been profoundly influenced by the writings of many ichthyologists that have passed on, especially George M. Hughes, Graham Shelton, Donald E. McAllister, and Karel Liem. George M. Hughes and Graham Shelton have been called "the fathers of fish respiration," and both have inspired me to think of more questions than I could ever hope to answer. I would like to thank the estate of GM Hughes for providing funding for scientists participating in the 2013 symposium "Challenges to Respiratory Gas Transport" at the annual meeting of the Society for Experimental Biology, at which I was a contributor supported by these funds. Donald E. McAllister was known for his support of ocean conservation and biodiversity, but through his writings, I have also greatly appreciated his detailed observations on branchiostegal rays. My copy of his volume on the evolution of the branchiostegal apparatus is well-worn. Surprisingly, though, my inspiration to study gill ventilation did not come from these authors initially. Rather, it came while I was studying Karel Liem's monograph on the functional morphology of nandid fishes as a first year doctoral student. His traces of skeletal kinematics during nandid ventilation confused me, and my attempts to understand them in the context of fish diversity sparked an intense interest in gill ventilatory anatomy and function. I am indebted to these authors, and many others, for their scholarship and inspiration.

My time as an undergraduate at the University of New Hampshire (UNH) and at Shoals Marine Laboratory (SML) set me on the path to graduate school, largely due to the impact of the many people that supported and guided me. My instructors at SML were Denny Taylor, Doug Fudge, Anne Todgham, and Jeanette Lim, and each one encouraged me and gave me the tools

that I needed to begin the transformation into an effective marine biologist. I am especially grateful to Jeanette, because her lectures on fish biomechanics were instantly intriguing to me, and I have been intrigued ever since. Jeanette also helped me to obtain a summer job at the Harvard MCZ fish collection, where I was introduced to many more fish biologists. On the UNH campus, I worked with then-doctoral-student Mick Walsh, who taught me about the research process and inspired me with her drive and the scope of her research. She helped me to obtain my first research grant and attend my first conference, and her enthusiasm, support, and friendship hasn't wavered since. During my time at UNH, I also took courses with Professors Jessica Bolker and Win Watson, both of whom were incredibly supportive in and out of the classroom. I would also like to extend my sincere gratitude to my academic and research advisor at UNH, Dr. Hunt Howell. Throughout my years at UNH, he remained steadfast in his belief in my abilities, even when I doubted myself, and his support and that of my other mentors gave me the courage and confidence to pursue my goal of graduate school.

Throughout my doctoral program, my fellow graduate students have been a tremendous source of support and discussions, and I am incredibly fortunate to count them among my colleagues. I am especially grateful to Drs. Amanda Cass, Misty Paig-Tran, Stephanie Crofts, Mick Walsh, Erin Blevins, Anabela Maia, Rayna Bell, Morgan Mouchka, and Anna Forsman. As I have watched you graduate and advance in your careers, it has been a tremendous source of encouragement to see such an incredible cohort of women scientists form. I could not ask for a better group of role models. I am also grateful to my graduate student colleagues from the FHL Functional Morphology and Ecology of Marine Fishes 2012 cohort, from the Department of Ecology and Evolutionary Biology, and from the Friday Harbor Laboratories student community, especially Callie Crawford, Cassandra Donatelli, Katie Dobkowski, Matt Kolmann,

Sarah Longo, and Katie Marchetto. I am especially indebted to my labmates, Kate Bemis, Andrea Cerruti, and Josh Moyer for their many hours of help and moral support.

I have also received considerable support and mentorship as I developed my skills as a teaching assistant working with professors and visiting lecturers at Cornell University, Shoals Marine Laboratory, and Friday Harbor Laboratories, especially: Willy Bemis, Andrew Clark, Jan Factor, Lara Ferry, Alice Gibb, Harry Greene, Patricia Hernandez, Amy McCune, Misty Paig-Tran, Katie Staab, Adam Summers, Kelly Zamudio, and Rick Zechman. I am especially indebted to Frank Fish, Betty McGuire, and Irby Lovette, with whom I have worked repeatedly over the last five years. They have shaped my teaching philosophy profoundly through their integrity and passion for undergraduate education, and their varying strategies converge on one theme: they care deeply about their students.

Finally, none of this would be possible without my loving and supportive family, especially my husband, Matthew Gibbons, who is truly my partner and my joy. My parents, Lou and Pam Farina, have been and continue to be there for me every step of the way. My sisters, Laura and Michele, inspire me every day with the delight and integrity with which they live their lives. My husband's family has been a source of strength and love that continues to grow. I am so fortunate and so grateful to be surrounded by an incredible community.

TABLE OF CONTENTS

CHAPTER 1

EVOLUTION OF THE BRANCHIOSTEGAL MEMRANE AND RESTRICTED GILL OPENINGS IN ACTINOPTERYGIAN FISHES[1]

Abstract

A phylogenetic survey is a powerful approach for investigating the evolutionary history of a morphological characteristic that has evolved numerous times without obvious functional implications. Restricted gill openings, an extreme modification of the branchiostegal membrane, are an example of such a characteristic. We examine the evolution of branchiostegal membrane morphology and highlight convergent evolution of restricted gill openings. We surveyed specimens from 433 families of actinopterygians for branchiostegal membrane morphology and measured head and body dimensions. We inferred a relaxed molecular clock phylogeny with branch length estimates based on nine nuclear genes sampled from 285 species that include all major lineages of Actinopterygii. We calculated marginal state reconstructions of four branchiostegal membrane conditions and found that restricted gill openings have evolved independently in at least 11 major actinopterygian clades, and the total number of independent origins of the trait is likely much higher. A principal component analysis revealed that fishes with restricted gill openings occupy a larger morphospace, as defined by our linear measurements, than do fishes with non-restricted openings. We used a decision tree analysis of ecological data to determine if restricted gill openings are linked to certain environments. We found that fishes with restricted gill openings repeatedly occur under a variety of ecological

[1] This chapter has been published as Farina, S.C., Near, T. J., Bemis, W.E. 2015. Evolution of the branchiostegal membrane and restricted gill openings in Actinopterygian fishes. Journal of Morphology 276, 681-694.

conditions, although they are rare in open-ocean pelagic environments. We also tested seven ratios for their utility in distinguishing between fishes with and without restricted gill openings, and we propose a simple metric for quantifying restricted gill openings called the RGO ratio, defined as a ratio of the distance from the ventral midline to the gill opening relative to half the circumference of the head. Functional explanations for this specialized morphology likely differ within each clade, but its repeated evolution indicates a need for a better understanding of diversity of ventilatory morphology among fishes.

Introduction

Gill chamber morphology varies extensively among the more than 31,000 living species of ray-finned fishes (Actinopterygii). This undoubtedly relates to performance of both gill ventilation and feeding, and understanding the evolutionary history of this variation can provide important context for functional studies (Lauder, 1990). Historically, broad surveys of morphological variation of actinopterygians categorized morphology without in-depth consideration of historical patterns. For example, with teleosts, McAllister's (1968) survey of branchiostegal rays, Monod's (1968) survey of the caudal skeleton, and Kusaka's (1974) survey of the urohyal, while anatomically detailed, could not be framed in a rigorous phylogenetic context because so little phylogenetic information for ray-finned fishes was available at that time. The more recent study of abdominal and caudal vertebral patterning by Ward and Brainerd (2007) exemplifies the continuing importance of broad morphological surveys as context for functional morphological research, but even in 2007, phylogenetic relationships among many subgroups of actinopterygians were poorly known (Stiassny et al., 2004). Recent large-scale efforts to improve resolution of the actinopterygian phylogeny using molecular data (Near et al., 2012; Betancur-R et al., 2013; Broughton et al., 2013; Near et al., 2013) now allow us to

consider ancestral state reconstruction (e.g., Stewart et al., 2014; Davis et al., 2014) and frame questions about patterns of variation in structure across a broad distribution of actinopterygian species.

As actinopterygians ventilate their gills, water is pumped into the mouth, passed over the gill tissue, and pumped out through openings at the posterior edge of the gill chamber. The movements of the mouth and the gill covers (= opercula) have inspired experimental and morphological investigations that established a two pump model for ventilation (Hughes and Shelton, 1958; Hughes, 1960). Far less obvious is the often-substantial skeleton ventral to the gill covers, the branchiostegal rays, which contribute to the 'suction' pump created by gill chamber expansion during ventilation. These rays are long struts of dermal bone that articulate with ventral elements of the hyoid arch to form the ventro-lateral surface of the gill chamber (Fig. 1). In extant actinopterygians, the number of branchiostegal rays varies from 0-51 pairs, along with substantial variation in length, shape, and cross-sectional area (McAllister, 1968). The rays are actuated by several muscles, primarily the hyohyoideus abductor and adductor muscles, which are highly variable in their arrangement (Winterbottom, 1974). The relative size of the branchiostegal apparatus has been linked to differences in ventilatory function, with larger or more numerous branchiostegal rays often indicating a more prominent suction pump (Baglioni, 1907; Hughes, 1960; Liem, 1970).

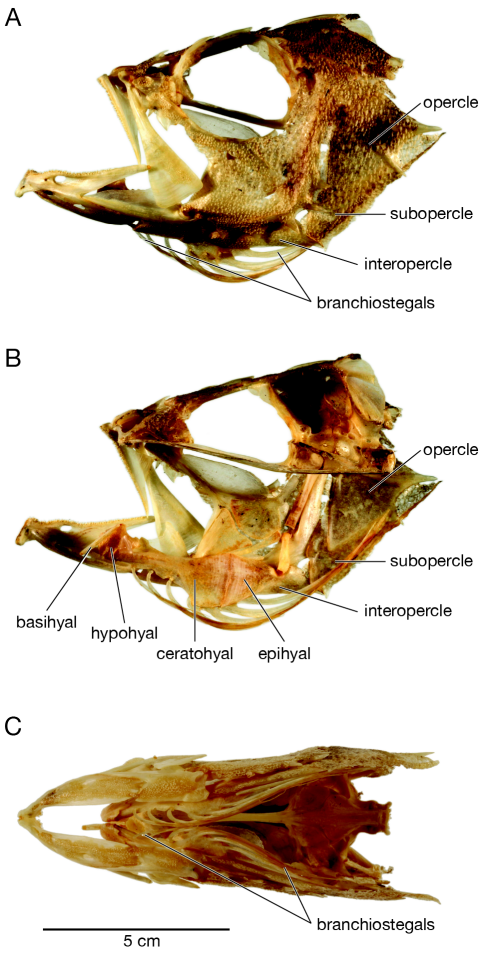

Figure 1. Photograph illustrating the branchiostegal rays. Branchiostegal rays are dermal bones that articulate with ventral elements of the hyoid arch to form the ventro-lateral surface of the gill chamber. The top photograph (A) is a lateral view of the cranial skeleton of Sebastes norvegicus. The middle photograph (B) is a lateral view of the interior cranial skeleton of S. norvegicus to demonstrate the ventral elements of the hyoid arch. The specimen has been bisected through the mid-sagittal plane, and the left half of the specimen is depicted. The photograph has been flipped to orient the mouth in the same direction as in the other photographs. The bottom photograph (C) is a ventral view of the cranial skeleton of S. norvegicus to depict a complete set of branchiostegal rays.

The branchiostegal rays support the branchiostegal membrane, often referred to as the gill membrane. The branchiostegal membrane is ideally situated to have a potent effect on water transport during ventilation as a wall of the gill chamber and as a valve to control the flow of water out of the gill openings. In addition to its primary function in gill ventilation, this

membrane can serve a variety of functions in fish behavior. For example, some males develop bright coloration of the branchiostegal membrane to attract females (Semler, 1971; Ragland and Fischer, 1987). Others flare their membranes in antagonistic displays against conspecific intruders or competitors (Baerends and Baerends-Van Roon, 1950). It is also a common substrate for photophores in light-producing fishes (Strum, 1969; Cavallaro et al., 2004). Our study focuses on an extreme modification of the branchiostegal membrane, the reduction of the gill opening to a small aperture, which presumably influences fluid flow in important though as yet poorly understood ways (Brainerd and Ferry-Graham, 2006; Graham, 2006).

Restricted gill openings are frequently mentioned as defining characteristics of taxonomic groups in classification references and field guides (e.g., Nelson, 2006; Lamb and Edgell, 2010). In species descriptions, these small gill openings are characterized relative to features such as eye size (e.g., Chernova, 2014) and position of the pectoral fin (e.g., Maldonado-Ocampo et al., 2014) to distinguish new species from close relatives. In some taxa, the gill opening is siphon-like or minuscule, presenting an obvious case of restricted gill openings that can be identified by qualitative assessment. For cases that are less obvious, a quantitative definition that can be applied across all ray-finned fishes may be useful for systematists. With only rare exceptions, "restricted gill openings" and related terms are applied to fishes in which the branchiostegal membrane is broadly joined to the ventral surface of the body, restricting the aperture. Therefore, a useful quantitative definition of this trait could include the relative broadness of this attachment in addition to gill opening size.

To examine the evolutionary history and variation of gill openings, we surveyed branchiostegal membrane morphology and mapped it onto a comprehensive time-calibrated phylogeny of major actinopterygian lineages. Our goals were to: (1) reconstruct the evolutionary

history of branchiostegal membrane morphology in Actinopterygii; (2) identify independent origins of restricted gill openings at the family level; (3) determine useful metrics for quantifying gill opening restriction; and (4) determine morphometric and ecological correlates of the occurrence of restricted gill openings. We highlight the extensive morphological, ecological, and phylogenetic diversity of actinopterygian fishes with restricted gill openings.

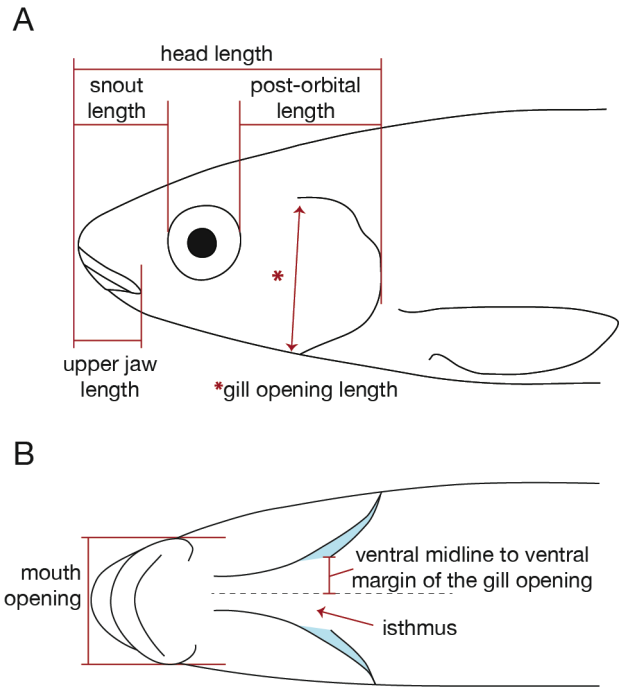

Figure 2. Morphological measurements taken during survey. (A) Measurements taken from a lateral perspective included head length, snout length, post-orbital length, upper jaw length, and gill opening length. (B) Measurements taken from a ventral perspective included mouth opening length and the length from the ventral midline to the ventral margin of the gill opening.

Methods

We surveyed branchiostegal membrane morphology in specimens from the Cornell University Museum of Vertebrates (CUMV), the Academy of Natural Sciences of Drexel University (ANSP), the University of Washington Fish Collection (UW), and the Harvard Museum of Comparative Zoology (MCZ). Nelson (2006) recognized 453 families of actinopterygians, and we examined one specimen from 433 of these families (see Appendix 1).

We selected individuals that were non-larval and had a fully intact branchiostegal membrane, and whenever possible, we chose taxa of the same genus and species as those in the molecular data set used for ancestral state reconstruction of branchiostegal membrane morphology (see below). Because we only examined one specimen from each family, we did not capture the entire extent of variation that exists within families. We measured the following on each specimen: standard length, head length, upper jaw length, snout length, post-orbital length (distance from posterior margin of orbit to posterior margin of the opercle), mouth opening (width of the maximum opening of the lower jaw near the jaw joint) and circumference of the head through the center of the opercle (or in the gill region in fishes without opercles, such as in saccopharyngiforms) (Fig. 2A). We also measured the length from the ventral midline of the body to the ventral margin of the gill opening (Fig. 2B). We characterized each specimen according to the following four branchiostegal membrane morphologies based on the terminology and descriptions of McAllister (1968).

"Separate and free from the isthmus" (Fig. 3A)

Left and right branchiostegal membranes are separate from each other. Often, the branchiostegal membranes overlap ventro-anteriorly, as in *Amia calva* (Fig. 3A, Amiidae). There is no attachment of the branchiostegal membrane to the isthmus of the body.

"United and free from the isthmus" (Fig. 3B)

Left and right branchiostegal membranes are united with each other ventrally, and there is no attachment of the membranes to the isthmus. In some species, the unity of the membranes is broad and obvious, as in *Lepisosteus osseus* (Fig. 3B, Lepisosteidae). However, in other species, the membranes are united by only a small amount of tissue ventro-anteriorly and can overlap slightly. This can make it difficult to distinguish between "separate" and "united" morphologies

in certain groups. For such specimens, we made the distinction based on a qualitative assessment of whether or not the left and right membranes were continuous with one another. McAllister (1968) reported many clades as having examples of both "separate" and "united" configurations.

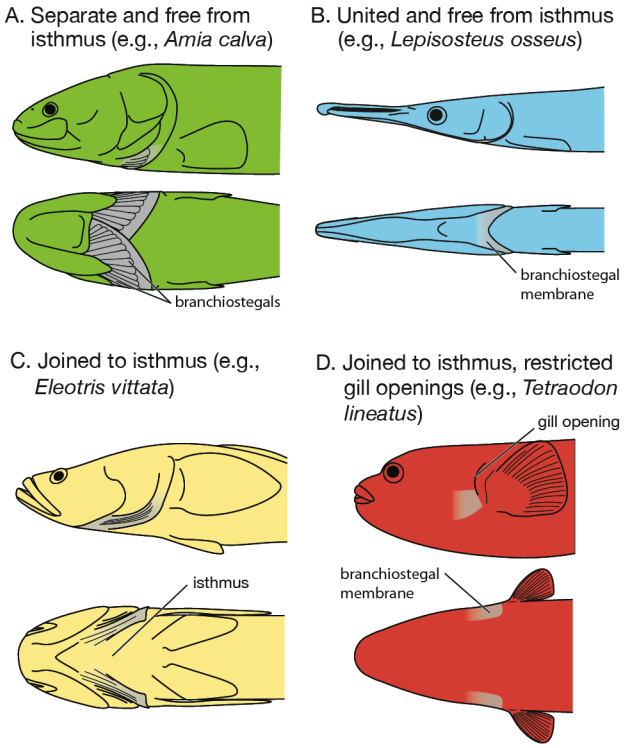

Figure 3. Four conditions of the branchiostegal membrane. (A) Left and right membranes are separate from one another, often overlapping. (B) Left and right membranes are continuous with one another and free from the isthmus. (C) Membranes are joined to the isthmus of the body. (D) Membranes are joined to the isthmus of the body with restricted gill openings.

"Joined to the isthmus" (Fig. 3C)

The branchiostegal membranes are joined to the ventral surface of the body, separating the gill openings. The distance between the left and right gill openings can be small ("narrowly joined to the isthmus" according to McAllister, 1968) or large ("broadly joined to the isthmus") as in *Eleotris vittata* (Fig. 3C, Eleotridae). The amount of space between gill openings exists along a continuum, and therefore we do not distinguish between "narrowly joined" and "broadly joined" in our survey, except that we consider extreme broadness to often indicate restricted gill

openings (Fig. 3D). In some species, branchiostegal membranes are joined to the isthmus but appear externally to be united in a continuous membrane (e.g., many species of Cottidae). McAllister refers to these fishes as having a "gill membrane joined to isthmus and forming a free fold over it," because it can result in a folded appearance. In our survey, we consider this to be a case of "joined to the isthmus" morphology.

"Joined to the isthmus, gill opening restricted" (Fig. 3D)

The branchiostegal membranes are joined very broadly to the ventral surface of the body, resulting in restricted gill openings, as in *Tetraodon lineatus* (Fig. 3D, Tetraodontidae). Fishes were categorized as having this morphology if the branchiostegal membrane was attached to the isthmus and the gill openings were considerably smaller or more siphon-like in appearance relative to the more typical actinopterygian condition.

Ancestral state reconstruction

To reconstruct character state evolution of branchiostegal membrane morphology across Actinopterygii (Fig. 4), we first inferred a phylogeny using sequence data from two recent studies (Near et al., 2012; Near et al., 2013). This data set included 285 taxa representing 284 families recognized by Nelson (2006) and included sequence data for nine nuclear markers (*glyt*, *myh6*, *plagl2*, *ptr*, *rag1*, *SH3PX3*, *sreb2*, *tbr1*, and *zic1*). We used one species from each family, with the exception of Polypteridae, our outgroup to all other actinopterygians, for which we used two species (*Polypterus ornatipinnis* and *Erpetoichthys calabaricus*, Polypteridae). Using BEAST software (Drummond, 2012), we inferred a relaxed molecular clock phylogeny with relative divergence time estimates, rooting the tree with outgroup taxa *P. ornatipinnis* and *E. calabaricus*. Sequence data were partitioned using BEAUti software (Drummond, 2012) into

nine unlinked GTR substitution models. An MCMC chain of 190 million generations was used to generate a maximum clade credibility tree in TreeAnnotator v1.8.0 software.

We assigned one of four branchiostegal membrane character states to each taxon, based on the condition for its family from our morphological survey (Appendix 1). Out of the 285 taxa used for phylogenetic reconstruction, 123 taxa (43%) are the same species that we examined in our survey. We calculated the marginal ancestral state reconstructions for each node using the `rerootingMethod` function with equal rates and symmetrical models from the phytools package in R (R Core Team, 2013; Revell, 2012), which is based on the re-rooting method of Yang et al. (1995).

Testing metrics to define restricted gill openings

We investigated simple metrics that can be used to define restricted gill openings. We tested seven ratios of measurements for the ability to distinguish between restricted and non-restricted gill openings. We only included data from specimens with an attachment to the isthmus (Fig. 3C and 3D; 138 families total). For each ratio, we determined the optimal cutoff value beyond or below which a fish could be considered to have restricted gill openings. To do this, we applied the `optimize` function from the stats package in R (R Core Team, 2013) to a function written to determine a cutoff value for each ratio based on presence or absence of restricted gill openings as determined by our qualitative assessment. The error (the number of individuals not properly categorized by each cutoff value) was used to calculate a precision estimate for the cutoff value for each ratio. A range of error values was calculated by performing this optimization procedure over 100 simulations, with each simulation using a randomly sampled 90% of the original data. We tested the following ratios in this manner: gill opening length relative to head length, distance from the ventral midline of the body to the ventral margin

of the gill opening (ventral midline to ventral margin, VMVM) relative to head length, VMVM relative to half the circumference of the head in the gill region multiplied by 100 (herein referred to as the restricted gill opening ratio, or RGO ratio), VMVM relative to gill opening length, RGO ratio divided by gill opening length, RGO ratio multiplied by the inverse of the ratio of gill opening length to head length, and gill opening length relative to half the circumference of the head in the gill region.

Morphometric and ecological features co-occurring with restricted gill openings

To investigate the morphospace occupied by fishes with different branchiostegal membrane morphologies, we used JMP Pro 10.0.0 to conduct a principal component analysis on measurements taken from the 433 specimens examined. We did not adjust for phylogenetic relationships because phylogenetic information is not available for all 433 families examined. We used the following ratios: head length relative to standard length, upper jaw length relative to head length, snout length relative to head length, post-orbital length relative to head length, mouth opening relative to head circumference, and half the head circumference relative to standard length; all ratios were arcsine transformed. We generated a plot of PC1 and PC2, a loading plot, and a table of factor loadings (Table 1). We performed a Bartlett's test of homogeneity in JMP Pro 10.0.0 to determine the number of components to retain and quantified the mean and standard deviation of each retained PC axis for each character state (Table 2).

Table 1. Loadings for ratios used in principal component analysis

Ratio	PC1	PC2	PC3	PC4
ArcSine(hl/sl)	0.527	0.712	0.286	0.183
ArcSine(ujl/hl)	-0.360	0.307	0.612	-0.633
ArcSine(snl/hl)	0.637	-0.466	0.523	0.084
ArcSine(pol/hl)	-0.828	0.316	-0.286	0.116
ArcSine(mo/circ)	-0.517	0.208	0.636	0.486
ArcSine(0.5*circ/sl)	0.603	0.665	-0.284	-0.051

hl = head length, sl = standard length, ujl = upper jaw length, snl = snout length, pol = post-orbital length, mo = mouth opening length, and circ = circumference of the head in the gill region.

Table 2. Means (M) and standard deviations (SD) for each significant PC axis of the principal component analysis for each branchiostegal membrane morphology condition

Condition	PC1 M	PC1 SD	PC2 M	PC2 SD	PC3 M	PC3 SD	PC4 M	PC4 SD
Separate	-0.323	**1.011**	0.015	**0.887**	0.181	**0.832**	-0.250	**0.784**
United	0.093	**1.283**	0.114	**1.008**	-0.134	**1.162**	-0.125	**0.779**
Joined to isthmus	0.309	**1.396**	-0.348	**1.007**	-0.014	**0.862**	0.252	**0.561**
Restricted	-0.018	**2.102**	-0.058	**1.839**	0.133	**1.514**	0.441	**0.978**
All conditions	0.004	**1.440**	-0.003	**1.186**	0.005	**1.139**	0.000	**0.834**

To examine the relationship between ecology and branchiostegal membrane morphology, we used ecological data from FishBase (Froese and Pauly, 2011) to determine the basic ecology (pelagic, demersal, or reef-associated) and environment (tropical, subtropical, temperate, deep-sea, boreal, or polar) for each species in our survey. We performed a decision tree analysis in JMP Pro 10.0.0 as a data-mining technique to determine which ecological variables are most recursively predictive of branchiostegal membrane morphology. No adjustment for phylogenetic relationships was made due to a lack of available molecular data for a large portion of the taxa surveyed.

Results

Ancestral state reconstruction (Fig. 4) showed that restricted gill openings have evolved independently in each of the following 11 clades: (1) Anguilliformes and Saccopharyngiformes; (2) Mormyridae; (3) Kneriidae; (4) Gymnotiformes; (5) Callichthyidae; (6) Opisthoproctidae; (7) Batrachoidiformes; (8) Syngnathidae, Pegasidae, Dactylopteridae, and Callionymidae; (9) Liparidae and Cyclopteridae; (10) Zanclidae; (11) Tetraodontiformes and Lophiiformes. Fishes with restricted gill openings are spread throughout the phylogeny. Out of the 433 families surveyed, 101 families had separate membranes (23.3%), 194 families had united membranes (44.8%), 58 families had membranes joined to the isthmus (13.4%), and 80 families had restricted gill openings (18.5%).

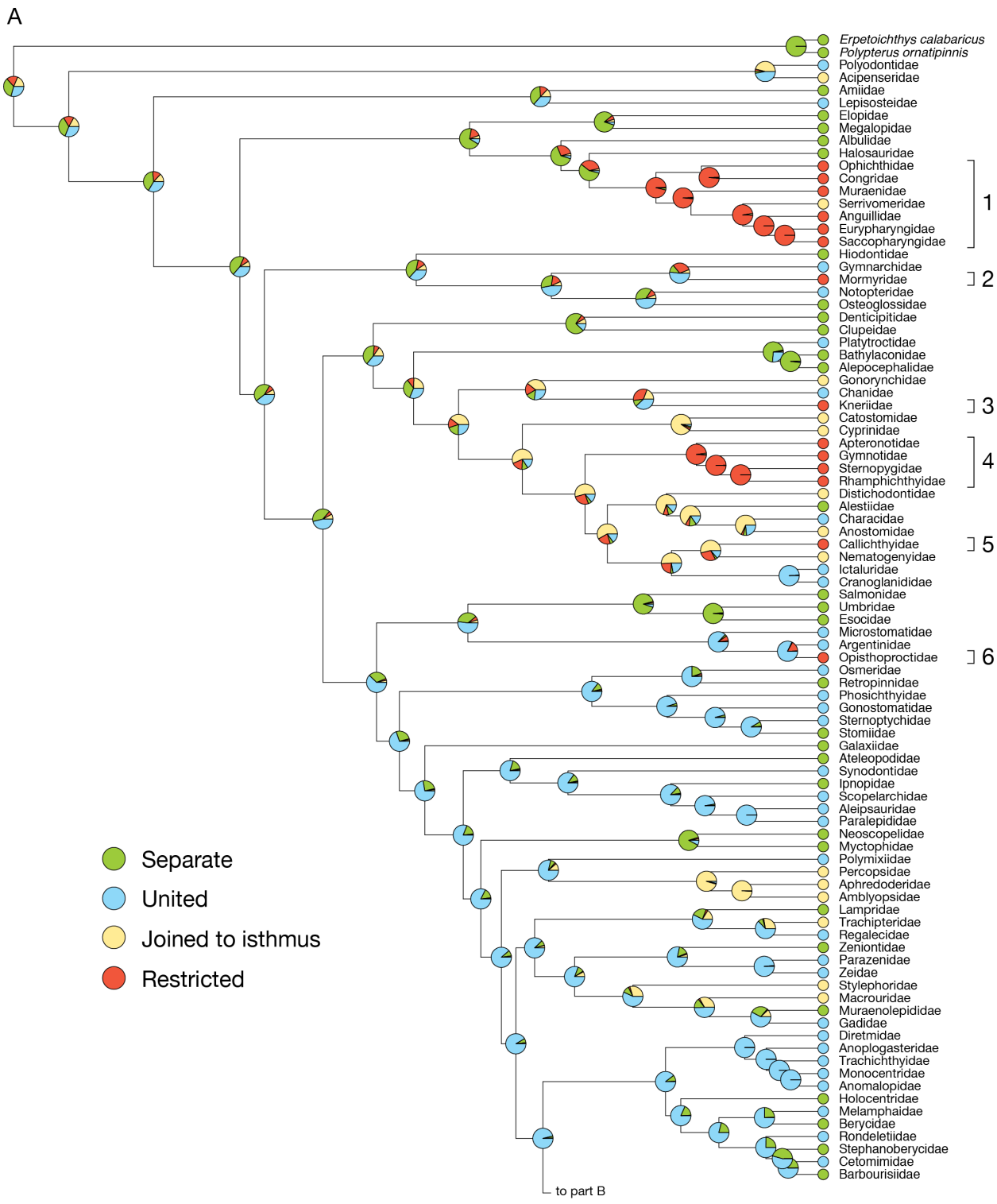
A
Erpetoichthys calabaricus
Polypterus ornatipinnis
Polyodontidae
Acipenseridae
Amiidae
Lepisosteidae
Elopidae
Megalopidae
Albulidae
Halosauridae
Ophichthidae
Congridae
Muraenidae
Serrivomeridae
Anguillidae
Eurypharyngidae
Saccopharyngidae
Hiodontidae
Gymnarchidae
Mormyridae
Notopteridae
Osteoglossidae
Denticipitidae
Clupeidae
Platytroctidae
Bathylaconidae
Alepocephalidae
Gonorynchidae
Chanidae
Kneriidae
Catostomidae
Cyprinidae
Apteronotidae
Gymnotidae
Sternopygidae
Rhamphichthyidae
Distichodontidae
Alestiidae
Characidae
Anostomidae
Callichthyidae
Nematogenyidae
Ictaluridae
Cranoglanidae
Salmonidae
Umbridae
Esocidae
Microstomatidae
Argentinidae
Opisthoproctidae
Osmeridae
Retropinnidae
Phosichthyidae
Gonostomatidae
Sternoptychidae
Stomiidae
Galaxiidae
Ateleopodidae
Synodontidae
Ipnopidae
Scopelarchidae
Aleipsauridae
Paralepididae
Neoscopelidae
Myctophidae
Polymixiidae
Percopsidae
Aphredoderidae
Amblyopsidae
Lampridae
Trachipteridae
Regalecidae
Zeniontidae
Parazenidae
Zeidae
Stylephoridae
Macrouridae
Muraenolepididae
Gadidae
Diretmidae
Anoplogasteridae
Trachichthyidae
Monocentridae
Anomalopidae
Holocentridae
Melamphaidae
Berycidae
Rondeletiidae
Stephanoberycidae
Cetomimidae
Barbourisiidae
1
2
3
4
5
6
Separate
United
Joined to isthmus
Restricted
to part B

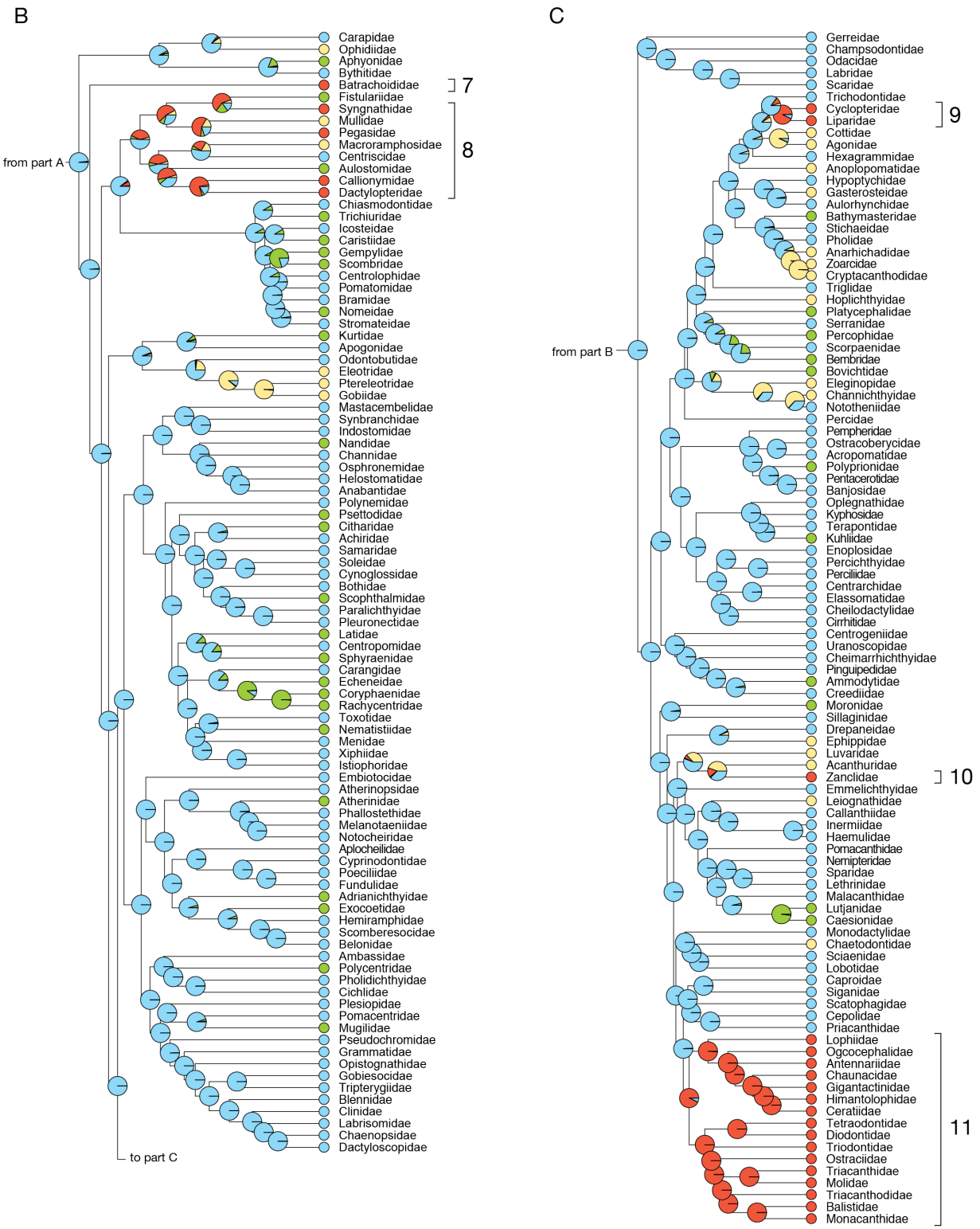

Figure 4. Ancestral state reconstruction of the distribution of branchiostegal membrane morphology across Actinopterygii. Relaxed molecular clock phylogeny of 285 species representing 284 actinopterygian families. Pie charts at nodes show marginal ancestral state reconstructions for four branchiostegal membrane conditions. Brackets indicate clades in which restricted gill openings have independently evolved.

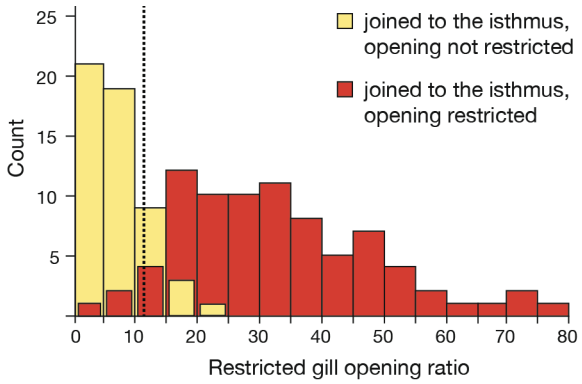

Figure 5. Quantitatively defining restricted gill openings. These histograms show the distribution of the RGO ratio for fishes with membranes joined to the isthmus (yellow) and with membranes joined to the isthmus, gill openings restricted (red). The dashed line indicates the calculated cutoff value of 12.5, above which fishes can be considered to have a restricted gill opening (error = 1.2 – 2.8%).

We tested different ratios of measurements for the ability to distinguish between restricted and non-restricted gill openings among fishes with an attachment to the isthmus. For each ratio, we determined a cut-off point between taxa with restricted and non-restricted gill openings and quantified the range of error. The ratio of gill opening length relative to head length had a cutoff value of 0.385 (error = 3.2 – 5.3%), below which fishes were classified as having a restricted gill opening. The ratio of VMVM relative to head length had a cutoff value of 0.127 (error = 3.2 – 5.1%), above which fishes were classified as having a restricted gill opening. The RGO ratio had a cutoff value of 12.53 (error = 1.2 – 2.7%), above which fishes were classified as having a restricted gill opening. The ratio of VMVM relative to gill opening length had a cutoff of 11.89 (error = 1.2 – 12.5%), above which fishes were classified as having a restricted gill opening. The RGO ratio divided by gill opening length had a cutoff value of 51.22 (error = 10.2 – 12.7%), above which fishes were classified as having a restricted gill opening. The RGO ratio multiplied by the inverse of the ratio of gill opening length to head length had a

cutoff value of 1231 (error = 1.4 – 12.9%), above which fishes were classified as having a restricted gill opening. The ratio of gill opening length to half the circumference of the head had a cutoff value of 0.41 (error = 7.5 – 13.4%). The RGO ratio (Fig. 5) was the value that consistently categorized fishes with low error. Gill opening length relative to head length was the only value incorporating size of the gill opening that consistently categorized fishes with low error.

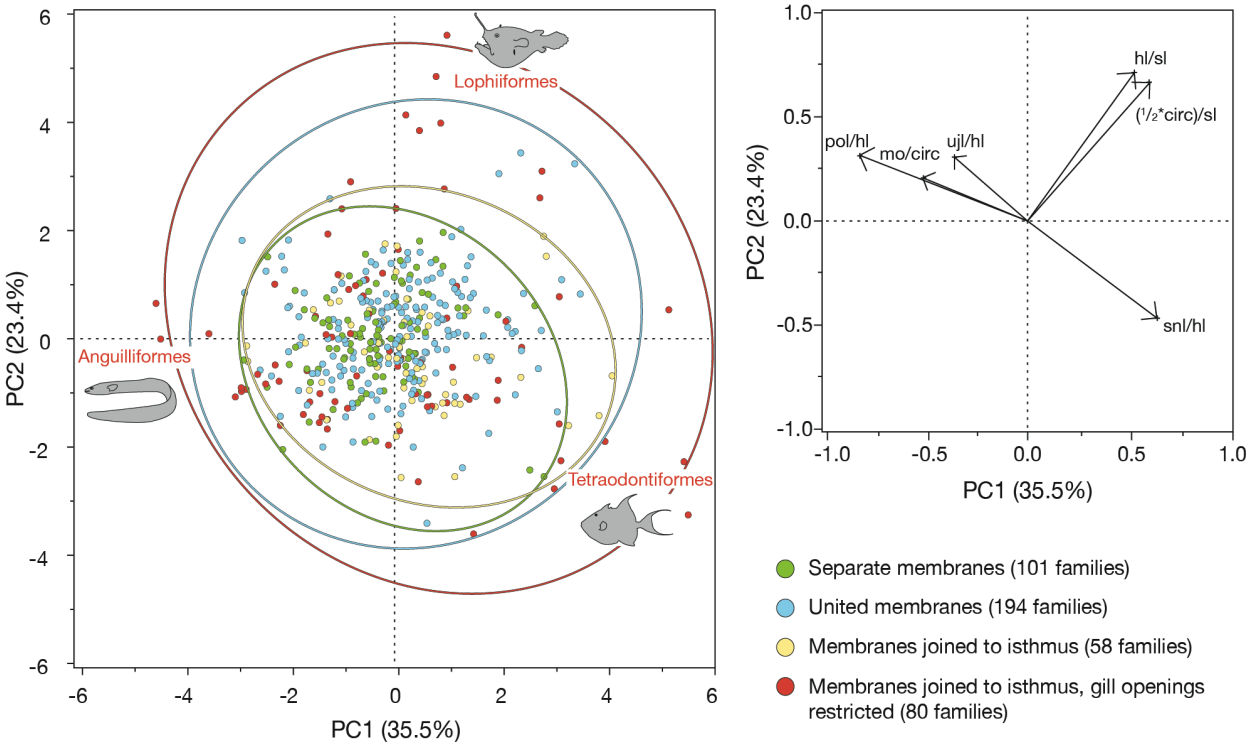

Figure 6. Principal component analysis of morphometric data. The plot of PC1 and PC2 for measurements taken from specimens representing 433 actinopterygian families (left) shows that fishes with restricted gill openings occupy a more widespread morphospace, as defined by our morphometric data, than fishes with other branchiostegal membrane morphologies. Fishes with restricted gill openings occur at many of the extremes of our plot, and we have indicated examples of groups that represent these extremes: the highly elongate Anguilliformes (eels), the large-headed Lophiiformes (anglerfishes), and the often large-snouted Tetraodontiformes (e.g., triggerfishes). All measurements were arcsine transformed, and colors follow Fig. 3. A corresponding loading plot for PC1 and PC2 is shown on the right.

A plot of PC1 and PC2 from our principal component analysis (Fig. 6) shows the morphospace occupied by fishes with each branchiostegal membrane morphology as quantified by six ratios of body shape based on standard measurements. Fishes with restricted gill openings, when considered as a whole, occupy a morphospace larger than fishes with all other membrane morphologies, even when compared with the most common morphology of united branchiostegal membranes. Fishes occupying the upper right quadrant of the plot (e.g., Lophiiformes) have large heads relative to body length and are globular in shape. Fishes occupying the lower right quadrant of the plot (e.g., Tetraodontiformes) have eyes that are positioned far posteriorly from the tip of the snout. Fishes occupying the lower left quadrant are elongate with short snouts. The components PC5 and PC6 were found to have eigenvalues with significantly different variances from the first four principal components based on the Bartlett's test of homogeneity (for PC5, $X^2 = 2.49$ and $p = 0.43$; for PC6, $X^2 = 0$, and $p = 1$), so PC loadings (Table 1) and descriptive statistics (Table 2) are only provided for PC1-4. For each of these four principal component axes, the standard deviation among fishes with restricted gill openings was higher than any of the other branchiostegal membrane conditions (Table 2).

Decision tree analysis shows that the most important ecological factor recursively predicting branchiostegal membrane morphology is whether or not the fish is pelagic ($p = 0.008$) (Fig. 7). Among pelagic families ($p = 0.010$), most fishes with restricted gill openings are deep-sea; Molidae is the only pelagic family in our survey that has restricted gill openings but does not live in the deep-sea. Based on the taxa used for this study, most families with restricted gill openings are demersal ($n = 49$), and the rest are bathypelagic ($n = 16$), pelagic ($n = 1$), or reef-associated ($n = 14$). A high number of fish families with membranes joined to the isthmus are demersal ($n = 44$), with the rest occurring in bathypelagic ($n = 4$), pelagic ($n = 3$), and reef-

associated (n = 7) habitats. The majority of reef fish families have membranes that are united and free from the isthmus (n = 47 out of 79), and most reef fishes (p = 0.014) with restricted gill openings inhabit subtropical waters.

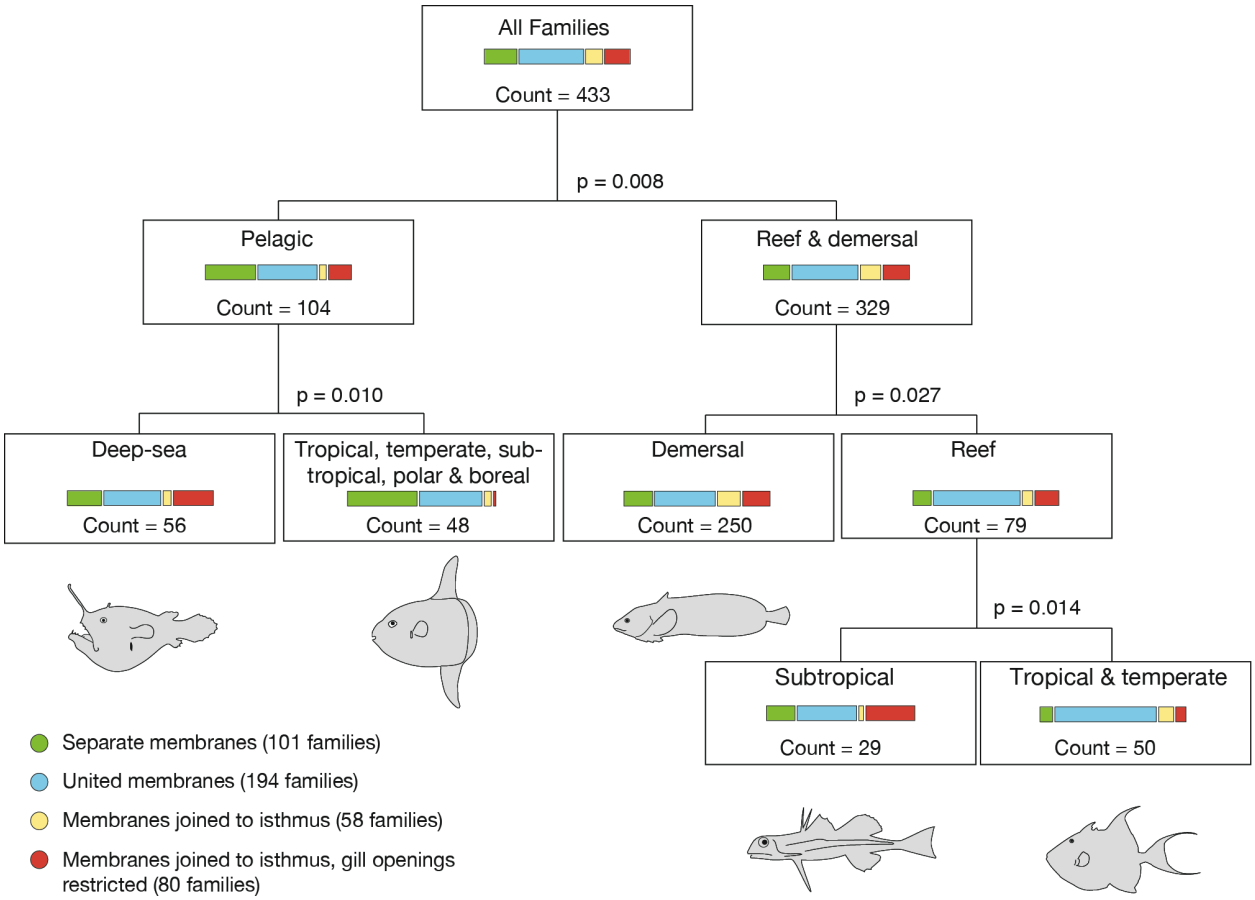

Figure 7. Decision tree analysis of ecological variation. A decision tree analysis shows ecological variables that are recursively predictive of branchiostegal membrane morphology. All environments that we considered showed examples of all four membrane conditions. The primary ecological factor recursively predicting branchiostegal membrane morphology is whether a fish is pelagic (p = 0.008). Most families with restricted gill openings are demersal (n = 49).

Discussion

Convergent evolution of restricted gill openings

Our phylogenetic analysis shows 11 independent origins of restricted gill openings within Actinopterygii, with the trait occurring in some of the earliest as well as the most recently

diverged lineages (Fig. 4). While the ubiquity of this trait has likely been obvious to ichthyologists for decades, recent efforts to complete robust molecular analyses with a large number of taxa and markers (Near et al., 2012; Betancur-R et al., 2013; Broughton et al., 2013; Near et al., 2013) greatly enhance our ability to identify the number of times that this trait has evolved and its distribution across the phylogeny. The repeated evolution of restricted gill openings suggests that it is likely beneficial under a variety of conditions.

There are several more instances of convergent evolution of restricted gill openings not represented in Fig. 4 due to the limited taxonomic coverage of the molecular phylogenetic data set. For example, within the species-rich clade of Siluriformes, restricted gill openings occur in each of the following clades: Loricarioidei, Cetopsidae, Aspredinidae (Auchenipteridae + Doradidae), Ariidae, Erethistidae, Chacidae, and Mochokidae (Malapteruridae + Amphiliidae). Based on hypothesized phylogenetic relationships among these clades (Sullivan et al., 2006), restricted gill openings have evolved at least three times within Siluriformes, while the actual number is likely higher. Giganturidae is another example of an independent origin of this trait as the only family within Aulopiformes to have restricted gill openings. Microdesmidae, placed as the sister group to Gobiidae by Betancur-R et al. (2013) also have restricted gill openings. Congiopodidae is a clade of uncertain phylogenetic position within Scorpaeniformes (Lautredou et al., 2013) and Rhamphocottidae is nested within Cottoidei (*sensu* Nelson, 2006) according to Knope (2013) and Smith and Busby (2014); both of these clades likely represent additional instances of independent evolution of restricted gill openings.

Although membrane morphology is relatively conserved at a family level, it can vary within families and even within genera. Large, species-rich families such as Cyprinidae and Blenniidae contain species that have restricted gill openings, as seen in *Gila*, *Hypsoblennius*, and

Chasmodes (Miller, 1945; Ditty et al., 2005). There can also be variation within species-depauperate families such as Aploactinidae, which contains species with membranes united and free from the isthmus as well as species with restricted gill openings (Poss and Johnson, 1991). As for intrageneric variation, *Ernogrammus hexagrammus* (Stichaeidae) has membranes joined to the isthmus whereas *Ernogrammus walkeri* has membranes united and free from the isthmus (Follett and Powell, 1988). There are also several families in which all or most members have an attachment of the branchiostegal membrane to the isthmus, with some members having restricted gill openings; these families include Cyprinidae, Auchenipteridae, Batrachoididae, Agonidae, and Gobiidae.

We identified a cryptic case of restricted gill openings in some barreleyes (Opisthoproctidae) that calls attention to the difficulty of determining branchiostegal membrane morphology from preserved specimens of deep-sea fishes. These specimens are typically delicate and easily damaged during collection and preservation, and tearing of the branchiostegal membrane can give the impression that membranes are free from the isthmus. This is exacerbated by the evolutionary trend of branchiostegal ray reduction in deep-sea fishes, because the rays cease to provide substantial skeletal support for the membrane (McAllister, 1968). Based on examination of two specimens in which the complete branchiostegal membrane is intact (*Opisthoproctus soleatus*, MCZ41536, and *Macropinna microstoma*, UW110014), we found that the gill opening is restricted to a small aperture covered by the opercular bones in these species. Other opisthoproctid genera such as *Dolichopteryx* and *Rhyncohyalus* have been noted to have united membranes that are free from the isthmus (Cohen, 1964), but the morphology of the gill opening was unambiguously restricted in the two aforementioned specimens of *O. soleatus* and *M. microstoma*. Among the Opisthoproctidae, these two taxa

represent more extreme forms, with some skeletal modifications potentially linked to restricted gill openings. For example, *O. soleatus* possesses a large ventral keel that extends far forward on the ventral surface of the head, supported by anterior projections of the cleithrum (Cohen, 1964). *Macropinna microstoma* has large expansions of the interopercle and preopercle that extend ventrally to cover the gular region (Chapman, 1942). These structures may require the ventral space on the head provided by restricted gill openings. Also, both species have dorsally-directed tubular eyes that require specialized configurations of the cranial elements, some of which may be facilitated by restriction of the gill openings.

Synbranchiform fishes (swamp eels) are often noted for their single, small gill opening on the ventral surface of the head. This is a specialized case of "united and free from the isthmus" (McAllister, 1968) in which the gill openings are covered with skin dorsally, giving the superficial appearance of one small ventral opening. Because the membranes remain free from the isthmus, we consider this to be a fundamentally different morphology from "restricted gill openings," as we have defined it in this study. This single opening likely has major functional consequences for the complex and unique synbranchiform aerial respiratory apparatus (Liem, 1980). Graham (1997) suggests that it may allow Synbranchiformes to better retain a volume of air in the gill chamber and keep out debris. Restricted gill openings may have similar functions in other air-breathing or burying fishes.

While restricted gill openings are distributed broadly throughout the ray-finned fishes, they are notably absent among much of the phylogenetic diversity of Percomorpha (Fig. 4B-C). The majority of families in these clades without restricted gill openings have previously been classified as belonging to "Percoidei," which has long been acknowledged as paraphyletic (Johnson, 1984). Many (but not all) "Percoidei" have a generalized, often perch-like form with

few distinguishing specializations and occur among reefs and other near-shore environments (Johnson, 1984). These historical and ecological trends help to explain the high number of reef fishes in our survey with united membranes that are free from the isthmus (Fig. 7).

Quantifying gill opening restriction

Although many species have clearly tiny gill openings, the difference between "membranes joined to the isthmus" and "restricted gill openings" morphology is frequently a matter of qualitative assessment by authors. Our survey provided an opportunity to use qualitative assessment of gill opening morphology to quantitatively define this feature. The most accurate and consistent metric tested in our study to quantify gill opening restriction was the RGO ratio, which is a consideration of how broadly the branchiostegal membrane is attached to the isthmus relative to head circumference, as expressed in the following equation:

$$RGO\ ratio = \left(\frac{VMVM}{1/2\ head\ circumference}\right) * 100$$

where VMVM is the distance from the ventral midline of the body to the ventral margin of the gill opening. This ratio quantifies the extent to which the gill openings are restricted ventrally by the branchiostegal membrane and the isthmus. Generally, a fish with an RGO ratio above 12.5 has restricted gill openings (Fig. 5), and this value can be used as a reference for species descriptions and other morphological assessments.

When diagnosing gill opening restriction, it is useful to consider gill opening length in addition to the RGO ratio. Gill opening length is a commonly reported metric that provides a direct indication of gill opening size. The ratio of gill opening length to head length had relatively low error in our subsampling simulations (error = 3.2 – 5.3%). Fishes with a gill opening length less than 38.5% of head length were most often characterized qualitatively as having restricted gill openings. Due to the importance of gill opening size in the definition of

restricted gill openings, we attempted to refine our RGO ratio by testing metrics that included both VMVM and gill opening length. However, these more complex metrics showed higher errors and were unreliable for consistently distinguishing fishes that were characterized as having restricted gill openings. Therefore, the RGO ratio and the relative length of the gill opening should be considered separately in assessment of gill opening morphology.

Based on our simulations, the RGO ratio mischaracterized morphology in 1.2 – 2.7% of taxa. These mischaracterizations occur in cases of fishes with restricted gill openings that are positioned very close to the ventral midline (e.g., *Muraenesox bagio*, Muraenesocidae), which have a small RGO ratio and will therefore be erroneously characterized as "joined to the isthmus." Additionally, fishes with large gill openings but a broad attachment to the isthmus (e.g., *Rhyacichthys aspro*, Rhyacichthyidae) have a large RGO ratio and will be erroneously characterized as "gill openings restricted." The ratio of gill opening length to head length mischaracterized taxa in 3.2 – 5.3% of cases. In taxa with small head lengths, as in Gymnotidae (knifefishes), this ratio can be large despite a restricted gill opening. Taxa with large snouts, such as Acipenseridae (sturgeons), can have a small ratio of gill opening length to head length, despite a large gill opening. When diagnosing the presence of restricted gill openings in a species, it is useful to consider the following factors: the RGO ratio ("restricted" above 12.5), the gill opening length as a percentage of the head length ("restricted" below 38.5%), the position and appearance of the gill opening, and the relative condition of closely related taxa.

Relationship of restricted gill openings with morphometric and ecological factors

We defined a morphospace based on six ratios of measurements taken as a part of our survey. These measurements were selected because of their ability to capture the major axes of actinopterygian body shape variation, specifically relative body elongation, head size, snout size,

horizontal position of the eye on the head, and mouth dimensions. Fishes with restricted gill openings occupy a large area of morphospace in our plot of PC1 and PC2 (Fig. 6), and for each of the first four principal components, the standard deviation is highest among fishes with restricted gill openings (Table 2). United branchiostegal membranes are the most common morphology in terms of number of families (n = 194 out of 433), and yet fishes with that condition occupy only a subset of the morphospace circumscribed by fishes with restricted gill openings (n = 80). Fishes with separate membranes and membranes joined to the isthmus occupy an even smaller portion of the overall morphospace. If fishes with restricted gill openings had occupied only a portion of our morphospace, then we could potentially infer body and head shapes that co-occur with restricted gill openings. However, fishes with a wide range of shapes possess restricted gill openings, indicating that small gill openings may be beneficial when co-occurring with a large variety of cranial morphologies. This trend is apparent even when superficially considering the diversity of fishes with restricted gill openings; moray eels, ocean sunfishes, and seahorses share very few similarities in body and head shape.

Furthermore, the presence of fishes with restricted gill openings at the extremes of this morphospace may indicate that a small, constrained gill opening is necessary for some extreme morphologies to be possible. Restricted gill openings co-occur with a number of highly specialized morphological systems. For example, some anguilliforms (eels) have evolved increased mobility of the pharyngeal jaws for prey capture and posteriorly displaced gill arches (Mehta and Wainwright, 2008; Nelson, 1966). Their ventilation relies mostly on a powerful buccal pump (Hughes, 1960), which may be due to the evolutionary restructuring of the pharyngeal chamber and a reduction of the branchiostegal apparatus. Lophiids (goosefishes) are cryptic ambush predators with large, up-turned mouths ideal for rapid ingestion of large prey.

Lophiids have limited range of cranial motion during ventilation as a result of their extreme feeding morphology (Elshoud, 1986), and therefore ventilation is primarily driven by the action of a large branchiostegal apparatus closed off by a siphon-like restricted gill opening uniquely positioned behind the base of the pectoral fin. The inflation mechanism of burrfishes (Diodontidae) involves a kinematically complex expansion and compression of the buccal cavity, facilitated in part by a greatly enlarged first branchiostegal ray (Wainwright et al., 1995). Syngnathids use a powerful elastic recoil system, spanning from the epaxial muscles to the snout, to quickly rotate the snout upward towards a prey item during suction feeding (van Wassenbergh et al., 2008), and their ventilation is primarily facilitated by a powerful gill-chamber pump (Hughes, 1960). While it is clear that restricted gill openings cannot be the sole explanation for the evolution of these complex biomechanical systems, it is possible that small gill openings played a critical role in their evolutionary history by freeing cranial morphology from the constraint of ancestrally large gill openings. Freeing constraints on morphological systems weakens evolutionary integration among structures and can result in rapid accumulation of disparities within a clade, producing extreme forms (Liem, 1973; Collar et al., 2014). The influence of the presence of restricted gill openings on patterns of diversification and morphological evolution could be tested in a group such as the catfishes (Siluriformes), in which the trait has evolved repeatedly in morphologically and ecologically disparate groups.

Our decision tree analysis (Fig. 7) demonstrates that fishes with all four branchiostegal membrane morphologies, including restricted gill openings, occur in a variety of habitats. However, fishes with restricted gill openings were notably sparse among pelagic (non-deep sea) fishes, with the Molidae as the only example in our survey (other pelagic species of Tetraodontiformes, such as the ocean triggerfish, *Canthidermis sufflamen*, Balistidae, have

restricted gill openings). This indicates that restricted gill openings are not ideal for the high levels of activity required for a typical pelagic fish. For example, a small gill opening may not be suitable for fishes such as paddlefishes (Polyodontidae) that rely on ram ventilation (Burggren and Bemis, 1991). Benthic and structure-associated fishes are, to some extent, released from the selective pressures for and morphological constraints of extreme drag reduction and therefore may be more likely to possess modified ventilatory structures such as restricted gill openings.

Functional implications of restricted gill openings

Direct investigations of ventilatory pressures have revealed that fishes with restricted gill openings exhibit a variety of patterns of ventilatory function, ranging from dominant buccal pumpers to dominant branchiostegal pumpers (Hughes, 1960). This variation spans the continuum of known functional diversity in aquatically ventilating ray-finned fishes, and therefore it is difficult to link restricted gill openings to specific aspects of ventilatory function without further study. However, by considering the nature of the trait and the diversity of taxa in which it occurs, we can discuss potential functional implications. For example, there may be functional benefits for separating the left and right gill openings through an attachment to the isthmus. In fishes with "united and free from the isthmus" morphology, the unification of the left and right membranes results in the formation of a single gill opening from which water leaves the gill chambers. Separation of these two openings allows the gill openings to be positioned more variably on the head; in extreme cases, the gill openings can be positioned as small apertures on the dorsal surface of the head (e.g., Palefin Dragonet, *Synchiropus goodenbeani*, Callionymidae) or posterior to the pectoral girdle (e.g., American Angler, *Lophius americanus*, Lophiidae). This flexibility in gill opening positioning may be of great importance to fishes that

rely on frequent and sustained contact of the ventral surface of the body with a substrate, because a gill opening that is pointed ventrally is likely to disturb sediment.

Broad attachment to the isthmus is also generally associated with a reduction in the size or number of branchiostegal rays, possibly because the branchiostegal membrane is more anchored by tissue and may not need robust and numerous rays to support it (McAllister, 1968). Reduction of the branchiostegals may be beneficial where general skeletal reduction is adaptive, as in deep-sea habitats. Also, reduction of the branchiostegal apparatus is associated with a reduced reliance on the gill chamber suction pump during ventilation (Liem, 1970; Hughes, 1960). This reduction is observed in many pelagic fishes and does not require an attachment to the isthmus. However, if selection favors a reduced branchiostegal apparatus and a stronger reliance on buccal pumping, a broad attachment to the isthmus may provide stability for the gill chamber and the opercular valve.

Some fishes have coopted their restricted gill openings for the more obvious function of opercular jetting. Many frogfishes (Lophiiformes: Antennariidae) force water from the gill openings to jet forward, either for a fast burst of movement or cryptic locomotion (Fish, 1987; Pietsch and Grobecker, 1987). Porcupine fishes (Tetraodontiformes: Diodontidae) expel a high-velocity jet of water from their gill openings, in conjunction with rapid movement of their fins and trunk, as an escape mechanism (Breder, 1924). Banjo catfishes (Siluriformes: Aspredinidae) use their ventrally-positioned restricted gill openings to propel themselves along the benthos (Gradwell, 1971). However, this behavior has been observed in only a small subset of fishes with restricted gill openings, and it is likely a secondary advantage of this feature.

Lastly, the branchiostegal apparatus may be under fewer functional constraints relative to other components of the gill chamber, which are the opercular bones (opercle, subopercle, and

interopercle) and pectoral girdle. The opercular bones are linked closely with the lower jaw and often function in feeding mechanics (Liem, 1970; Westneat, 2005); for example, these bones have been demonstrated to be strongly evolutionarily integrated with feeding structures in suction-feeding eels (Collar et al., 2014). The pectoral girdle functions in both feeding and locomotion and presumably experiences strong evolutionary pressures related to feeding and locomotor performance. However, the branchiostegal apparatus has a weaker association with feeding and locomotion, and therefore it is likely the structure that is most directly influenced by selective pressures on ventilatory mechanics. Functional studies of variation in aquatic gill ventilatory systems in fishes will undoubtedly benefit from a closer examination of the branchiostegal apparatus.

While the direct effects of gill opening restriction on ventilatory biomechanics have yet to be determined (Brainerd and Ferry-Graham, 2006), the feature is associated with a large amount of morphological and ecological variation. It has evolved repeatedly throughout the evolutionary history of the ray-finned fishes, without a clear indication of its adaptive purpose. This relatively common modification of the gill chamber draws attention to the potentially critical influence of ventilatory morphology on the ecology, behavior, and evolutionary history of fishes.

Acknowledgments

This chapter was written in collaboration with William E. Bemis and Thomas Near. For access to specimens, we thank John P. Friel and Charles M. Dardia (CUMV), John Lundberg (ANSP), Karsten Hartel and Andrew Williston (MCZ), and Theodore W. Pietsch and Katherine Maslenikov (UW). For feedback on statistical analyses, we thank Collin B. Edwards, Nicholas A. Mason, Liam Revell, Peter C. Wainwright, and Francoise Vermeylen. For help with data

collection and entry, we thank Matthew T. Gibbons. For comments on the manuscript, we thank John P. Friel, Harry Greene, Amy McCune, Adam Summers, and two anonymous reviewers. We thank our funding sources, including an NSF Doctoral Dissertation Improvement Grant (DEB-1310812). No live animals were used in this research.

REFERENCES

Baerends GP, Baerends-Van Roon JM. 1950. An Introduction to the study of the ethology of the cichlid fishes. Behaviour Suppl 1(1950):1-243.

Baglioni S. 1907. Der Atmungsmechanismus der Fische. Ein Beitrag zur vergleichenden Physiologie des Atemrhythmus. Z Allg Physiol 7:177-282.

Betancur-R R, Broughton RE, Wiley EO, Carpenter K, López JA, Li C, Holcroft NI, Arcila D, Sanciangco M, Cureton JC, Zhang F, Buser T, Campbell MA, Ballesteros JA, Adela Roa-Varon A, Willis S, Borden WC, Rowley T, Reneau PC, Hough DJ, Lu G, Grande T, Arratia G, Ortí1 G. 2013. The tree of life and a new classification of bony fishes. PLOS Currents Tree of Life Edition 1.

Brainerd EL, Ferry-Graham LA. 2006. Mechanics of respiratory pumps. In: Shadwick RE, Lauder GV, editors. Fish biomechanics. Amsterdam: Elsevier, Inc. p 1-28.

Breder CM. 1924. Respiration as a factor in locomotion of fishes. Am Nat 58:145-155.

Broughton RE, Betancur-R R, Li C, Arratia G, Ortí G. 2013. Multi-locus phylogenetic analysis reveals the pattern and tempo of bony fish evolution. PLOS Currents Tree of Life Edition 1.

Burggren WW, Bemis WE. 1991. Metabolism and ram gill ventilation in juvenile paddlefish, *Polyodon spathula* (Chondrostei: Polyodontidae). Physiol Zool 65(3):515-539.

Cavallaro M, Mammola CL, Verdiglione R. 2004. Structural and ultrastructural comparison of photophores of two species of deep-sea fishes: *Argyropelecus hemigymnus* and *Maurolicus muelleri*. J Fish Biol 64(6):1552-1567.

Chapman WM. 1942. XXIV.—The Osteology and Relationship of the Bathypelagic Fish *Macropinna microstoma*, with Notes on its Visceral Anatomy. Ann Mag Nat Hist Series 11. 9(52): 272-304.

Chernova NV. 2014. New species of the genus *Careproctus* (Liparidae) from the Kara Sea with notes on spongiophilia, reproductive commensalism between fishes and sponges (Rossellidae). J Ichthyol 54(5):508-519.

Cohen DM. 1964. Suborder Argentinoidea. In: Fishes of the Western North Altantic. Sears Fdn Mar Res 1(4):1-70.

Collar DC, Wainwright PC, Alfaro ME, Revell LJ, Mehta RS. 2014. Biting disrupts integration to spur skull evolution in eels. Nat Commun 5:5505.

Davis MP, Holcroft NI, Wiley EO, Sparks JS, Smith WL. 2014. Species-specific bioluminescence facilitates speciation in the deep sea. Mar Biol 161(5):1139-1148.

Ditty JG, Shaw RF, Fuiman LA. 2005. Larval development of five species of blenny (Teleostei: Blenniidae) from the western central North Atlantic, with a synopsis of blennioid family characters. J Fish Biol 66(5):1261-1284.

Drummond AJ, Suchard MA, Xie D, Rambaut A. 2012. Bayesian Phylogenetics with BEAUti and the BEAST 1.7. Mol Biol Evol 29(8):1969-1973.

Elshoud GCA. 1986. Fish and chips: computer models and functional morphology of fishes (Doctoral Dissertation). Rijksuniversiteit, Leiden, Netherlands.

Fish FE. 1987. Kinematics and power output of jet propulsion by the frogfish genus *Antennarius* (Lophiiformes: Antennariidae). Copeia 1987(4):1046-1048.

Follett WI, Powell DC. 1988. *Ernogrammus walker*, a new species of prickleback (Pisces: Stichaeidae) from South-central California. Copeia 1988(1):135-152.

Froese R, Pauly D. Editors. 2011. FishBase. Electronic Publication. www.fishbase.org.

Gradwell N. 1971. Observations on jet propulsion in banjo catfishes. Can J Zool 49:1611-1612.

Graham JB. 1997. Air-breathing fishes. San Diego: Academic Press. 299p.

Graham JB. 2006. Aquatic and Aerial Respiration. In: Evans DH, Claiborne JB, editors. The Physiology of Fishes, third edition. Boca Raton: CRC Press, Taylor and Francis Group. p 85-117.

Hughes GM. 1960. A comparative study of gill ventilation in marine teleosts. J Exp Biol 37:28-45.

Hughes GM, Shelton G. 1958. The mechanism of gill ventilation in three freshwater teleosts. J Exp Biol 35(4):807-823.

Johnson GD. 1984. Percoidei: Development and relationships. In: Moser HG, Richards, WJ, Cohen DM, Fahay MP, Kendall AW, Richardson SL, editors. Ontogeny and Systematics of Fishes Special Publication. Lawrence: American Society of Ichthyologists and Herpetologists. p 464-498.

Knope ML. 2013. Phylogenetics of the marine sculpins (Teleostei: Cottidae) of the North American Pacific Coast. Mol Phylogenet Evol 66:341-349.

Kusaka T. 1974. The urohyal of fishes. Tokyo: University of Tokyo Press. 320p.

Lamb A, Edgell P. 2010. Coastal fishes of the Pacific Northwest, revised and expanded second edition. Madeira Park, BC: Harbour Publishing. 352p.

Lauder GV. 1990. Functional morphology and systematics: studying functional patterns in an historical context. Annu Rev Ecol Syst 21:317-340.

Lautredou AC, Motomura H, Gallut C, Ozouf-Costaz C, Cruaud C, Lecointre G, Dettai A. 2013. New nuclear markers and exploration of the relationships among Serraniformes

(Acanthomorpha, Teleostei): The importance of working at multiple scales. Mol Phylogenet Evol 67:140-155.

Liem KF. 1970. Comparative Functional Anatomy of the Nandidae (Pisces: Teleostei). Fieldiana 56:1-166.

Liem KF. 1973. Evolutionary strategies and morphological innovations: cichlid pharyngeal jaws. Syst Biol 22(4):425-441.

Liem KF. 1980. Air ventilation in advanced teleosts: Biomechanical and evolutionary aspects. In: Ali MA, editor. Environmental Physiology of Fishes, Volume 35. New York: Springer. p 57-91.

Maldonado-Ocampo JA, López-Fernández H, Taphorn DC, Bernard CR, Crampton WGR, Lovejoy NR. 2014. *Akawaio penak*, a new genus and species of Neotropical electric fish (Gymnotiformes, Hypopomidae) endemic to the upper Mazaruni River in the Guiana Shield. Zool Scripta 43(1):24-33.

McAllister DE. 1968. Evolution of branchiostegals and classification of teleostome fishes. Bull Natl Mus Canada 221:1-237.

Mehta R, Wainwright PC. 2008. Functional morphology of the pharyngeal jaw apparatus in moray eels. J Morphol 269(5):604-619.

Miller RR. 1945. A new cyprinid fish from southern Arizona, and Sonora, Mexico, with the description of a new subgenus of *Gila* and a review of related species. Copeia 1945(2):104-110.

Monod T. 1968. Le complexe urophore des poissons téléostéens. Dakar: IFAN. 709p.

Near TJ, Dornburg A, Eytan RI, Keck BP, Smith WL, Kuhn KL, Moore JA, Price SA, Burbrink FT, Friedman M, Wainwright PC. 2013. Phylogeny and tempo of diversification in the superradiation of spiny-rayed fishes. Proc Natl Acad Sci USA 110(31):12738-12743.

Near TJ, Eytan RI, Dornburg A, Kuhn KL, Moore JA, Davis MP, Wainwright PC, Friedman M, Smith WL. 2012. Resolution of ray-finned fish phylogeny and timing of diversification. Proc Natl Acad Sci USA 109:13698-13703.

Nelson GJ. 1966. Gill arches of teleostean fishes of the order Anguilliformes. Pac Sci 20(4): 391-408.

Nelson JS. 2006. Fishes of the World, 4th Edition. New York: John Wiley & Sons. 601p.

Pietsch TW, Grobecker DB. 1987. Frogfishes of the World. Stanford: Stanford University Press. xxii + 420p.

Poss SG, Johnson GD. 1991. *Matsubarichthys inusitatus*, a new genus and species of velvetfish (Scorpaeniformes: Aploactinidae) from the Great Barrier Reef. Proc Biol Soc Wash 104(3):468-473.

R Core Team. 2013. R: A language and environment for statistical computing. R Foundation for Statistical Computing, Vienna, Austria. http://www.R-project.org/.

Ragland HC, Fischer EA. 1987. Internal fertilization and male parental care in the scalyhead sculpins, *Artedius harringtoni*. Copeia 1987(4):1059-1062.

Revell LJ. 2012. phytools: an R package for phylogenetic comparative biology (and other things). Methods Ecol Evol 3(2):217–223.

Semler DE. 1971. Some aspects of adaptation in a polymorphism for breeding colours in the threespine stickleback (*Gasterosteus aculeatus*). J Zool, Lond 165:291-302.

Smith WL, Busby MS. 2014. Phylogeny and taxonomy of sculpins, sandfishes, and snailfishes (Perciformes: Cottoidei) with comments on the phylogenetic significance of their early-life-history specializations. Mol Phylogenet Evol 79:332-352.

Stewart TA, Smith WL, Coates MI. 2014. The origins of adipose fins: an analysis of homoplasy and the serial homology of vertebrate appendages. Proc R Soc B 281: 20133120.

Stiassny MLJ, Wiley EO, Johnson GD, de Carvalho MR. 2004. Gnathostome fishes. In: Cracraft J, Donoghue MJ, editors. Assembling the tree of life. Oxford, UK: Oxford University Press. p 410-429.

Strum JM. 1969. Fine structure of the dermal luminescent organs, photophores, in the fish, *Porichthys notatus*. Anat Rec 164(4):433-461.

Sullivan JP, Lundberg JG, Hardman M. 2006. A phylogenetic analysis of the major groups of catfishes (Teleostei: Siluriformes) using rag1 and rag2 nuclear gene sequences. Mol Phylogenet Evol 41(3):636-662.

Van Wassenbergh S, Strother JA, Flammang BE, Ferry-Graham LA, Aerts P. 2008. Extremely fast prey capture in pipefish is powered by elastic recoil. J R Soc Interface 5(20):285-296.

Wainwright PC, Turingan RG, Brainerd EL. 1995. Functional morphology of pufferfish inflation: mechanism of the buccal pump. Copeia 1995(3):614-625.

Ward AB, Brainerd EL. 2007. Evolution of axial patterning in elongate fishes. Biol J Linn Soc 90:97-116.

Westneat MW. 2005. Feeding mechanics of teleost fishes (Labridae; Perciformes): A test of four-bar linkage models. J Morphol 205(3):269-295.

Winterbottom R. 1974. A descriptive synonymy of the striated muscles of the Teleostei. Proc Acad Nat Sci Philadelphia 125(12):225-317.

Yang Z, Kumar S, Nei M. 1995. A new method of inference of ancestral nucleotide and amino acid sequences. Genetics 141:1641-1650.

CHAPTER 2

FUNCTIONAL MORPHOLOGY OF THE GILL VENTILATION SYSTEM OF THE GOOSEFISH, *LOPHIUS AMERICANUS* (LOPHIIFORMES: LOPHIIDAE)

Abstract

The Goosefish, *Lophius americanus*, is a dorso-ventrally compressed marine fish that spends most of its life sitting on the substrate waiting to ambush prey. Fishes in the genus *Lophius* have some of the slowest ventilatory cycles recorded in fishes, with a typical cycle lasting more than 90 seconds. They have long branchiostegal rays and a siphon-like gill opening positioned underneath and behind the base of the pectoral fin, creating a large gill chamber that fills during inspiration. Our goals were to characterize the kinematics of gill ventilation in *L. americanus* relative to those of more typical ray-finned fishes, address previous assertions about ventilation in this genus, and describe the anatomy of the gill opening. We found that the duration of Phase 1 of ventilation (during which both the buccal and gill chamber are expanding) is greatly increased relative to that of typical fishes, and during this phase, the branchiostegals are slowly expanding. This slow expansion is almost visually imperceptible, especially from a dorsal view. Despite this unusually long Phase 1, the general pattern of skeletal movements follows that of a typical actinopterygian fish, refuting previous assertions that *Lophius* does not use its jaws, suspensorium, and operculum during ventilation. When fishes were disturbed from their cryptic sand recesses, they tended to breathe more rapidly (termed "rapid ventilation") by decreasing the length of Phase 1. Dissections of the gill opening revealed a previously undocumented dorsal extension of the adductor hyohyoideus muscle, which passes from between

the branchiostegal rays, through the ventro-medial wall of the gill opening, and to the dorsal midline of the body. This morphology of the adductor hyohyoideus shares similarities with that of many Tetraodontiformes, and therefore, we suggest that it may be a synapomorphy for Lophiiformes + Tetraodontiformes. The specialized anatomy and function of the gill chamber of *Lophius* represents an extreme modification that provides insight into the potential and the limits of the actinopterygian gill ventilatory system.

Introduction

Pumping water over the gills is energetically expensive for ray-finned fishes (Actinopterygii), comprising 5-15% of the total metabolic budget (Cameron and Cech, 1970; Edwards, 1971; Farrell and Steffensen, 1987). Fishes have evolved many adaptations for increased efficiency of respiration, including maximizing surface area of the gill tissue, minimizing diffusion distance across the gill epithelium, and maximizing the oxygen partial pressure gradient (Hughes, 1966). The latter is achieved through a system of counter-current exchange in which blood in vessels of the gill lamellae flows in the opposite direction of oxygenated water (Hughes and Shelton, 1958). Establishing this unidirectional flow of water over the gills requires coordination of many cranial components. Given the diversity in cranial morphology and metabolic requirements among ray-finned fishes, we can expect to find a great variety of strategies for efficient pumping. However, functional variation in aquatic ventilatory pumps has received little attention.

Gill ventilation in most species of ray-finned fishes relies on changes in pressure driven by pumps in two chambers: the mouth (buccal chamber) and gill chamber. As shown in Figure 1, these pumps alternate between suction (expansion to create negative pressure, drawing in water) and pressure (compression to create positive pressure, forcing out water; Hughes and Shelton,

1958; Hughes, 1960; Brainerd and Ferry-Graham, 2006). A ventilatory cycle begins with expansion of the buccal chamber, which draws water into the mouth (Phase 1, Fig. 1). In Phase 2, the gill chamber is expanded, which draws water from the mouth over the gills. In Phase 3, the buccal chamber is compressed to force water from the mouth over the gills. Finally, in Phase 4, compression of the gill chamber forces water out of the gill opening. The gill tissues introduce resistance between the two chambers, limiting backflow during the transition from pressure back to suction. Changes in buccal chamber pressure are driven by movements of the jaw, suspensorium, and hyoid apparatus, and changes in gill chamber pressure are driven by the opercular series (opercle, subopercle, and interopercle) and the branchiostegal apparatus (Liem, 1970). The relative timing of these movements and the resulting pressure changes vary considerably among taxa (Hughes, 1960), and there is substantial variation in the skeletal elements and musculature involved, particularly in the branchiostegal apparatus (McAllister, 1968). There is also significant morphological variation in the external openings of the buccal and gill chambers; for example, gill openings can be very large with a wide valve, or they can be restricted to a tiny aperture variably positioned on the head (McAllister, 1968; Farina et al., 2015).

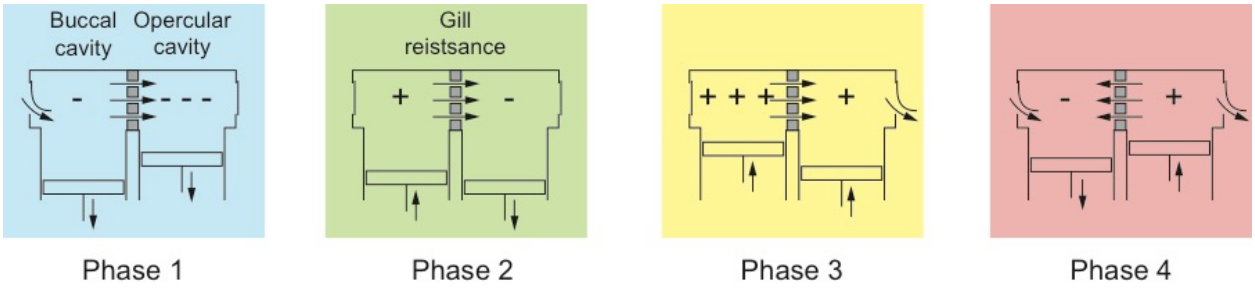

Figure 1. Four phases of gill ventilation used by Actinopterygians. During Phase 1, both the buccal and gill chambers are expanding to produce negative pressure and take in water. During Phase 2, the buccal chamber begins to compress. During Phase 3, both chambers compress to produce positive pressure and force water out of the gill opening. During Phase 4, the buccal chamber begins to expand, transitioning back to negative pressure to draw in water. Based on Brainerd and Ferry-Graham (2006), Summers and Ferry-Graham (2002), and Hughes (1960).

The Goosefish, *Lophius americanus*, is a commercially important marine fish common in waters off the northeastern coast of North America at depths ranging from subtidal to over 900 meters (Bigelow and Schroeder, 1953; Caruso, 2002; Richards et al., 2008). It is dorso-ventrally flattened, and its head is large for its body size (Fig. 2). As in other anglerfishes (Lophiiformes) such as frogfishes, batfishes, and seadevils, it has elongate dorsal spines that have migrated to the front of the skull and support a fleshy lure known as an esca. Members of the genus *Lophius* differ primarily in pectoral fin ray counts, shape of the esca, and dorsal spine length (Caruso, 1983). All are ambush predators that spend most of their adult life sitting on sandy, muddy, or rocky substrates, using their lure to attract fishes and other prey (Chadwick, 1929; Wilson, 1937; Gudger, 1945). When suction feeding, they rapidly expand the buccal cavity by means of hyoid and jaw depression combined with a large degree of cranial elevation (Elshoud, 1986). When not feeding, they remain cryptic by matching skin colors to the substrate and using the pectoral fins to create recesses in the sediment (Wilson, 1937; Laurenson, 2004).

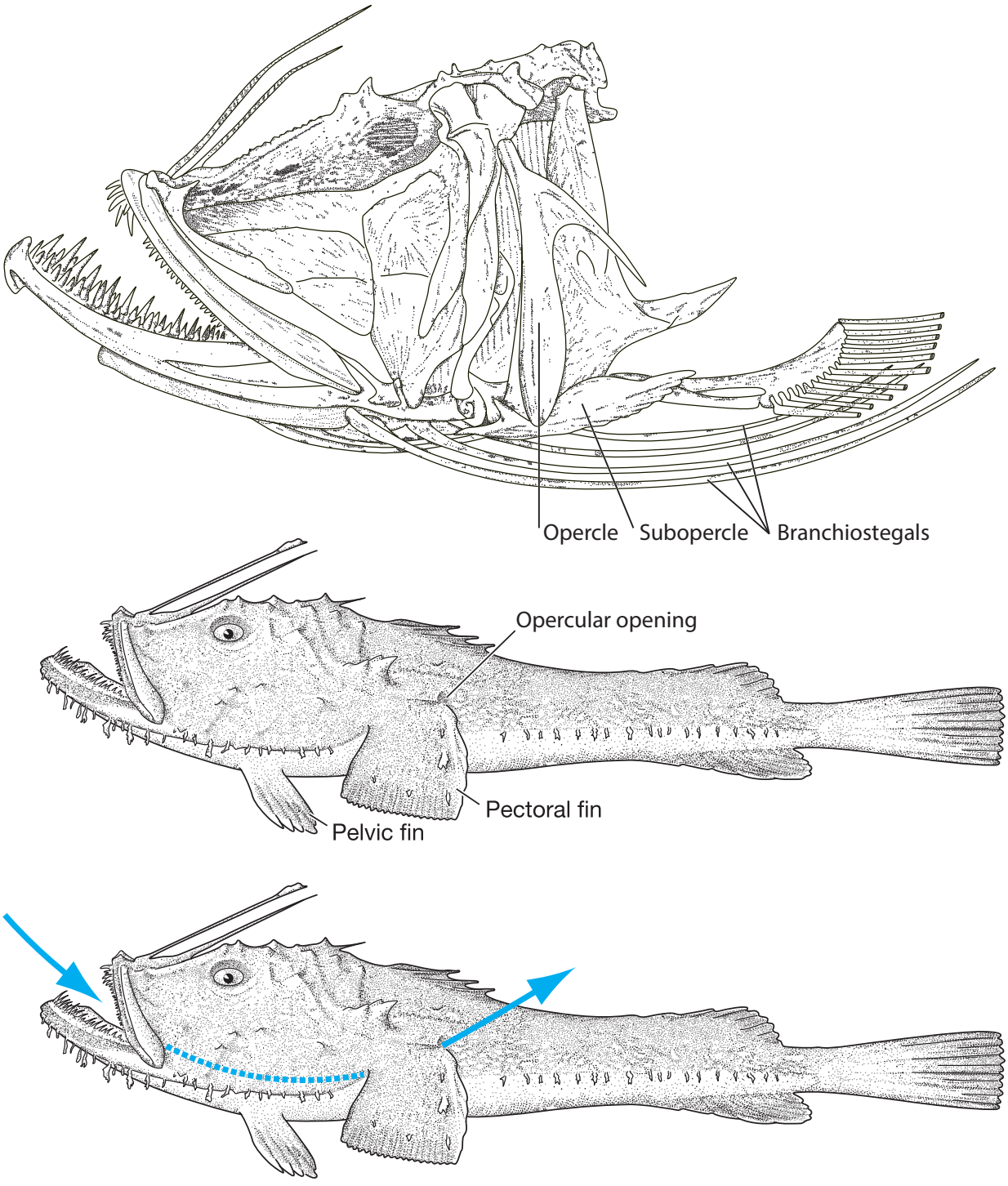

Figure 2. Cranial skeletal and external anatomy of *Lophius*. The large gill chamber consists of an L-shaped operculum and elongated branchiostegal rays that pass under the pectoral girdle (A). The gill opening is located in the axillary region, posterior and ventral to the pectoral fins (B). Water comes in through the mouth and passes over the gills to enter the large gill chamber. It then passes under the pectoral fin and out the gill opening.

While at rest, species of *Lophius* have exceptionally slow ventilation, taking approximately 60 – 180 seconds to complete a single ventilatory cycle (Wilson, 1937). Most other species of ray-finned fishes take between 0.5 – 6 seconds to complete a ventilatory cycle (Hughes, 1960). We term this "slow ventilation" and consider that it is likely related to low metabolic demands, which is evident from their low total gill lamellae surface area relative to body weight (Hughes, 1966), and a need to remain cryptic as intermittent and opportunistic feeders (Armstrong et al., 1996; Laurenson and Priede, 2005; Fariña et al., 2008; Valentim et al., 2008). They increase their ventilatory rate considerably immediately after feeding events (Wilson, 1937) or when they are disturbed from their sediment recesses, and we term this "rapid ventilation." Their ventilatory anatomy consists of a large buccal cavity with a pronounced oral valve, an L-shaped operculum, six elongate branchiostegal rays, and a gill opening ventral and posterior to the pectoral fin (Fig. 2). As in other Lophiiformes, the gill opening is relatively small and siphon-like, forming a tube upon exhalation. The long branchiostegal rays and posterior position of the gill opening create a much larger gill chamber than is typical for actinopterygians.

With its exceptionally slow ventilation and enormous gill chamber, *Lophius americanus* represents an extreme of fish ventilatory anatomy and function. It is therefore an important species to investigate when considering limits of the gill ventilation system of ray-finned fishes. Our first goal is to characterize the kinematics of gill ventilation in *L. americanus* and make comparisons to those of more typical ray-finned fishes. We also address some previous assertions and predictions about ventilation in *Lophius*. Our second goal is to describe the anatomy of the gill chamber, specifically the musculature of the gill opening, and discuss our findings in the context of gill ventilatory function and evolution.

Methods

Animals and videography

From June to August 2011, we made observations and video recordings of gill ventilation in five specimens of *Lophius americanus* collected in the Gulf of Maine, ranging in size from 40 to 55 cm TL. Four individuals obtained by bottom trawl were transported to Shoals Marine Laboratory (SML) and studied for one to three weeks in flow-through seawater tanks. Detailed observations and videography at SML commenced after fish were allowed to acclimate to tanks for at least three days. A fifth individual was studied in its exhibit at the Seacoast Science Center (SSC) in Rye, NH. Animal care and use followed protocols approved by Cornell University's Institutional Animal Care and Use Committee (IACUC protocol #2011-0028).

We recorded high definition video at 30 frames per second using a Canon 5D Mark II camera equipped with a 24-70mm lens. For two individuals housed at SML, we recorded both slow and rapid ventilation. To study "slow ventilation," we minimized any disturbances or human activity in the tank room for at least one hour prior to videography, and only recorded individuals when they were sitting undisturbed in a sand recess. If a fish became alarmed by the presence of a researcher, it would leave its sand recess and swim around the tank. When it ceased swimming and rested above the sand, it would ventilate much more rapidly until it returned to its sand recess or created a new one. We termed this "rapid ventilation" and recorded and analyzed it separately (Table 1). The two additional individuals housed at SML did not create sand recesses and only exhibited rapid ventilation during our week of observation. The individual at the SSC had been on exhibit for two months and had been in its sand recess for more than one hour prior to our videography of slow ventilation. It remained in its recess throughout filming, so we were unable to record its rapid ventilation.

Table 1. Relative timing of each phase of gill ventilation in each individual recorded.

	Mean ventilation rate (Hz)	Phase 1 (s)	Phase 2 (s)	Phase 3 (s)	Phase 4 (s)
L. americanus 1 (Slow)	0.013	74.05 (6.19)	0.14 (0.03)	2.79 (0.09)	0.51 (0.08)
L. americanus 1 (Rapid)	0.037	24.88 (1.87)	0.16 (0.06)	1.77 (0.09)	0.39 (0.03)
L. americanus 2 (Slow)	0.014	70.36 (2.93)	0.13 (0.05)	2.03 (0.33)	0.91 (0.16)
L. americanus 2 (Rapid)	0.041	20.86 (0.70)	0.21 (0.02)	1.8 (0.23)	1.45 (0.34)
L. americanus 3 (Slow)	0.008	120.04 (24.28)	0.69 (0.13)	2.41 (0.12)	0.41 (0.08)

Kinematic analyses

We analyzed ventilatory cycles using ImageJ to record the timing of each phase of ventilation through a visual frame-by-frame inspection. Following the scheme shown in Figure 1, we used the following movements to denote the start of each of the four phases: Phase 1 started with branchiostegal abduction, Phase 2 started with mouth closing, Phase 3 started with the opening of the gill opening, and Phase 4 started with mouth opening. The start of Phase 1 was impossible to observe in fishes buried in a sand recess because the branchiostegals were not visible. In these cases, we used the abduction of the opercle (which occurs slightly later) as the start of Phase 1, which may introduce small errors into our estimates of the lengths of Phases 1 and 4. Using a digitizing tool developed for MatLab (Hedrick, 2008), we tracked two-dimensional movements of points on the head throughout a typical rapid ventilatory cycle to demonstrate kinematic patterns seen during ventilation (because much of the fish is obscured when it is buried in a sand recess and breathing cryptically, we only digitized a rapid ventilatory cycle). As markers, we used spots of pigmentation that contrasted with the rest of the skin color to track the lower jaw, the opercle, the suspensorium, and the eye. The eye was used as a fixed

point on the head so that jaw, opercle, and suspensorial movements could be corrected for head movements. We used the location of the eye relative to the substrate to track cranial elevation during ventilation by measuring vertical displacement on each frame of a video recorded from a lateral view of the fish (Fig. 3). Additionally, we visualized flow out of the gill opening by introducing food dye mixed with seawater into the mouth of an individual and allowing the fish to expel the colored water; we analyzed the jet of water by using ImageJ to track the speed.

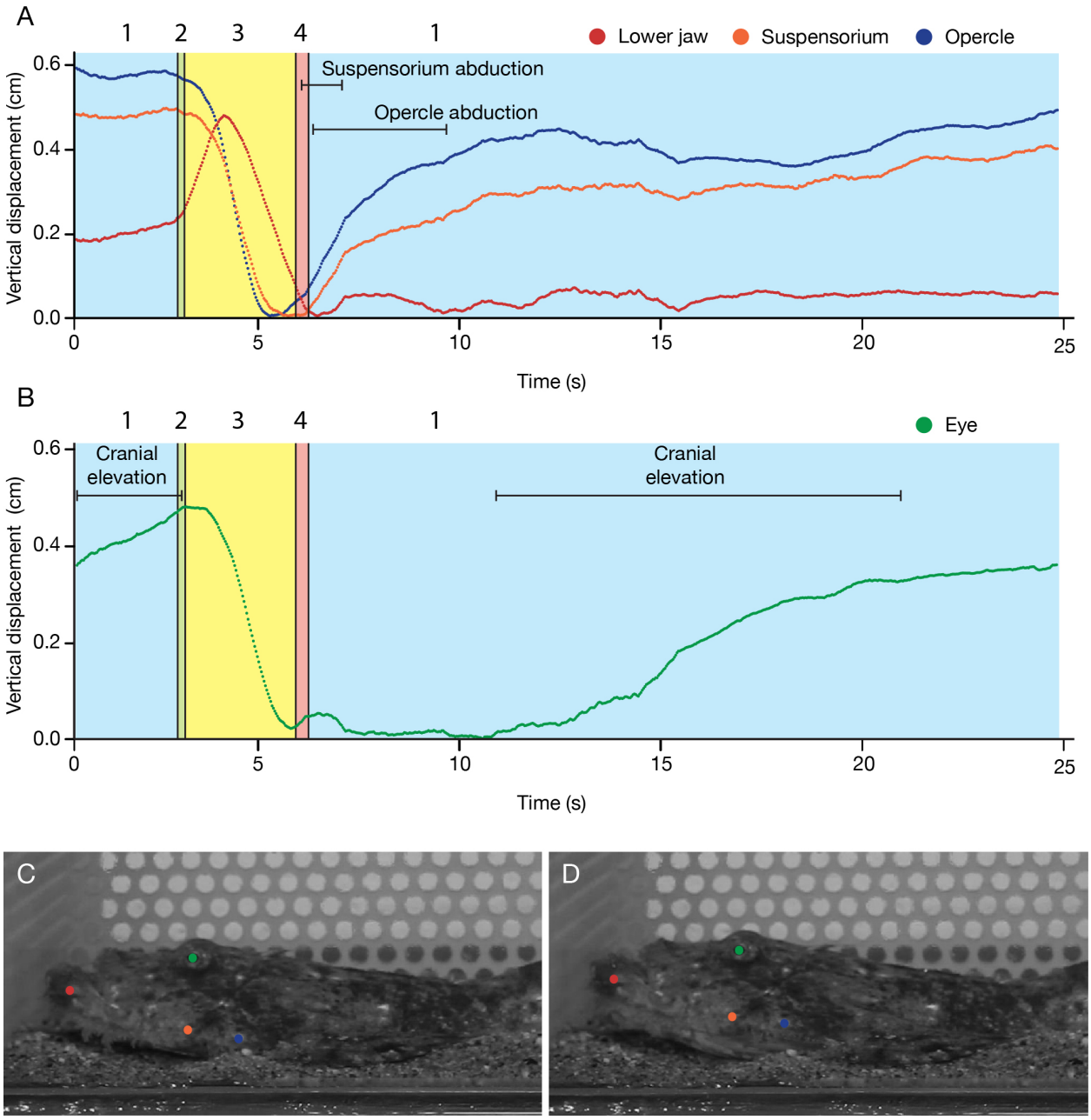

Figure 3. An example ventilatory cycle of *Lophius americanus*. Digitized vertical movements of the jaw, suspensorium, operculum, and eye show that *L. americanus* pumps water throughout the ventilatory cycle. The position of the eye was subtracted from each of the vertical movements of the jaws, suspensorium, and operculum to show movement independent of head position (A). Eye movement is plotted separately (B) to demonstrate when cranial elevation occurs. Stills from the analyzed video show the position of the fish at the start of Phase 1 (C) and at the start of Phase 3 (D), with colored markers indicating locations of points tracked for kinematic plots shown parts A and B.

Anatomy of the gill chamber

We dissected eight specimens of *L. americanus* collected by the Northeast Fisheries Science Center (NEFSC) in Woods Hole, MA, on annual bottom trawl surveys between 2008 and 2012. Muscles of the gill chamber were exposed by careful removal of the loose skin covering the branchiostegals and trunk. Dissections of three specimens were photographed using a Canon 5D Mark II camera equipped with a 24-70mm lens. We removed the entire branchiostegal apparatus of a particularly large specimen (30 kg, 1.3 meters total length) and photographed it on a light table. We also removed a square of tissue from the dorsal extension of the adductor hyohyoideus (*hyohyoidei adductores*; Winterbottom, 1973) muscle and examined it using an Olympus SZX12 Stereozoom microscope. Additionally, we dissected the gill opening region of two other Lophiiformes: *Histrio histrio* (CUMV 79429) and *Chaunax pictus* (CUMV 43866).

Results

The average length of a ventilatory cycle of the *Lophius americanus* in our study was 91.5 seconds (SE ± 9.9 seconds; n = 3), or approximately 0.011 cycles per second, during slow ventilation. The longest ventilatory cycle analyzed for this study is from the individual at the SSC, which lasted 210.5 seconds. Phase 1 was the longest phase of ventilation, and it varied considerably among individuals (Table 1) and with factors such as time of day and time spent in its sand recess. The shortest phase was Phase 2 (the transition from suction to pressure). When the fish were out of the sand, rapid ventilation occurred primarily through the reduction of Phase 1. Phase 3 was also shorter during rapid ventilation, but Phases 2 and 4 remained approximately the same length in both slow and rapid ventilation. The duration of Phase 2 was consistently very short (Table 1), regardless of the individual or the conditions.

Movements occur throughout the ventilatory cycle (Fig. 3). Phase 1 began with a slow abduction of both the opercle and the branchiostegals, with residual movements of the jaw and suspensorium that started in Phase 4. Approximately three seconds after the start of Phase 1, the operculum reached maximum abduction (Figure 3). However, the branchiostegals continued to expand throughout Phase 1. The fish slowly elevated its head using its pectoral and pelvic fins throughout this phase to accommodate the extreme expansion of the branchiostegal apparatus (Fig. 3). The oral valve remained open for most of this phase, although it would occasionally partially close. Phase 2 began with raising the lower jaw and hyoid apparatus, followed shortly thereafter by the start of suspensorial adduction, which compressed the buccal chamber. Phase 3 began almost immediately after the start of Phase 2, and it was signaled by the opening of the valve of the gill chamber and adduction of the operculum and branchiostegals. Phase 4 began with depression of the lower jaw and hyoid while the gill chamber valve was still open and while adduction of the operculum and branchiostegals was still occurring. Phase 4 was very short relative to the total ventilatory cycle.

In dorsal view, ventilatory movements were almost imperceptible (Fig. 4), except during exhalation, when the gill opening could be seen from above as a siphon-like aperture (Fig. 4F). During such exhalations (Phases 3 and 4), water was ejected out the gill opening in a large dorsally-directed jet (Fig. 5), which traveled upward at a speed of approximately 0.1 m/s (0.21 body lengths per second). The position of the pectoral fins relative to the substrate influences water flow out of the gill opening; when an individual is sitting in its sand recess, the pectoral fins are extended laterally, holding the opening in its typical siphon shape (Fig. 6A). However, when the fish is above the substrate or housed on a glass substrate, it uses its pectoral fins to prop itself up, producing a flap-like gill opening shape (Fig. 6B).

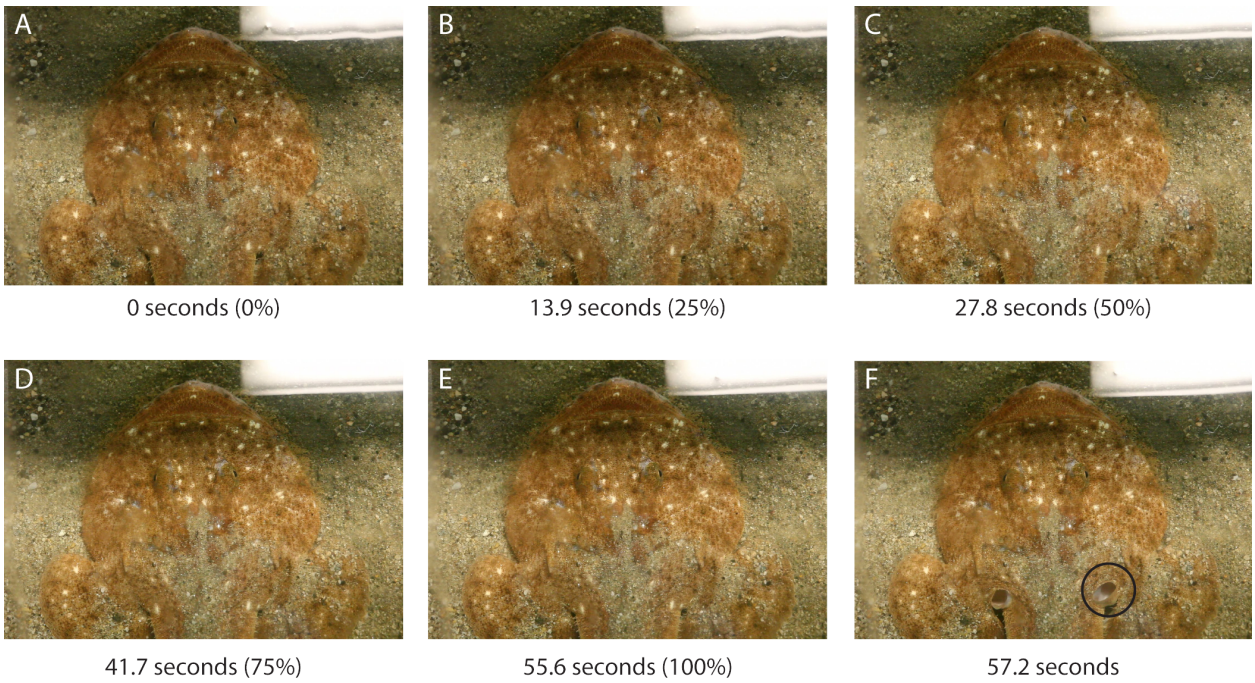

Figure 4. Dorsal view of *Lophius americanus* during slow ventilation. Parts A-E show Phase 1 at 0% (A), 25% (B), 50% (C), 75% (D), and 100% (E) of the phase. From a dorsal perspective, motion of *L. americanus* is almost imperceptible, except during exhalation (F).

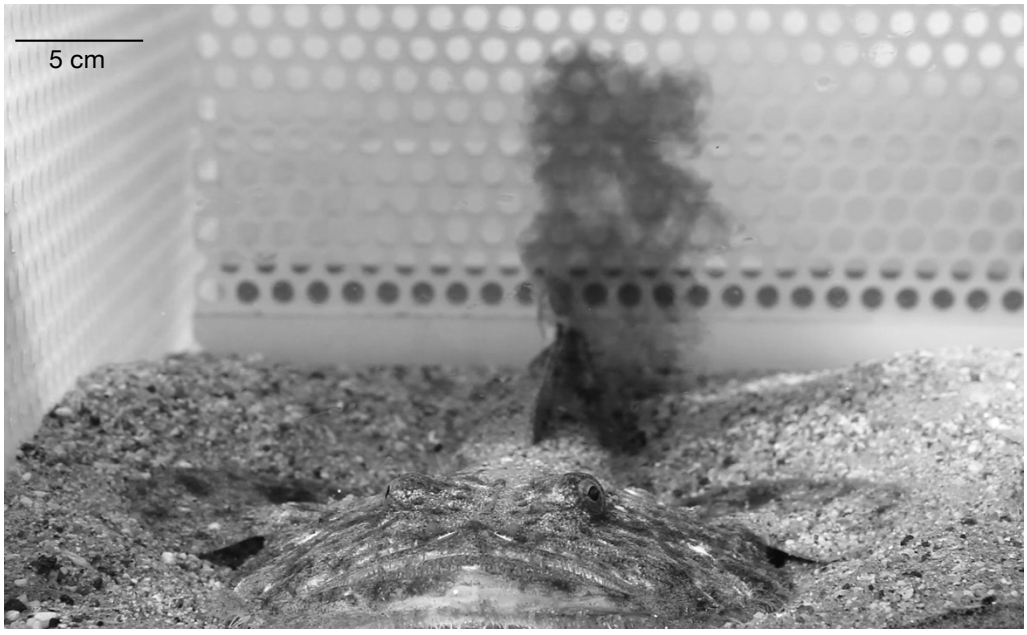

Figure 5. Visualization of flow from the gill openings during exhalation. The ventilatory current leaving the gill opening is forced upward, as shown by water seeded with dye expelled from the opening. The resulting jet traveled upward at approximately 0.1 m/s.

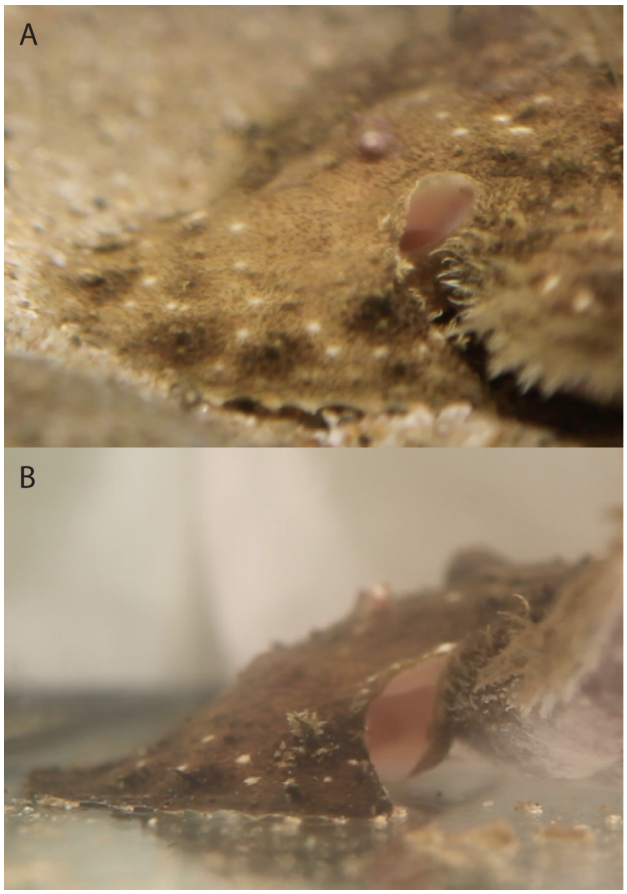

Figure 6. The role of fin positioning in gill opening aperture shape. Posterior views of the gill opening during Phase 3 show that the positioning of the fins is impacted by the substrate and changes the shape of the gill opening. When the fish is in its sand recess (A), its pectoral fins extend laterally from the body, and the gill opening forms a vertically directed siphon-like shape. When the same individual is removed from the substrate (B), the pectoral fins are extend laterally and ventrally, causing the gill opening to have a flap-like shape directed posteriorly.

The gill opening sits ventrally and posteriorly to the pectoral fin base (Fig. 7A) and is formed by several tissues, including muscles, fascia, and two large masses of connective tissue (Figs. 7 and 8; CT). The thick connective tissue masses provide a lining for the occluding parts of the valve, which consists of a dorsal and ventral lip. The dorsal lip of the valve sits between the pectoral fin and the body and is supported by one of the connective tissue masses (Fig. 7; CT1). The ventral lip begins at the anterior base of the pectoral fin and ends at the posterior

margin of the dorsal lip, where it is supported by a second connective tissue mass (Fig. 7; CT2). The tips of branchiostegals 3-5 sit in the gill opening, actuating the ventral half of the gill opening. In dissections of the gill openings, we observed that the adductor hyohyoideus extends posteriorly from between each branchiostegal to surround the medial and ventral walls of the gill opening. There is also a large dorsal extension of this muscle. We followed these dorsally-extending muscle fibers from their origin between branchiostegals 2-5, where they form a cross-hatching pattern with the muscle fibers that transversely join neighboring branchiostegals (Figs. 8C and 8D). These muscle pass by the medial surface of the gill opening, pass over one of the connective tissue masses and continue dorsally up the side of the body. A narrow band of this extension of the adductor hyohyoideus muscle sits just lateral to the trunk and abdominal muscles in a thin sheet of fascia (Figs. 7 and 8B). The left and right extensions meet at the dorsal midline of the trunk, just posterior to the dorsal fin spines. We examined the tissue of this narrow band using microscopy and found it consists of muscle fibers. We also noted similar expansions of the adductor hyohyoideus muscles of *Chaunax pictus* and *Histrio histrio*.

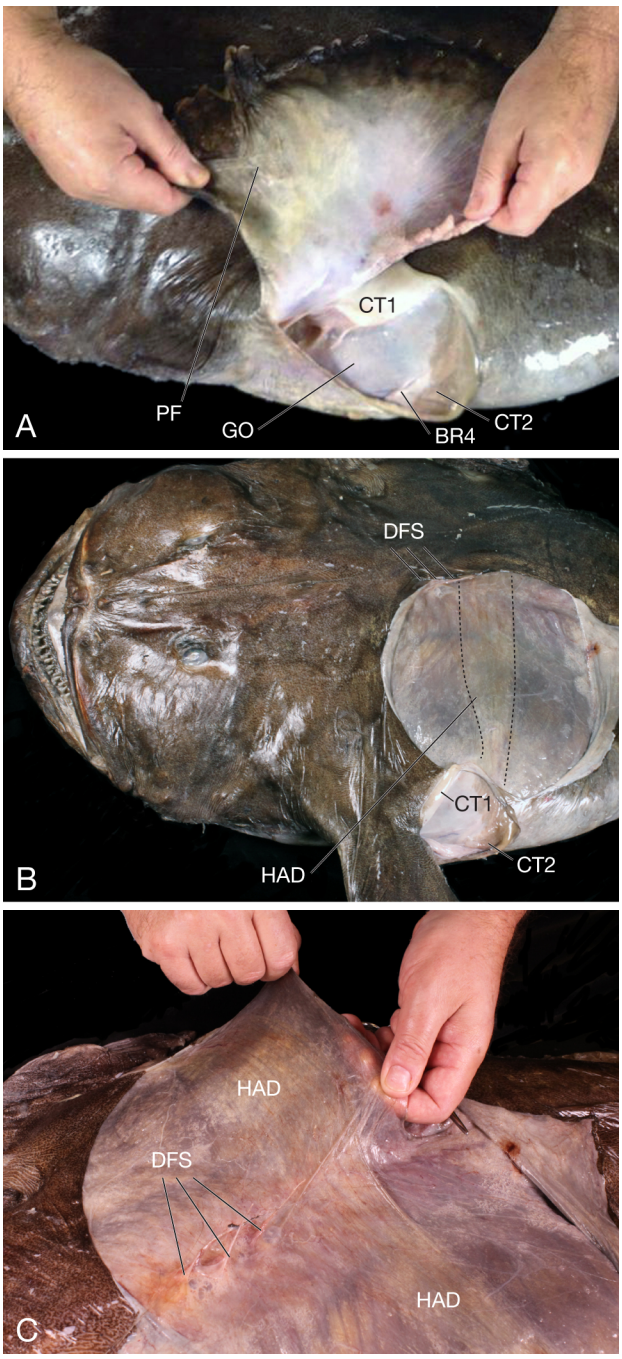

Figure 7. Position of the gill opening and associated musculature. The gill opening is positioned ventrally and posteriorly to the pectoral fin, and two connective tissue masses that we term lips form the occluding margins of the opening (A). When the skin is removed from the dorsal surface of the trunk, a dorsal extension of the adductor hyohyoideus is visible as a thin band of muscle embedded in the fascia of the trunk (B). This adductor hyohyoideus extends dorsally from the gill openings to meet its antimere at the dorsal midline behind the dorsal spines (C). Abbreviations: BR = branchiostegal ray, CT = connective tissue mass, DFS = dorsal fin spines, GO = gill opening, HAD = adductor hyohyoideus.

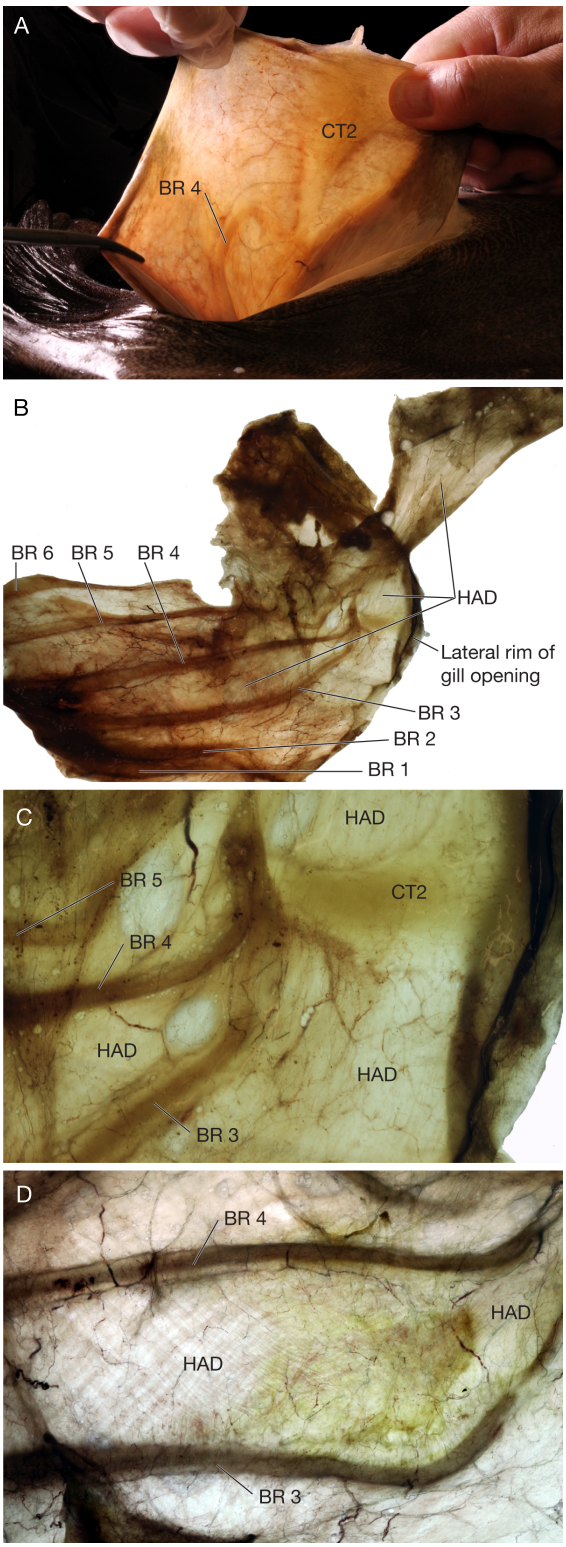

Figure 8. Anatomy of the gill opening. The ventral wall of the gill opening is supported by a branchiostegal and a connective tissue mass (A). We removed the gill chamber (branchiostegal rays and gill opening) from the fish and placed it on a light table. The gill opening is lined with

adductor hyohyoideus muscle (B), which extends across the second connective tissue mass before extending dorsally up the body (C). The adductor hyohyoideus stretches transversely (anteriorly) or obliquely (posteriorly) between the branchiostegal rays until the tips of the rays, at which point the muscle fibers form a cross-hatching pattern as they meet and continue posteriorly beyond the branchiostegals. Abbreviations: BR = branchiostegal ray, CT = connective tissue mass, HAD = adductor hyohyoideus.

Discussion

Lophius americanus has an extremely slow ventilatory cycle, which exceeds the duration of typical actinopterygian ventilation by at least 30 times. This is accomplished with a long Phase 1 (Fig. 1), and so the majority of the cycle consists of inspiration with a short period of exhalation (Fig. 3). A large gill chamber allows *Lophius* to take in a large volume of water over the course of Phase 1, and their siphon-like gill opening allows them to eject this water without much disturbance to sediments around them (Fig. 5). Phase 3 is also much longer than that of a typical actinopterygian, but this is likely due to the large volume of water that must be expelled as the fish exhale. While the operculum in most fishes contributes substantially to the expansion of the gill chamber, in the case of *L. americanus*, the operculum only abducts for approximately 3 s at the beginning of Phase 1 (Fig. 3). However, the branchiostegal rays expand throughout Phase 1, and for most of the ventilatory cycle, they are the only structures involved in driving the ventilatory current. Even after the operculum reaches maximum abduction, the branchiostegals continue to expand, drawing water from the mouth over the gills. The oral valve also stays open for Phase 1, allowing water to enter the mouth. Continual expansion of the gill chamber by the branchiostegals combined with a continuously open oral valve is strong evidence that *L. americanus* maintains a constant flow of water over the gills despite its slow pumping.

Although this extremely slow expansion of the branchiostegals represents a major deviation from typical actinopterygian ventilation, the rest of the ventilatory movements follow

the same general pattern as other actinopterygians, with all of the same phases of buccal and gill chamber expansion and compression occurring (Hughes and Shelton, 1958; Hughes, 1960) and the same skeletal structures actuating the chambers. In a dissertation on the feeding of *Lophius piscatorius*, Elshoud (1986) referred to the enlarged gill chamber as a "ventro-caudally situated muscular respiratory sack" and suggested that this "sack" operates independently of feeding-associated structures (jaws and suspensorium) during gill ventilation. He went so far as to state: "*Lophius* has invented a new respiratory system." He proposed that *Lophius* reduces or eliminates abduction of the suspensorium during ventilation because such abduction would produce cranial elevation that would lift the fish from the sediment and compromise its concealment. Likewise, in a separate study of feeding anatomy, Field (1966) noted the relatively small muscles actuating the suspensorium and operculum of *Lophius* and inferred that they were "fixation muscles" with no role in ventilation. However, we observed suspensorial adduction during Phases 2 and 3 and suspensorial abduction during Phase 4 and at the beginning of Phase 1 (Fig. 3A). We also observed opercular adduction during Phases 3 and 4 and abduction at the beginning of Phase 1 (Fig. 3A). There was also substantial elevation of the head during Phase 1 (Fig. 3B). When the fish were in their sand recesses, it was impossible to quantify their movements because much of the head was obscured and the fish was not optimally positioned for videography. Therefore, we were unable to directly quantify these movements for slow ventilatory cycles, and it is possible though unlikely that these movements are reduced considerably during slow ventilation. However, visual inspection of videos of cycles up to 210 seconds show movements of the jaws, suspensorium, and operculum that appear to be very similar to those exhibited in our example sequence (Fig. 3). While Field (1966) and Elshoud (1986) were correct about the importance of the branchiostegal apparatus, the ventilatory

movements of *Lophius* are more similar to those of a typical ray-finned fish than these authors suggested.

The slow ventilation of *Lophius* is possibly an adaptation for crypsis. Lophiiformes generally have many adaptations for their cryptic feeding strategy, which involves ambushing prey that is attracted to the deceptive lure on their dorsal spine. *Lophius* species in particular are highly cryptic, and their slow ventilatory movements during Phase 1 are likely visually imperceptible to predators and prey, especially in dorsal view (Figure 4 A-E). Exhalation is much more obvious, but it is infrequent because the long inspiration time allows them to draw water continuously over the gills without the need for a rapid ventilation rate. This strategy is almost certainly impossible in fishes with a higher basal metabolic rate because the low rate of water passing over the gills would not provide enough oxygen to support an active fish. *Lophius* has been noted for having a much smaller total gill surface area relative to body weight (Hughes, 1966), which indicates that its metabolic demands are low and its ventilatory mechanism does not bring a large amount of oxygenated water across the tissues.

The gill openings of *Lophius* are positioned in the axillary region behind and underneath the pectoral fin (Fig. 7A), which is an atypical position for the gill opening of a ray-finned fish. Typical gill openings are positioned immediately behind the opercular bones, and thus often are called "opercular openings." The unusual L-shaped opercle and subopercle of *Lophius* (Fig. 2A) are far away from the actual gill opening. Instead, there is a close association between the pectoral fin and the gill opening, and the shape of the gill opening changes based on the position of the pectoral fins. When the fish is in its sand recess (Fig. 6A), its pectoral fins extend from the body laterally, resting on the edge of the recess, and the gill opening has a siphon-like shape. However, when the same individual is moved to a tank without substrate (Fig. 6B), its pectoral

fins extend laterally and ventrally to support the body by fanning out along the bottom, and the gill opening has a flap-like shape. The siphon-like shape allows the fish to exhale in a dorsally-directed jet (Fig. 5A; Wilson, 1937) which does not disturb the sediment, and it pushes the fish down further into its recess, increasing its concealment. While fishes were acclimating to tanks and forming their recesses, they would occasionally exhale forcefully, pushing themselves further into the sand. Additionally, the position of the gill opening allows for a short transition between the suction and pressure phase (Phase 2; Table 1), allowing the fish to quickly begin exhalation. The posteriorly positioned gill openings can be seen to open almost immediately after the lower jaw begins to close, so that the buccal and gill chambers can be emptied nearly simultaneously.

Previous studies of the cranial anatomy of *Lophius* primarily focused on the enlarged buccal skeleton that allows them to rapidly engulf large prey, but several authors also comment on the specialized skeletal anatomy of the gill chamber (Gregory, 1933; Field, 1966; Elshoud, 1986), including the large branchiostegals. Regarding musculature of *Lophius*, Field (1966) and Winterbottom (1973) described the enlarged hyohyoideus muscles that actuate the branchiostegal rays. The abductor hyohyoideus in *Lophius* consist of thick transverse bands of muscle that originate on the fascia of the ventral midline and insert onto the first two branchiostegals (Field, 1966). The inferior hyohyoideus consists of much thinner strips of obliquely positioned muscle that originate on the ceratohyal and insert on the first four branchiostegal rays (Field, 1966; Winterbottom, 1973). Together, these two muscles control the expansion of the branchiostegals during inhalation (Field, 1966). The adductor hyohyoideus consists of thin sheets of muscle positioned transversely or obliquely between each of the branchiostegals and between the sixth branchiostegal and the subopercle (Field, 1966; Winterbottom, 1973). These muscles are

responsible for the contraction of the gill chamber during exhalation. Given the length of the branchiostegal rays, these muscles have tremendous surface area. We found that these muscles extend posteriorly from branchiostegal rays 2-5 to form a complex musculature that helps to control the gill opening (Fig. 8). There is a large and previously undocumented dorsal extension of this muscle, with muscle fibers extending dorsally through the medial surface of the gill opening and continuing up the side of the body in the thin sheet of fascia (Fig. 7). These muscles only appear to be active during exhalation (Phases 3 and 4), and therefore, likely function to pull the gill opening into a siphon shape when the fish exhales and the pectoral fins are positioned normally (Fig. 6A).

All Lophiiformes lack a close association between the gill opening and the opercular bones and show a restriction of the gill opening to a small aperture. In most Lophiiformes, the gill opening is posterior and ventral to the pectoral fin base, sitting in the axillary region of the fin, as in *Lophius*, although in some cases it is positioned much farther back on the body, including in Chaunacidae, *Antennarius analis* and *A. duescus* (Pietsch and Grobecker, 1987). Antennariid frogfishes use their siphon-like restricted gill opening to produce a slow jetting behavior (Fish, 1987; Pietsch and Grobecker, 1987). We found extensions of the adductor hyohyoideus muscles beyond the branchiostegal rays in *Chaunax pictus* and *Histrio histrio*. In *C. pictus*, these muscles surround the gill opening before passing dorsally into the fascia covering the trunk musculature. In *H. histrio*, these muscles extend from between the branchiostegals and surround the tiny gill opening, most noticeably in the ventral portion of the aperture. In his studies of teleost muscles, Winterbottom (1973; 1974) noted that the adductor hyohyoideus frequently extends dorsally to the opercular bones, but in Tetraodontiformes, these muscles are often greatly enlarged, lining the lateral and sometimes ventro-medial surfaces of the gill

chamber, sometimes muscularizing the gill opening valves. In some tetraodontiforms, the adductor hyohyoideus also extends to the pectoral girdle and the epibranchials. These expansions of the adductor hyohyoideus beyond the branchiostegal rays and the medial surfaces of the opercular bones may be homologous with the expansion of the adductor hyohyoideus we observed in Lophiiformes studied here. Lophiiformes and Tetraodontiformes have been proposed as closely related clades (e.g., Miya et al., 2003; Alfaro et al., 2009; Betancur-R et al., 2013), and were resolved as sister taxa by Near et al. (2013). We propose that this expansion of the adductor hyohyoideus as well as the presence of restricted gill openings (Chanet et al., 2013; Farina et al., 2015) may be a synapomorphy for Tetraodontiformes + Lophiiformes. However, further investigation into the musculature of related taxa is needed.

The specialized gill chamber anatomy of *Lophius americanus* allows slow gill ventilation. However, even with these specializations, *L. americanus* maintains a basic pattern of pumping similar to that of other actinopterygians. *Lophius* is therefore an excellent example of the robustness of the actinopterygian ventilatory pattern, while showcasing potential for evolutionary modulation of this system. Understanding the diversity and extremes of gill ventilation can be expected to provide new insights into actinopterygian evolution.

Acknowledgements

This chapter was written in collaboration with William E. Bemis. This research was supported by an award from the Edward C. Raney Fund from the American Society of Ichthyologists and Herpetologists and by an NSF Doctoral Dissertation Improvement Grant (DEB-1310812) awarded to Stacy C. Farina and William E. Bemis. Captain Jim Ford (F/V Lisa Ann II), Captain David Goethel (F/V Ellen Diane), and John Galbraith (NMFS/NEFS) collected specimens used in this study. Wendy Lull generously allowed us to record videos of the

specimen of *Lophius americanus* at the Seacoast Science Center in Rye, New Hampshire. Frank Fish assisted with flow visualization experiments at SML and talked extensively with the senior author about gill openings and functional morphology. Beth Brainerd, Harry Greene, Amy McCune, and Adam Summers provided feedback on the project and manuscript. We also thank the staff and community of Shoals Marine Laboratory, especially Hal Weeks, Philip Thompson, Robin Hadlock Seeley, and Kevin Wells.

REFERENCES

Alfaro, M.E., Santini, F., Brock, C., Alamillo, H., Dornburg, A., Rabosky, D.L., Carnevale, G., Harmon, L.J., 2009. Nine exceptional radiations plus high turnover explain species diversity in jawed vertebrates. Proc. Acad. Nat. Sci. Philadelphia. 106, 13410-13414.

Armstrong M.P., Musick, J.A., Colvocoresses J.A., 1996. Food and ontogenetic shifts in feeding of the goosefish, *Lophius americanus*. J. Northwest Atl. Fish. Sci. 18, 99-103.

Betancur-R R., Broughton, R.E., Wiley, E.O., Carpenter, K., López, J.A., Li, C., Holcroft, N.I., Arcila, D., Sanciangco, M., Cureton, J.C., Zhang, F., Buser, T., Campbell, M.A., Ballesteros, J.A., Adela Roa-Varon, A., Willis, S., Borden, W.C., Rowley, T., Reneau, P.C., Hough, D.J., Lu, G., Grande, T., Arratia, G., Ortí, G., 2013. The tree of life and a new classification of bony fishes. PLOS Currents Tree of Life Edition 1.

Brainerd, E.L., Ferry-Graham, L.A., 2006. Mechanics of respiratory pumps. In: Shadwick, R.E., Lauder, G.V. (Eds.), Fish Physiology: Volume 23. Elsevier Academic Press, San Diego, pp. 1-28.

Bigelow, H.B., Schroeder, W.C., 1953. Fishes of the Gulf of Maine. Fish and Wildlife Service, Fish. Bull., 53.

Cameron, J.N., Cech, J.J., 1970. Notes on the energy cost of gill ventilation in teleosts. Comp. Biochem. Physiol. 34(2), 447-455.

Caruso, J.H., 1983. The systematics and distribution of the lophiid anglerfishes: II. Revisions of the genera *Lophiomus* and *Lophius*. Copeia 1983(1), 11-30.

Caruso, J.H., 2002. Goosefishes or Monkfishes. Family Lophiidae. In: Collette, B.B., Klein-MacPhee, G. (Eds.) Bigelow and Schroeder's Fishes of the Gulf of Maine. Third Edition. Smithsonian Institution Press, Washington, pp. 264-270.

Chadwick, H.C., 1929. Feeding habits of the angler-fish, *Lophius piscatorius*. Nature 124:337.

Chanet, B., Guintard, C., Betti, E., Gallut, C., Dettaï, A., Lecointre, G., 2013. Evidence for a close phylogenetic relationship between the teleost orders Tetraodontiformes and Lophiiformes based on an analysis of soft anatomy. Cybium: Int. J. Ichthyol. 37, 179-198.

Edwards, R.R.C., 1971. An assessment of the energy cost of gill ventilation in the plaice (*Pleuronectes platessa* L.). Comp. Biochem. Physiol., A: Comp. Physiol. 40(2), 391-398.

Elshoud, G.C.A., 1986. Fish and chips. Computer models and functional morphology of fishes. Thesis Rijksuniversiteit, Leiden, The Netherlands.

Farina, S.C., Near, T. J., Bemis, W.E. 2015. Evolution of the branchiostegal membrane and restricted gill openings in Actinopterygian fishes. J. Morphol. 276, 681-694.

Fariña, A.C., Azevedo, M., Landa, J., Duarte, R., Sampedro, P., Costas, G., Torres, M.A., Cañás, L., 2008. *Lophius* in the world: A synthesis of the common features and life strategies. ICES J. Mar. Sci. 65, 1272-1280.

Farrell, A.P., Steffensen, J.F., 1987. An analysis of the energetic cost of the branchial and cardiac pumps during sustained swimming in trout. Fish Physiol. and Biochem. 4(2), 73-79.

Fish, F.E., 1987. Kinematics and power output of jet propulsion by the frogfish genus *Antennarius* (Lophiiformes: Antennariidae). Copeia 1987, 1046-1048.

Field, J.G., 1966. Contributions to the functional morphology of fishes. Part II. The feeding mechanism of the angler-fish, *Lophius piscatorius* Linnaeus. Zool. Afr. 2, 45-67.

Gregory, W.K., 1933. Fish Skulls: A study of the evolution of natural mechanisms. Trans. Amer. Phil. Soc. 23(2), 1-481.

Gudger, E.W., 1945. The angler-fishes, *Lophius piscatorius* et *americanus*, use the lure in fishing. Am. Nat. 79(785), 542-548.

Hedrick, T., 2008. Software techniques for two- and three-dimensional kinematic measurements of biological and biomimetic systems. Bioinspir Biomim. 3, 034001.

Hughes, G.M., 1960. A comparative study of gill ventilation in marine teleosts. J. Exp. Biol. 37, 28-45.

Hughes, G.M., 1966. The dimensions of fish gills in relation to their function. J. Exp. Biol. 45, 177-195.

Hughes, G.M., Shelton, G., 1958. The mechanism of gill ventilation in three freshwater teleosts. J. Exp. Biol. 35(4), 807-823.

Laurenson, C.H., Hudson, I.R., Jones, D.O.B, Priede, I.G., 2004. Deep water observations of *Lophius piscatorius* in the north-eastern Atlantic Ocean by means of a remotely operated vehicle. J. Fish Biol. 65, 947-960.

Laurenson, C.H., Priede, I.G., 2005. The diet and trophic ecology of anglerfish *Lophius piscatorius* at the Shetland Islands, UK. J. Mar. Biol. Assoc. UK 85, 419-424.

Liem, K.F., 1970. Comparative functional anatomy of the Nandidae (Pisces: Teleostei). Fieldiana: Zool. 50, 1-175.

McAllister, D.E., 1968. Evolution of branchiostegals and classification of teleostome fishes. Bull. Natl. Mus. Canada 221, 1-237.

Miya, M., Takeshima, H., Endo, H., Ishiguro, N.B., Inoue, J.G., Mukai, T., Satoh, T.P., Yamaguchi, M., Kawaguchi, A., Mabuchi, K., Shirai, S., Nishida, M., 2003. Major

patterns of higher teleostean phylogenies: a new perspective based on 100 complete mitochondrial DNA sequences. Mol. Phylogenet. Evol., 26, 121-138.

Near, T.J., Dornburg, A., Eytan, R.I., Keck, B.P., Smith, W.L., Kuhn, K.L., Moore, J.A., Price, S.A., Burbrink, F.T., Friedman, M., Wainwright P.C., 2013. Phylogeny and tempo of diversification in the superradiation of spiny-rayed fishes. Proc. Natl. Acad. Sci. USA 110(31), 12738-12743.

Pietsch, T.W., Grobecker, D.B., 1987. Frogfishes of the World: Systematics, Zoogeography, and Behavioral Ecology. Stanford University Press, Stanford, California.

Richards, R.A., Nitschke, P.C., Sosebee, K.A., 2008. Population biology of monkfish Lophius americanus. ICES J. Mar. Sci., 65, 1291-1305.

Summers, A. P., and Ferry-Graham, L. A. (2002). Respiration in elasmobranchs: New models of aquatic ventilation. In: Bels, V. L., Gasc, J. P., and Casinos, A. (Eds.), Vertebrate Biomechanics and Evolution. pp. 87–100. Bios Scientific Publishers Ltd., Oxford.

Valentim, M.F.M., Caramaschi, E.P., Vianna, M., 2008. Feeding ecology of monkfish Lophius gastrophysus in the south-western Atlantic Ocean. J. Mar. Biol. Assoc. U.K. 88, 205-212.

Wilson, D.P., 1937. The habits of the angler-fish *Lophius piscatorius* L., in the Plymouth Aquarium. J. Mar. Biol. Assoc. U.K. 21, 477-496.

Winterbottom, R., 1973. A descriptive synonymy of the striated muscles of the Teleostei. Proc. Acad. Nat. Sci. Philadelphia. 1973, 225-317.

Winterbottom, R., 1974. The familial phylogeny of the Tetraodontiformes (Acanthopterygii: Pisces) as evidenced by their comparative myology. Smithson. Contr. Zool. 155, 1-201.

CHAPTER 3

THE CONTRIBUTION OF THE BRANCHIOSTEGAL APPARATUS TO DRIVING VENTILATORY CURRENT IN FOUR SPECIES OF SCULPINS (SUPERFAMILY COTTOIDEA)

Abstract

The branchiostegal apparatus forms the ventro-lateral wall of the gill chamber of ray-finned fishes and consists of a membrane supported by many long bony branchiostegal rays that articulate with ventral elements of the hyoid arch. Its role in ventilation is to expand and compress the gill chamber, working with the operculum. Across ray-finned fishes, there is great diversity in skeletal and soft tissue components of the branchiostegal apparatus, and previous authors have qualitatively linked the diversity of this structure to variation in ventilatory pressures. Here, we focus on the Cottoidea (sculpins), a group of mostly benthic fishes that exhibits much variation in branchiostegal morphology. We collected functional (pressure recordings in the buccal and opercular chamber) and anatomical measurements for four cottoid species. For analysis of pressure recordings, we subtracted pressures in the opercular chamber from those of the buccal chamber to create differential pressure profiles, allowing a calculation of the relative contributions of the buccal and opercular pumps to driving pressure changes. *Leptocottus armatus* (Cottidae) has a powerful buccal pressure pump, *Hemilepidotus hemilepidotus* (Agonidae) and *Dasycottus setiger* (Psychrolutidae) have powerful opercular suction pumps, and *Myoxocephalus polyacanthocephalus* (Psychrolutidae) has an intermediate condition. We propose and calculate a new metric, the "pump ratio," to characterize the relative

contributions of the buccal and opercular pumps. Using recently published sequence data, we used phylogenetically corrected generalized least squares models to assess the relationships between pump ratio and each of our anatomical variations. We found that the relative size of the branchiostegal apparatus explains much of the variation in the pump ratio ($p = 0.0278$). Therefore, we propose the addition of a third pump, the branchiostegal apparatus, to the standard Hughes model. This third pump works in parallel with the operculum, and by explicitly modeling its contributions to ventilatory mechanics, we can provide a better framework for understanding phylogenetic variation in patterns of gill ventilation.

Introduction

Since the work of G.M. Hughes and G. Shelton more than 50 years ago, the general mechanics of gill ventilation in ray-finned fishes (Actinopterygii) have been well understood. Fishes drive water over their gills by cyclically expanding and compressing the buccal and opercular chambers, alternating between positive and negative pressures (Hughes and Shelton, 1958). This establishes a system of counter-current exchange of oxygen and carbon dioxide between blood in the vessels of the secondary lamellae and water passing over the gills (Hughes and Shelton, 1962). Counter-current exchange is considered to be the most efficient arrangement for transfer of gasses in vertebrate respiration (Piiper and Scheid, 1972), and this increased efficiency is needed due to the high viscosity and low oxygen content of water relative to air. However, the pumping mechanism needed to ventilate the gills can require up to 15% of total metabolic activity during rest and even more during activity (Cameron and Cech, 1970; Farrell and Steffensen, 1987), and therefore the structures involved with this pumping are likely under selective pressures for efficient gill ventilatory performance throughout the evolutionary and ecological diversity of fishes.

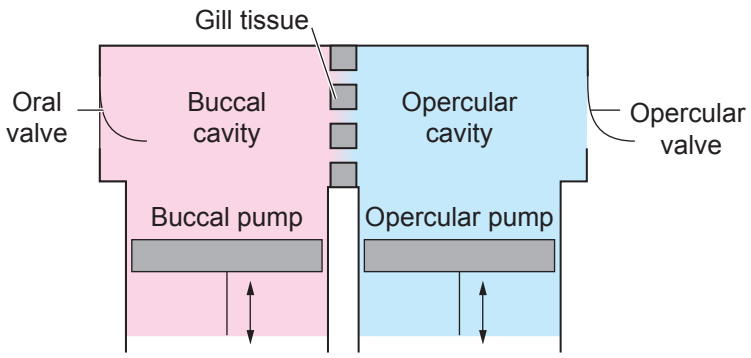

Figure 1. Schematic model of gill ventilatory anatomy. Hughes (1960) modeled anatomy of the gill ventilatory system as a simple system of pistons and chambers. The two chambers, the buccal cavity and the opercular cavity, each contain a pump and a valve. Gill tissue between the chambers provides some resistance to water flow between the chambers.

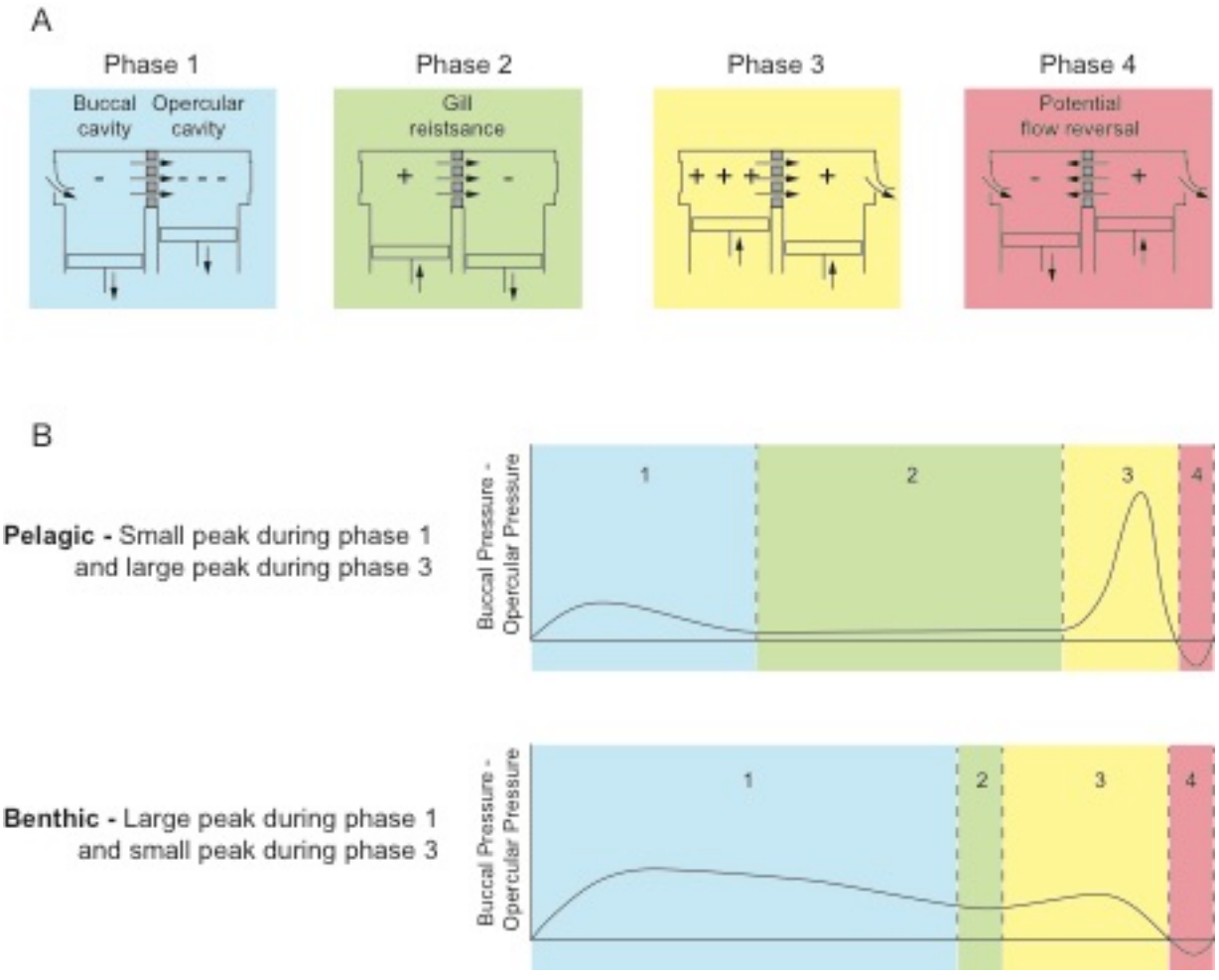

Figure 2. Changes in pressures during a ventilation cycle. There are four phases in a ventilatory cycle, further defined in the text, during which each of the chambers expands and

contracts, creating pressure differences that draw water continuously over the gills. Hughes (1960) observed that fishes that were highly active and swam continuously tended to have a large peak of differential pressure during Phase 3 (indicating a dominant buccal pump), while benthic and more sedentary fishes tended to have a large peak during Phase 1 (indicating a dominant opercular pump). Models of ventilation (A) are based on Brainerd and Ferry-Graham (2006), Summers and Ferry-Graham (2002), and Hughes (1960), and differential pressure profiles (B) are redrawn from Hughes (1960).

In the Hughes (1960) model of gill ventilation for ray-finned fishes (Fig. 1), the buccal and opercular cavities are treated as two chambers with some resistance to flow between them, and each chamber has a pump and a valve. The chambers cycle through four phases (Hughes, 1960; Brainerd and Ferry-Graham, 2006; Fig. 2A) during a single ventilation event. In Phase 1, the buccal and opercular chambers expand, drawing water into the mouth and over the gill tissue. During Phase 2, the buccal chamber begins to compress while the opercular chamber is still expanding, forcing water over the gill tissue. In Phase 3, both the buccal and opercular chambers compress, forcing water over the gills and out the gill openings, and in Phase 4 the buccal chamber begins to expand, transitioning back to negative pressure, causing the potential for temporary reversal of water flow (Summers and Ferry-Graham, 2001). The pump in the buccal chamber consists of the lower jaw, suspensorium, and hyoid apparatus, and the pump in the opercular chamber consists of the opercular bones (opercle, subopercle, and interopercle) and the branchiostegal rays (Fig. 3). Filamentous gills extend from the gill arches and into the opercular chamber. They interlock to form a curtain, which limits water flow between the buccal and opercular chambers.

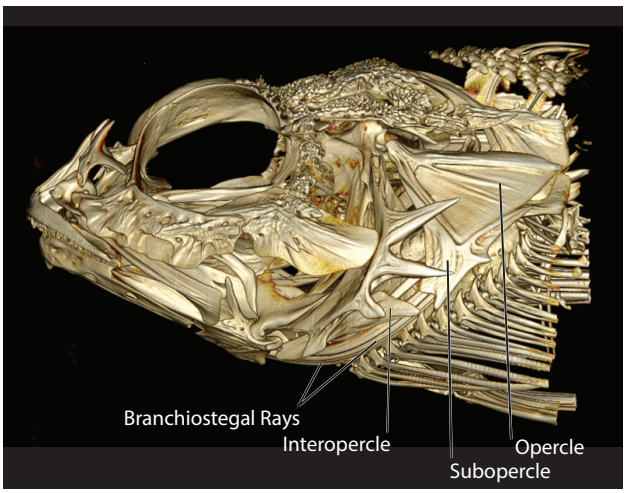

Figure 3. Skeletal anatomy of the opercular chamber. Skeletal elements of the opercular chamber of ray-finned fishes, here exemplified by a cottoid *Hemilepidotus hemilepidotus*, consist of the opercular series (opercle, subopercle, and interopercle) and branchiostegal rays. The medial wall of the chamber is supported by the pectoral girdle.

Attempts to characterize fishes according to their ventilatory morphology and behavior began with Baglioni (1907), who emphasized the role of branchiostegal rays in generating respiratory current. Branchiostegal rays are long, thin dermal bones that articulate with ventral elements of the hyoid arch (Fig. 3). They support a thin membrane of skin, connective tissue and muscle fibers called the branchiostegal membrane, which forms the ventral wall of the opercular chamber. Together, the branchiostegal rays, membrane, and associated muscles form the branchiostegal apparatus. Baglioni focused on the relative size of this feature, because benthic fishes appear to rely on a well-developed branchiostegal apparatus to drive more respiratory current than do pelagic fishes. Hughes (1960) tested the validity of Baglioni's characterizations by recording pressures in the buccal and opercular chambers during ventilation in several marine fishes. He subtracted buccal pressure and opercular pressure to calculate differential pressure curves for each species. Hughes found that, generally, pelagic fishes had larger differential pressures during Phase 3 (Fig. 2B), as they predominantly used their "buccal pressure pump" to

drive ventilatory current with positive pressures in the buccal chamber. In contrast, benthic fishes had larger differential pressures during Phase 1 of ventilation (Fig. 2B) because the opercular chamber generated large negative pressures; he considered fishes with this condition to have a predominant "opercular suction pump" (Hughes, 1960). However, much of the variation in differential pressure profiles of the species examined by Hughes (1960) could not be explained by Baglioni's predictions, likely due to large evolutionary divergence among the taxa Hughes studied. Comparisons of gill ventilatory pressures are likely to be more informative if they are made within a group of closely related, morphologically and ecologically similar species.

Sculpins (Cottoidea; Yabe, 1985) are benthic marine and freshwater fishes consisting of least 114 extant genera. They are an ideal group for comparative studies of gill ventilation because many aspects of their morphology and ecology are similar, thus minimizing some of the complications that arise from comparing very disparate species. Most sculpins rest on the substrate and use suction feeding as a primary prey-capture method. However, sculpins vary in cranial anatomy (Yabe, 1985), suction feeding performance (Norton, 1995), and hypoxia tolerance (Mandic et al., 2009), and therefore, we expect that there will be biologically relevant differences in gill ventilation.

The primary goal of our study is to characterize ventilatory patterns in four benthic species of cottoids to test predictions based on models proposed by Hughes (1960) and shown in Figure 2B. Secondarily, we sought to explore the potential for improving Hughes' double pump model for gill ventilation (Fig. 1) using phylogenetically-corrected generalized least squares models to assess the relationships between ventilatory function and anatomical components of the ventilatory pumps.

Methods

Research was conducted at Friday Harbor Laboratories (FHL) during summer 2012. The four species chosen for this study were *Leptocottus armatus* (Cottidae), *Myoxocephalus polyacanthocephalus* (Psychrolutidae), *Hemilepidotus hemilepidotus* (Agonidae), and *Dasycottus setiger* (Psychrolutidae). Family-level classification follows Smith and Busby (2014). Three individuals of similar sizes were used for each species: *L. armatus* (194-213mm), *M. polyacanthocephalus* (229-260mm), *H. hemilepidotus* (220-237mm), and *D. setiger* (82-153mm). *Leptocottus armatus*, *M. polyacanthocephalus*, and *H. hemilepidotus* were caught by seine net, and *D. setiger* was caught by bottom trawl in the waters surrounding San Juan Island in Washington, USA. Fishes were held in sea tables with a constant flow of seawater from the San Juan Marine Preserve off the coast of the FHL campus when they were not in use for experimentation. Animal care and use followed protocols approved by University of Washington's Institutional Animal Care and Use Committee (IACUC protocol # 4238-03).

Videography

Videos of gill ventilation were recorded for each individual prior to all other experimentation. Resting ventilation rate was obtained prior to videography while the fishes were still in their holding sea table. Each fish was then placed in the filming tank and acclimated for one hour or longer until it reached its resting ventilation rate. The filming tank had a constant flow of seawater from the same water system as the holding tanks, so water conditions were similar. Temperature ranged from 10-13°C. Videos were taken from dorsal and lateral views. Videography was used to confirm that ventilation kinematics did not change as a result of pressure transducer implantation. Videos were also used to obtain ventilation rates, timing of

skeletal movements, and lengths of the four phases of ventilation for 10 ventilation cycles in each fish.

Pressure Transducer Recordings

For each individual, pressure transducer recordings were obtained from the buccal and opercular chambers simultaneously. Pressures were obtained using three transducers connected to two pressure control units (Millar Instruments®, PCU-2000), converted from analog to digital using a PowerLab 8/30 data acquisition system (ADInstruments®, Model ML870), recorded on Apple MacIntosh computers, and read with LabChart® v7.2.4 (ADInstruments®). Cannulae made from polyethylene tubing were surgically implanted in anesthetized fish (MS-222) with a 15-gauge needle in the buccal cavity (dorsal to the metapterygoid or between the premaxillary and maxillary bones) and the opercular cavity (between the dorsal surface of the opercle and the posttemporal bone). One transducer was fed through each of the two cannulae, and a third transducer was fed through a cannula affixed to the buccal cannula outside the fish as a measure of the ambient pressure. Fishes were allowed to recover from anesthesia for a minimum period of one hour, and pressure recordings were obtained for at least an additional one hour after the recovery period. Video was also recorded during pressure recordings for at least ten ventilatory cycles. Video records were synchronized with pressure recordings by using an LED light connected to the PowerLab system with a BNC cable. The light was manually flashed in the video using variable patterns so that voltage recordings from the light could be matched to the flashing visible in video recordings.

Analyses of pressure data included obtaining the area under the curve of the differential pressure during Phase 1 and Phase 3. This curve was obtained by subtracting the buccal and opercular chamber pressures using LabChart® software. Integrals were obtained for Phase 1 and

Phase 3 of ventilation by measuring the area under the differential curves in ImageJ. For each individual, we calculated an average ratio of the integrals of Phase 1 and Phase 3 as a metric of the relative dominance of the opercular suction vs. buccal pressure pump (herein referred to as the pump ratio).

Anatomical Data

After all experiments were completed, individuals were killed using a lethal dose of MS-222 and studied for anatomical analyses. Photographs were taken in dorsal, lateral, and ventral views with the branchiostegal membrane both closed and expanded. Standard measurements were made with calipers, including standard length, total length, head length, and snout length. The opercle, subopercle, and branchiostegal membrane (including branchiostegal rays) were removed from the fishes, laid flat on a sheet of paper, and photographed. Surfaces areas of the branchiostegal membrane and opercular bones (opercle + subopercle) were measured from these photographs in ImageJ. Molds of the buccal and opercular chambers were obtained by filling the chambers with a thermoplastic adhesive polymer while the chambers were held at maximum expansion. Volumes of the chambers were obtained by measuring the masses of the molds. We also made 3D micro-computed tomography reconstructions of museum specimens of the same four species (CUMV 98019, 97968, 98210, and 97976) to visualize buccal and opercular chamber anatomy. For *Leptocottus armatus* (Fig. 4E and 4I), *Myoxocephalus polyacanthocephalus* (Fig. 4F and 4J), and *Dasycottus setiger* (Fig. 4H and 4L), we used a GE eXplore CT-120 to scan with 50 µm resolution. For *Hemilepidotus hemilepidotus*, we used a Zeiss (Xradia) Versa XRM-520 to scan with 47 µm resolution.

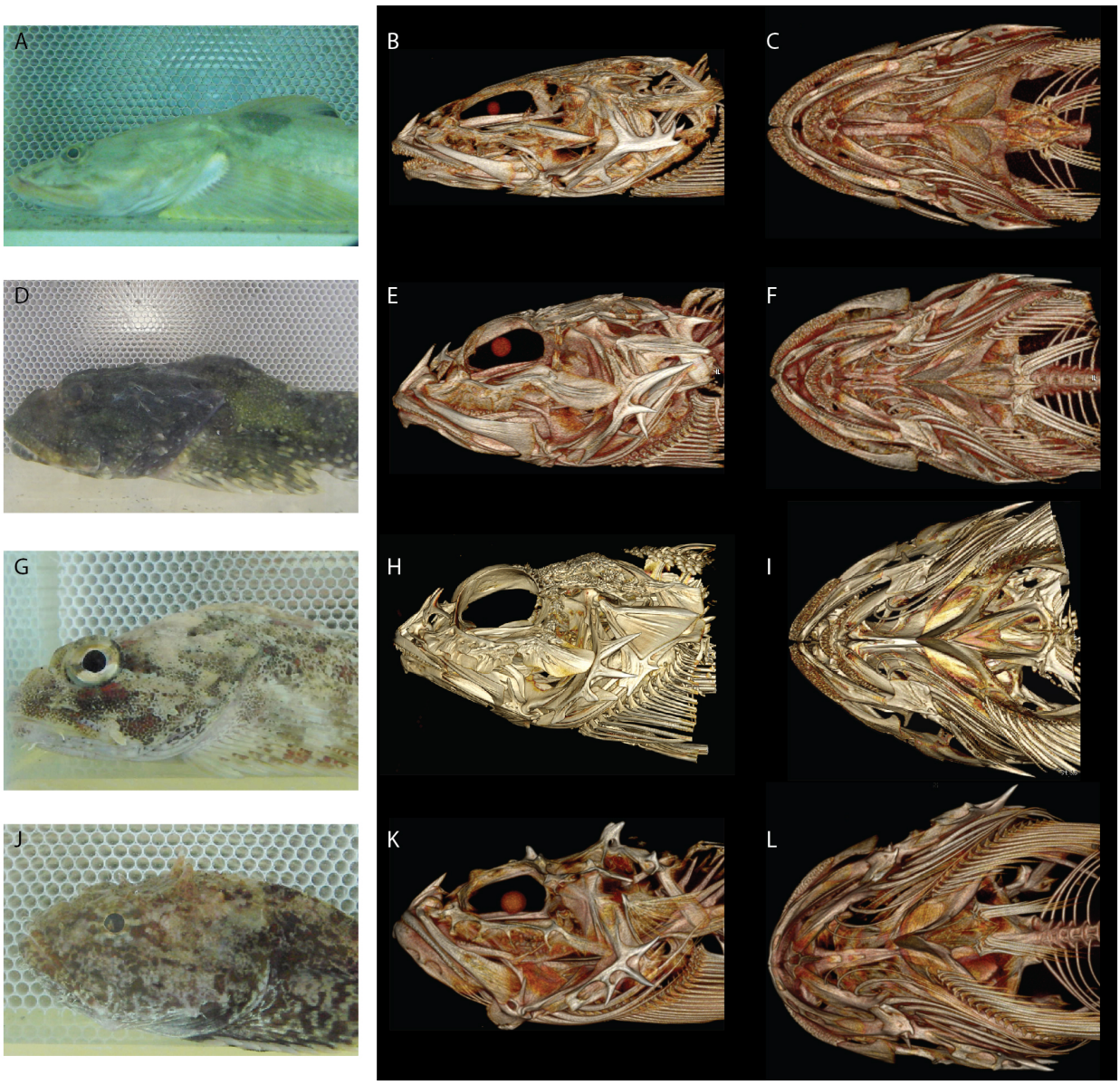

Figure 4. Four species of cottoids studied. We studied ventilatory pressures and kinematics in four species: *Leptocottus armatus* (A, B, C), *Myoxocephalus polyacanthocephalus* (D, E, F), *Hemilepidotus hemilepidotus* (G, H, I), and *Dasycottus setiger* (J, K, L). We used micro-computed tomography scans to visualize the anatomy of each species.

Analyses

To facilitate phylogenetically corrected data analyses, we constructed a phylogeny using molecular data for 102 species of Cottoidea and six outgroup species, *Hexagrammos*

decagrammus, *H. stelleri*, *Trichodon trichodon*, *Cyclopterus lumpus*, *Liparis dennyi*, and *L. florae*. We used a molecular dataset from Knope (2013), which included sequences from mitochondrial gene cytochrome b (*cytb*) and the first nuclear intron of the S7 ribosomal protein (*S7*) for 99 cottoid species. We supplemented these data with sequences from GenBank (Benson et al., 2013), including *cytb* from nine additional and *S7 H. decagrammus* and *H. stelleri*. We also included GenBank sequences from mitochondrial gene cytochrome c oxidase I (*COI*) for a subset of 72 taxa. Sequences from each gene were aligned individually using MUSCLE (Edgar, 2004) on the EMBL-EBI bioinformatics web tool (Li et al., 2015). The complete alignment had 86.7% amplicon and 69.3% base pair coverage. Best-fit nucleotide substitution models were chosen using jModelTest v2.1.7 (Guindon and Gascuel, 2003; Darriba et al., 2012) based on AIC values calculated for 24 candidate models. To reconstruct the phylogeny, we ran MrBayes v3.2.3 (Ronquist et al., 2012) on the CIPRES Science Gateway v3.3 for four runs using an MCMC chain length of 20,000,000. Each run was evaluated in Tracer v1.6 (Rambaut et al., 2014) and trees from the run with the highest log-likelihood were used to construct a maximum clade credibility tree in Tree Annotator v1.8.0.

All character analyses were conducted in R (R Core Team, 2013). We first pruned our maximum clade credibility tree to include only our four study species using the *drop.tip* function in the *ape* package (Pardis et al., 2004). Phylogenetic generalized least squares (PGLS) analyses were used to evaluate the relationship between the pump ratio and seven anatomical ratios (branchiostegal membrane surface area relative to opercular surface area, maximum volume of the opercular chamber relative to the buccal chamber, gill opening length relative to standard length (SL), upper jaw length relative to SL, mouth opening diameter relative to SL, snout length relative to SL, and head length relative to SL). All ratios were log-transformed prior to PGLS

analyses. PGLS tests were performed using the *gls* function in the *nlme* package (Pinheiro et al., 2014) by applying a Brownian correlation structure based on phylogenetic difference using the *corBrownian* function in the *ape* package (Pardis et al., 2004).

Results

The average length of a ventilatory cycle was 1.25 s (± 0.33 s) for *Leptocottus armatus*, 2.26 s (± 0.27 s) for *Myoxocephalus polyacanthocephalus*, 2.00 s (± 0.36 s) for *Hemilepidotus hemilepidotus*, and 12.30 s (± 2.74 s) for *Dasycottus setiger*. The relative timing of skeletal movements during ventilation closely followed those previously reported for other ray-finned fishes. Videos of *L. armatus* showed considerable movements of the lower jaw during gill ventilation that were far more pronounced than the jaw movements of the other three species. Pumping movements of the branchiostegals in *M. polyacanthocephalus, H. hemilepidotus*, and *D. setiger* were substantial, and these species only opened small portions of their opercular valve (a dorsal and ventral flap) during phases 3 and 4. For all species, Phase 1 of ventilation was the longest phase. However, the ventilatory cycle of *D. setiger* consisted of an unusually long Phase 1.

By subtracting pressure in the opercular chamber from that of the buccal chamber during each ventilatory cycle, we observed differential pressure profiles. These profiles showed considerable variation among the four species (Fig. 5). *Leptocottus armatus* exhibited a large peak of differential pressure during Phase 3, with high positive pressures in the buccal chamber during this phase. *Myoxocephalus polyacanthocephalus* and *Hemilepidotus hemilepidotus* showed moderate peaks during Phase 3, but also maintained high negative pressures in the opercular chamber during Phase 1. *Dasycottus setiger* had the largest peak during Phase 1 of

ventilation, showing large differences in the negative pressures of the two chambers throughout this phase.

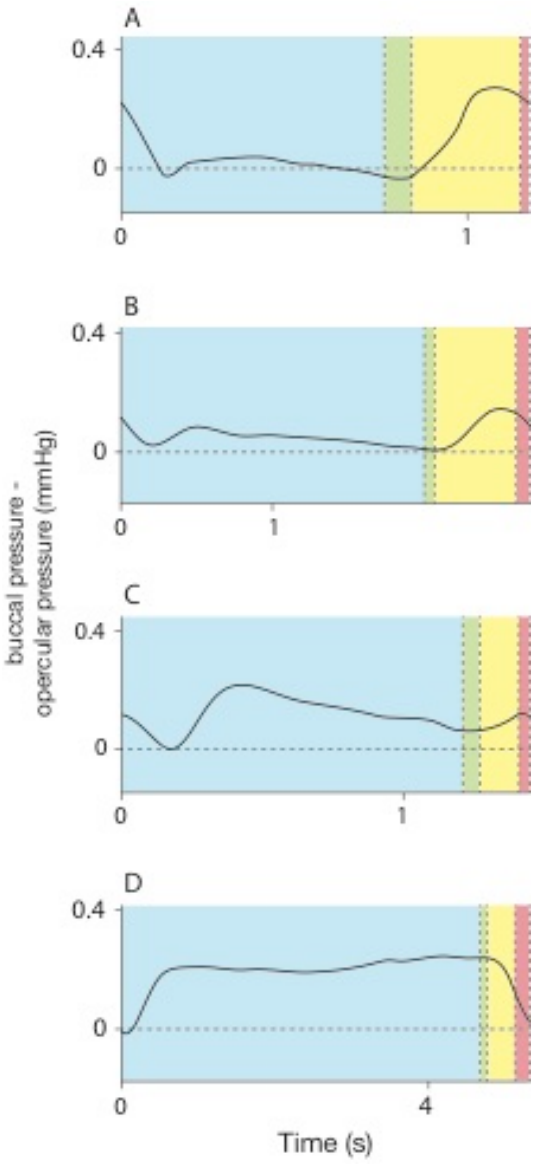

Figure 5. Differential pressure profiles for four cottoid species. We subtracted opercular chamber pressure from buccal chamber pressure over the course of each ventilatory cycle to produce differential pressure profiles. A representative cycle from each species shows substantial differences in the pressure patterns among the taxa. *Leptocottus armatus* (A) has a pressure profile similar to pelagic fishes, with a dominant buccal pump. *Myoxocephalus polyacanthocephalus* (B) has an intermediate pressure profile, with powerful buccal and opercular pumps. *Hemilepidotus hemilepidotus* (C) and *Dasycottus setiger* (D) have pressure profiles similar to other benthic fishes, with D. setiger having a long Phase 1.

We used the pump ratio (average ratio of the integrals of Phase 1 and Phase 3) as a metric for the relative dominance of the "opercular suction pump" and the "buccal force pump." Using phylogenetic generalized least squares analyses, we found that this pump ratio was significantly correlated with surface area of the branchiostegal apparatus relative to the combined surface area of the opercle and subopercle (Fig. 6; $p = 0.0278$). There was no significant correlation between the pump ratio and the other anatomical ratios measured ($p > 0.05$), including maximum volume of the opercular chamber relative to the buccal chamber, gill opening length relative to SL, upper jaw length relative to SL, mouth opening diameter relative to SL, snout length relative to SL, and head length relative to SL.

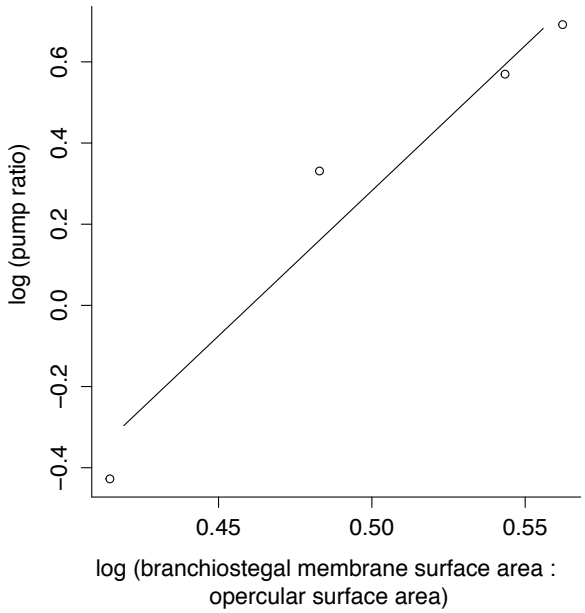

Figure 6. Phylogenetically corrected generalized least squares model for relative size of the opercular chamber elements versus the pump ratio. A bivariate plot of the log-transformed ratios of these two variables is plotted with the PGLS model indicated by the line. As relative surface area of the branchiostegal apparatus increased, so did the pump ratio, indicating that fishes with larger branchiostegals tend to exhibit a more "benthic" pressure profile, with a dominant opercular suction pump.

Discussion

Differential pressure profiles computed in this study varied among taxa to a much greater extent than we predicted based on pressures recorded by Hughes (1960). Hughes observed that fishes could have many different shapes of differential pressure profiles, but he attributed these differences to large ecological and anatomical disparities among the taxa that he examined. However, he did not compare closely related species with similar ecologies, perhaps because he assumed that the pressure profiles would be highly similar. All four species of Cottoidea we studied are benthic fishes that rely on suction feeding as their primary source of prey capture, yet their differential pressure profiles are considerably different. This allowed us to investigate the relationships among ventilatory biomechanics, physiological ecology, and cranial anatomy within a clade, removing the substantial evolutionary distances among taxa that confounded Hughes' interpretation.

Hughes (1960) noted a dominant "buccal pressure pump" among highly active pelagic species and a dominant "opercular suction pump" among more sedentary benthic fishes. In our study, *Leptocottus armatus* possessed a clearly dominant buccal pressure pump, despite being a benthic and largely sedentary fish. However, relative to other sculpins, *Leptocottus armatus* is generally more tolerant to hypoxia (Mandic et al., 2009) and can maintain high levels of oxygen consumption during alterations in the salinity of its environment (Henriksson et al., 2008). Our captive specimens frequently darted around the holding tanks, and this species has been studied for its rapid escape responses (Paglianti and Domenici, 2006). Therefore, *L. armatus* is a relatively active sculpin that may require a strong buccal pressure pump to move a large volume of water across the gills quickly. The buccal pump is able to rapidly expand and contract, allowing for a higher ventilation rate. The species with the most benthic profile was *Dasycottus*

setiger. Among the sculpins of the Pacific Northwest, *D. setiger* has one of the largest mouths (Norton, 1995). It is only found in subtidal habitats and likely relies on sit-and-wait predation and does not experience high levels of activity. The dominant opercular suction pump seen in *D. setiger* involves slow expansion of the branchiostegal rays. It is likely that this slow behavior is efficient in terms of metabolic energy usage, but it does not permit an easy transition to rapid pumping should the fish need to escape a predator. Within this group of closely related species, there is enough ecological variation to produce dramatic differences in ventilatory pressures that are of similar scale to the differences among highly disparate taxa examined by Hughes (1960).

Both Baglioni (1907) and Hughes (1960) asserted that the relative size of the branchiostegal apparatus should have important implications for ventilation behavior and mechanics. Our data support this relationship of anatomy to function among the four taxa that we studied. Among these taxa, the relative importance of the buccal pump and the opercular pump (the pump ratio) was closely correlated with the surface of the branchiostegal membrane relative to the surface area of the operculum (Fig. 6). The relative size of these two structures is a metric of the composition of the opercular chamber pump. A larger operculum indicates a pattern of ventilation dominated by the buccal pressure pump, whereas a larger branchiostegal apparatus indicates a pattern of ventilation dominated by the opercular suction pump. The branchiostegal apparatus plays a large role in fishes with a dominant opercular suction pump, and its slow expansion and compression appear to contribute substantially to driving the ventilatory current. Therefore, a larger branchiostegal apparatus, relative to other skeletal elements of the gill chamber, provides the anatomical basis for a strong opercular suction pump. Surprisingly, the size of the buccal pump (as indicated by the length of the lower jaw) did not correlate with relative importance of the pumps. This is perhaps because the buccal pump is also used in

suction feeding, and, therefore, it is specialized for the production of large negative pressures during feeding and is not limited by constraints of gill ventilatory performance.

The interpretation of differential pressure curves merits further study because of several confounding factors. A change in pressure can result from a change in volume or a change in water velocity, and therefore pressure measurements alone do not permit calculations of the relative contributions of each pump to the ventilatory cycle. To quantify the "dominance" of the buccal or opercular pump in a given species, one would need also to measure volume change or water velocity, at which point, calculations of biomechanical contributions of each chamber, such as work and power, can be made. However, accurately quantifying volume change temporally within the skulls of fishes is a notoriously difficult challenge.

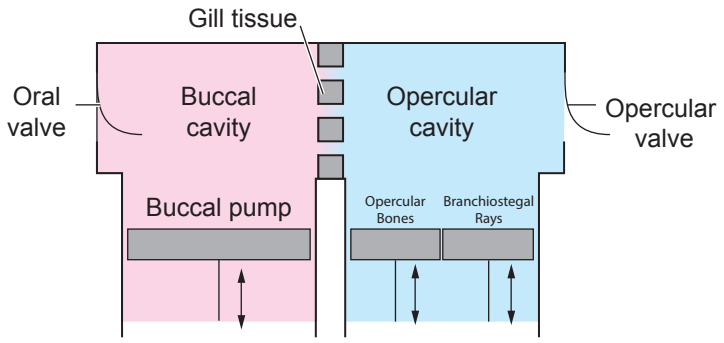

Figure 7. Revised model of gill ventilatory pumps. Ventilatory pressures among even closely related species are highly variable, with much of this variation explained by the relative size of the branchiostegal apparatus. Therefore, we propose that the addition of a third pump, the branchiostegal apparatus, working in parallel with the operculum, can provide a useful framework for better understanding this variation.

The investigation of ventilatory structures and their relationships with biomechanical aspects of the gill ventilation system is greatly enhanced by comparative work among closely related species. Using such an approach, we quantitatively established that the relative size of the branchiostegal apparatus is a predictor of ventilatory pumping function. While the opercular

bones and the branchiostegal rays work together to pump water in and out of the gill chamber, it is clear that their contributions to driving ventilatory current are neither identical nor interchangeable. Therefore, we propose that the Hughes model of the gill ventilatory dual pump system would be enhanced by the addition of a third pump, the branchiostegal apparatus, working in parallel with the operculum (Fig. 7). Given the importance of the branchiostegal apparatus in explaining variation in ventilatory biomechanics among fishes, consideration of the this structure as a third pump provides a useful framework for comparative work.

Acknowledgements

This work was completed in collaboration with Lara A. Ferry, Matthew Knope, Adam P. Summers, and William E. Bemis. For assistance with animal collection and husbandry, we thank David Duggins, Kristy Kull, the staff of Friday Harbor Laboratories (FHL), and the faculty and students of the FHL 2012 course in Functional Morphology and Ecology of Marine Fishes. For feedback and discussions, we thank Beth Brainerd, Amy McCune, John Friel, and Harry Greene. This research was supported by an NSF Doctoral Dissertation Improvement Grant (DEB-1310812) awarded to Stacy C. Farina and William E. Bemis and a Graduate Research Award from the Stephen and Ruth Wainwright Endowment from Friday Harbor Laboratories.

REFERENCES

Baglioni, S. (1907). Der Atmungsmechanismus der Fische. Ein Beitrag zur vergleichenden Physiologie des Atemrhythmus. *Zeitschrift für allgemeine Physiologie.* 7, 177-282.

Benson, D. A., M. Cavanaugh, K. Clark, I. Karsch-Mizrachi, D. J. Lipman, J. Ostell, and E. W. Sayers. (2013). GenBank. Nucleic acids research 41(D1), D36-D42.

Brainerd, E. L., Ferry-Graham, L. A. (2006). Mechanics of respiratory pumps. In: Shadwick, R.E., Lauder, G.V. (Eds.), Fish Physiology: Volume 23. Elsevier Academic Press, San Diego, pp. 1-28.

Cameron, J. N. and Cech, J. J. (1970). Notes on the energy cost of gill ventilation in teleosts. Comp. Biochem. Physiol. 34, 447-455.

Darriba, D., G. L. Taboada, R. Doallo, and D. Posada. (2012). jModelTest 2: more models, new heuristics and parallel computing. Nature Methods 9(8), 772.

Edgar, R. C. (2004). MUSCLE: multiple sequence alignment with high accuracy and high throughput. Nucleic acids research 32(5), 1792-1797.

Farrell, A. P. and Steffensen, J. F. (1987). An analysis of the energetic cost of the branchial and cardiac pumps during sustained swimming in trout. Fish Physiol. and Biochem. 4, 73-79.

Guindon S., and O. Gascuel. (2003). A simple, fast and accurate method to estimate large phylogenies by maximum-likelihood. Systematic Biology 52, 696-704.

Henriksson, P., Mandic, M. Richards J.G. (2008). The osmorespiratory compromise in sculpins: impaired gas exchange is associated with freshwater tolerance. Physiological and Biochemical Zoology. 81, 310-319.

Hughes, G. M. (1960). A comparative study of gill ventilation in marine teleosts. *Journal of Experimental Biology.* 37, 28-45.

Hughes, G. M. and Shelton, G. (1958). The mechanism of gill ventilation in three freshwater teleosts. *Journal of Experimental Biology*. 35, 807-823.

Hughes, G. M. and Shelton, G. (1962). Respiratory mechanisms and their nervous control in fish. *Advances in Comparative Physiology & Biochemistry.* 1, 275-364.

Knope, M. L. (2013). Phylogenetics of the marine sculpins (Teleostei: Cottidae) of the North American Pacific Coast. Molecular Phylogenetics and Evolution 66, 341-349.

Li , W., A. Cowley, M. Uludag, T. Gur, H. McWilliam, S. Squizzato, Y. M. Park, N. Buso, and R. Lopez. (2015). The EMBL-EBI bioinformatics and programmatic tools framework. Nucleic Acids Research doi:10.1093/nar/gkv279

Mandic, M., Todgham, A. E., and Richards, J. G. (2009). Mechanisms and evolution of hypoxia tolerance in fish. Proceedings of the Royal Society B 276, 735-744.

Norton, S. F. (1995). A functional approach to ecomorphological patterns of feeding in cottid fishes. Environmental Biology of Fishes 44, 61-78.

Paglianti, A. and P. Domenici. (2006). The effect of size on the timing of visually mediated escape behavior in staghorn sculpin *Leptocottus armatus*. Journal of Fish Biology. 68, 1177-1191.

Paradis, E., J. Claude, and K. Strimmer. (2004). APE: analyses of phylogenetics and evolution in R language. Bioinformatics 20, 289-290.

Piiper, J. and Scheid, P. (1972). Maximum gas transfer efficacy of models for fish gills, avian lungs, and mammalian lungs. Respiratory Physiology. 14, 115-124.

Pinheiro, J., D. Bates, S. DebRoy, D. Sarkar, and R Core Team. (2014). nlme: Linear and Nonlinear Mixed Effects Models. R package version 3.1-115.

R Core Team. (2013). R: A language and environment for statistical computing. R Foundation for Statistical Computing, Vienna, Austria. URL http://www.R-project.org/.

Rambaut, A., M. A. Suchard, D. Xie, and A. J. Drummond. (2014). Tracer v1.6. Available from http://beast.bio.ed.ac.uk/Tracer.

Ronquist, F., M. Teslenko, P. van der Mark, D. L. Ayres, A. Darling, S. Höhna, B. Larget, L. Liu, M. A. Suchard, and J. P. Huelsenbeck. (2012). MrBayes 3.2: efficient Bayesian phylogenetic inference and model choice across a large model space. Systematic Biology 61(3), 539-542.

Smith, W. L., and M. S. Busby. (2014). Phylogeny and taxonomy of sculpins, sandfishes, and snailfishes (Perciformes: Cottoidei) with comments on the phylogenetic significance of their early-life-history specializations. Molecular Phylogenetics and Evolution 79:332-352.

Smith, W. L., and W. C. Wheeler. (2004). Polyphyly of the mail-cheeked fishes (Teleostei: Scorpaeniformes): Evidence from mitochondrial and nuclear sequence data. Molecular Phylogenetics and Evolution 32, 627-646.

Summers, A. P. and Ferry-Graham, L. A. (2001). Ventilatory modes and mechanics of the hedgehog skate (Leucoraja erinacea): testing the continuous flow model. Journal of Experimental Biology 204, 1577-1587.

Summers, A. P., and Ferry-Graham, L. A. (2002). Respiration in elasmobranchs: New models of aquatic ventilation. In: Bels, V. L., Gasc, J. P., and Casinos, A. (Eds.), Vertebrate Biomechanics and Evolution. pp. 87–100. Bios Scientific Publishers Ltd., Oxford.

Yabe, M. 1985. Comparative osteology and myology of the superfamily Cottoidea (Pisces: Scorpaeniformes) and its phylogenetic classification. Memoirs of the Faculty of Fisheries-Hokkaido University (Japan).

CHAPTER 4

EVOLUTION OF CRANIAL ANATOMY OF COTTOIDS (PERCIFORMES) AND THE ANATOMICAL COUPLING OF SUCTION FEEDING AND GILL VENTILATION

Abstract

Among ray-finned fishes, suction feeding and gill ventilation use many of the same skeletal and muscular components, resulting in a strong evolutionary coupling between the two functions. Suction feeding involves rapid expansion of the buccal cavity through a series of linkages in the head, including a linkage between the opercular bones and the jaw joint. Gill ventilation involves cyclical expansion of the buccal and gill chambers to pump water continuously over the gill tissue. The gill chamber consists of the opercular bones and branchiostegal rays. Sculpins and relatives (Cottoidei) form an ecomorphologically diverse clade of suction feeders. We reconstructed Cottoidei phylogeny using previously published molecular data for three genes from 106 cottoids and two outgroup and used this tree to analyze the relationships among linear measurements of cranial bones from a subset of 23 cottoids and one outgroup taxon. Using phylogenetic generalized least squares models and a phylogenetic principal components analysis, we found that suction-feeding associated characters (lower jaw, upper jaw, and operculum) are correlated. However, there is only weak correlation among the branchiostegals and these structures. We conclude that the branchiostegal apparatus may be a source of modularity within the gill ventilatory system that releases some of the constraints imposed by the close coupling of feeding and ventilation.

Introduction

Organisms are highly integrated, with complex interactions among genes, developmental networks, morphology, physiology, and behavior (Gould and Lewontin, 1979; Cheverud, 1982; Klingenberg, 2008). There are many examples of integrated morphological systems in which multiple structures, such as skeletal elements, work together to perform a single function (e.g., Claverie and Patek, 2013; Kane and Higham, 2015). A single structure can also perform more than one function (Bels et al., 1994; Tsuboi et al., 2015). Studies of the evolution of morphology and function must therefore consider relationships among co-evolving structures that likely interact in highly complex ways. Among ray-finned fishes (Actinopterygii), suction feeding and gill ventilation require the coordination of many structures, and there is considerable overlap in skeletal structures used for both functions. These two systems are closely functionally and evolutionarily linked, making them ideal systems for evolutionary studies of morphological integration and functional coupling.

Suction feeding is the most common mechanism of prey capture in ray-finned fishes, and it has been proposed to be the ancestral feeding strategy for jawed vertebrates (Wainwright et al., 2015). Its prevalence among actinopterygians (Lauder, 1982a) and basal sarcopterygians (Bemis and Lauder, 1986; Bemis 1987a) makes it a critical functional system in studies of vertebrate evolution. Suction feeding involves rapid expansion of the buccal chamber, creating large negative pressures that draw water into the mouth. Skeletal components that facilitate this rapid buccal expansion include the upper and lower jaws, the suspensorium, the hyoid apparatus, and the opercular bones (Liem, 1970). All of these structures, with the exception of the upper jaw, are also involved in active gill ventilation in ray-finned fishes.

Active ventilatory pumping in ray-finned fishes relies on changes in pressure driven by pumps in the buccal chamber and the gill chamber. These chambers expand and compress cyclically to produce a unidirectional flow over the gills (Hughes and Shelton, 1958; Hughes, 1960). The buccal pump includes the lower jaw, suspensorium, and hyoid apparatus, while the gill chamber pump consists of the opercular bones and the branchiostegal rays (Figure 1). The buccal pump, called the "buccal force pump" by Hughes (1960), primarily uses positive pressures to force water from the mouth over the gills, and it also generates negative pressures to draw water into the mouth during inspiration. The gill chamber pump, called the "opercular suction pump" by Hughes (1960), mainly generates negative pressures to draw water over the gills and into the gill chamber, and it also produces positive pressures to force water out the gill openings during expiration. While the movements of the two chambers are synchronous with one another, they perform different tasks in the process of moving water over the gills.

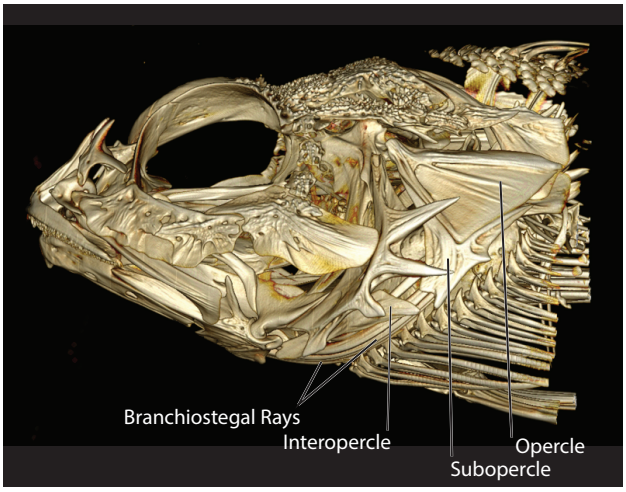

Figure 1. Anatomy of the gill chamber of cottoid fishes. CT scan reconstruction of *Hemilepidotus hemilepidotus* showing morphological components of the gill chamber, including the opercular bones and the branchiostegals.

Functional integration is defined as a high amount of coordination among structures that work together to perform the same function. Evolutionary integration occurs when these

structures show a high degree of correlation when phylogenetic distance is taken into account (Cheverud, 1996; Olson and Miller, 1958). Modularity refers to the presence of structural units, or modules, within a functional system that are working together to perform the function but are not evolutionarily integrated with one another. There is often a high degree of integration within each module and a lack of integration between modules (Klingenberg, 2008; Claverie and Patek, 2013). A lack of evolutionary integration among structures that coordinate to perform the same function can be a signal of modularity within a functional system (Claverie and Patek, 2013). Active gill ventilation represents a potentially modular functional system, in which the buccal and gill chambers are discrete units performing different aspects of one function. Alternatively, suction feeding is a functional system that shows little modularity, employing a large number of components that must be coordinated for rapid expansion and therefore tend to be highly integrated (Collar et al., 2014; Kane and Higham, 2015). Because of the overlap in structures used for both suction feeding and gill ventilation, these systems are functionally coupled, which is defined as one structure or group of structures performing multiple functions (Tsuboi et al., 2015). However, it is unclear how a functional system with a high degree of modularity, such as gill ventilation, can be so closely coupled with a system with a high degree of integration, such as suction feeding.

Sculpins and relatives (Cottoidei) are an ideal clade in which to examine evolutionary integration and modularity in suction feeding and gill ventilation morphology of fishes. Cottoidei (*sensu* Smith and Busby, 2014) consists of sculpins, poachers, snailfishes, lumpsuckers, and sandfishes. Sculpins and poachers (Cottoidea, *sensu* Yabe, 1985) are highly diverse, with at least 114 extant genera. They are also highly diverse from an ecomorphological perspective, with species ranging from intertidal to deep sea habitats, from sit-and-wait predators to active hunters,

and with total lengths ranging from 2 to 58 cm at maturity. However, they are almost exclusively suction feeders, with some variation in prey choice and feeding performance (Norton, 1995). The clade has recently been the subject of extensive phylogenetic revision (Buser and Andrés López, 2015; Knope, 2013; Ramon and Knope, 2008; Smith and Wheeler, 2004; Smith and Busby, 2014), and relationships among families and genera have not been adequately resolved.

In this study, we use available molecular data to reconstruct the phylogeny of Cottoidei using maximum likelihood and Bayesian methods. We then analyze continuously variable characters associated with suction feeding and gill ventilation for degree of evolutionary integration and modularity. We expect to find a high degree of evolutionary integration among structures involved with suction feeding, and do not expect modularity within this system. Among gill ventilatory structures, we expect to find a high degree of evolutionary integration within the functional units of the buccal chamber and the gill chamber but a lack of integration between these two units.

Methods

Phylogenetic reconstruction

To reconstruct cottoid phylogeny, we used molecular data for 106 species of cottoids and two outgroup species, *Hexagrammos decagrammus* and *H. stelleri* (Appendix 2). We used a molecular dataset from Knope (2013), which included sequences from mitochondrial gene cytochrome b (*cytb*) and the first nuclear intron of the S7 ribosomal protein (*S7*) for 99 cottoid species. We supplemented these data with sequences from GenBank (Benson et al., 2013), including *cytb* from seven additional species of cottoids and the two outgroup species as well as *S7* for the two outgroup species. We also included GenBank sequences from mitochondrial gene cytochrome c oxidase I (*COI*) for a subset of 72 taxa. Sequences from each gene were aligned

individually using MUSCLE (Edgar, 2004) on the EMBL-EBI bioinformatics web tool (Li et al., 2015). The complete alignment had 86.7% amplicon and 69.3% base pair coverage. Best-fit nucleotide substitution models were chosen using jModelTest v2.1.7 (Guindon and Gascuel, 2003; Darriba et al., 2012) based on AIC values calculated for 24 candidate models.

We constructed trees using maximum likelihood and Bayesian approaches. For the maximum likelihood tree, we ran RAxML (version 8; Stamatakis, 2014) on the CIPRES Science Gateway v3.3 with *Hexagrammos decagrammus* and *H. stelleri* constrained as a monophyletic outgroup. For this analysis, we split the data set into seven partitions, with a single partition for *S7* and the two mitochondrial genes split into three codon partitions each. Bayesian analyses were conducted using MrBayes v3.2.3 (Ronquist et al., 2012) on the CIPRES portal. Four MrBayes runs resulting in two consensus trees were performed with seven gene partitions and an MCMC chain length of 20,000,000. Nucleotide substitution models were chosen for our seven partitions based on jModelTest results. We used a general time-reversible model (Tavaré, 1986) with invariable sites and rate variation among sites (GTR + I + G) for *S7* and *cytb* (codon positions 1,2, and 3). For the *COI* gene, we used a general time-reversible model with equal state frequencies (SYM) for codon position 1, the F81 model (Felsenstein, 1981) for codon position 2, and a general time-reversible model with rate variation among sites (GTR + G) for codon position 3. Each of the four MrBayes runs were evaluated in Tracer v1.6 (Rambaut et al., 2014) and trees from the run with the highest log-likelihood (see Table 1) were used to construct a maximum clade credibility tree in Tree Annotator v1.8.0.

Table 1. Phylogenetic reconstruction summary statistics. Four trees were constructed, including one maximum likelihood and three Bayesian analyses. Two Bayesian consensus trees were constructed based on MrBayes runs, and a maximum clade credibility tree was constructed from the best MrBayes run.

	Run	Log-likelihood	SE	ESS	Tree log-likelihood	p-value (diff from best?)	Cottoidei support	Cottoidea support
Maximum Likelihood		-	-	-	-66857.93	< 0.0001	100*	30*
Bayesian Consensus Tree 1		-35778.12	0.16	6572.34	-47530.78	0.2547	100%	51.97%
	R1	-35777.96	0.26	2328.06	-			
	R2	-35778.28	0.20	4042.49	-			
Bayesian Consensus Tree 2		-35777.78	0.17	5484.21	-47531.05	0.2551	100%	70.79%
	R1	-35778.30	0.22	3305.12	-			
	R2	-35777.26	0.27	2193.09	-			
Best Bayesian MCC Tree		-35777.26	0.27	2193.09	-47181.91	(best)	100%	66.93%

*Bootstrap values

Character Analysis

We measured cranial skeletal elements from 23 cottoids and one outgroup taxon (*H. stelleri*). We collected and measured 16 species of cottoids from marine habitat surrounding Friday Harbor Laboratories on San Juan Island (Cornell University IACUC 2013-0017; CUMV 97968, 97973, 97975, 97977, 97978, 97981, 97986, 97998, 98023, 98024, 98029, 98033, 98035, 98036, 98039, 99999). This dataset was supplemented with measurements from specimens in the collection (CUMV 3318, 22666, 54050, 55962, 55996, 56207, 71854, 78131, 90894). Linear measurements were made using digital calipers, and standard lengths (SL) for size correction were measured using a ruler. The following measurements were obtained: upper jaw length (ujl), lower jaw length (ljl), mouth opening diameter (mod), opercular length (ol), average length of the shortest and longest branchiostegals multiplied by the total number of rays (brl), snout length (snl), eye diameter (ed), post-orbital length (pol), head depth measured at the hyomandibula-opercular joint (hd), and length of the gill opening (gol). All data were log-transformed prior to analysis.

All character analyses were conducted in R (R Core Team, 2013). We first pruned our maximum clade credibility tree to include only the 24 taxa for which we had continuous characters using the *drop.tip* function in the *ape* package (Pardis et al., 2004). We used the *phyl.resid* function in the *phytools* package (Revell, 2009; Revell, 2012) to obtain the residuals from PGLS regressions (all characters regressed against standard length), and these residuals were used as phylogenetically size corrected data for PGLS and PCA analyses, as recommended by Revell (2009). Phylogenetic generalized least squares analyses were performed for each of pair of size-corrected linear measurements using the *gls* function in the *nlme* package (Pinheiro et al., 2014) by applying a Brownian correlation structure based on phylogenetic difference using the *corBrownian* function in the *ape* package (Pardis et al., 2004). A phylogenetically corrected principal components analysis was run using the *phyl.pca* function in the *phytools* package (Revell, 2009; Revell, 2012), and a plot of PC1 and PC2, including loadings, was graphed using the *biplot* function in the *stats* package (R Core Team, 2013). We also used the *contMap* function in the *phytools* package (Revell, 2012) to visualize three continuous characters (lower jaw length, opercular length, and average branchiostegal length) on our pruned phylogeny.

Results

Phylogenetic reconstruction

Among the four trees tested (RAxML tree, two MrBayes consensus trees, and maximum clade credibility tree), the maximum clade credibility tree best fit the data, although the two MrBayes consensus trees were not significantly different from the best tree (Table 1). The maximum likelihood tree did not fit the molecular dataset as well as the best tree and showed low bootstrap values for internal nodes (Appendix 3, Figure 1). All trees recovered the Cottoidei and Cottoidea clades proposed by Smith and Busby (2014), with differing levels of support

(Table 1). The maximum clade credibility tree (Appendix 3, Figure 2) based on the best MrBayes run was pruned (Figure 2) and used for character analysis.

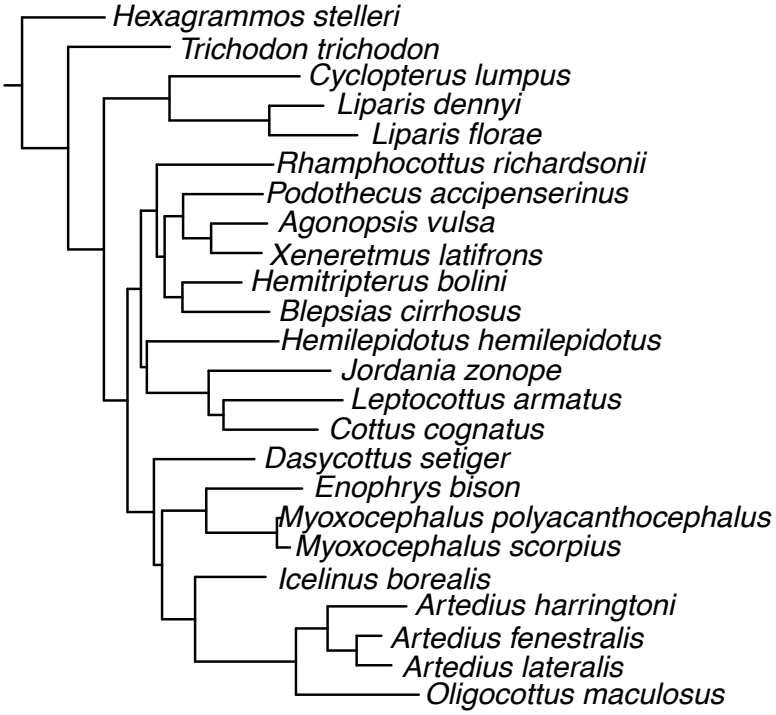

Figure 2. Pruned cottoid phylogeny. This is the pruned tree of 24 taxa used for analysis of continuous characters.

Character Analysis

Table 2 and Figure 3 summarize the results of the phylogenetic generalized least squares analyses. Opercular length was closely correlated with upper jaw length, lower jaw length, and mouth opening diameter. Average branchiostegal length showed weak correlation with opercular length, upper jaw length, lower jaw length, and mouth opening diameter. Maps of phylogenetically size-corrected continuous characters (Figure 4) show that lower jaw length, opercular length, and average branchiostegal length change across the phylogeny, with multiple transitions to small and large values for all three characters. Lower jaw length and opercular length have very similar continuous character maps, while the character map for average

branchiostegal length shows more instances of reductions across the phylogeny. The principal components analysis (Figure 5) indicated that upper jaw length, lower jaw length, mouth opening diameter, and opercular length are closely correlated, but that average branchiostegal length is not closely correlated with these feeding traits.

Table 2. PGLS results. P-values were calculated from phylogenetic generalized least squares analyses to determine the relative degree of correlation among continuous characters.

	ed	pol	brl	ujl	ljl	mod	ol	hd	gol
snl	0.1226	0.0011	0.0119	0.0165	0.1611	0.0072	0.0048	0.0314	0.1612
ed	X	0.0025	0.6201	0.0908	0.0607	0.0305	0.0036	0.0082	0.0003
pol		X	0.0131	< 0.0001	0.0002	< 0.0001	< 0.0001	< 0.0001	< 0.0001
brl			X	0.0032	0.03	0.0126	0.024	0.1198	0.0503
ujl				X	< 0.0001	< 0.0001	< 0.0001	0.0331	< 0.0001
ljl					X	< 0.0001	0.0001	0.0446	< 0.0001
mod						X	< 0.0001	0.0192	0.0001
ol							X	< 0.0001	< 0.0001
hd								X	0.0001
gol									X

0.05 > p > 0.01
p > 0.001
p >= 0.0001
p < 0.0001

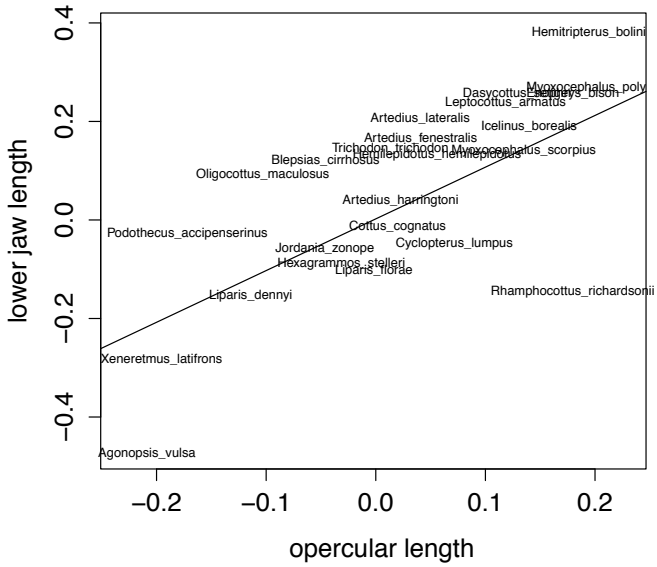

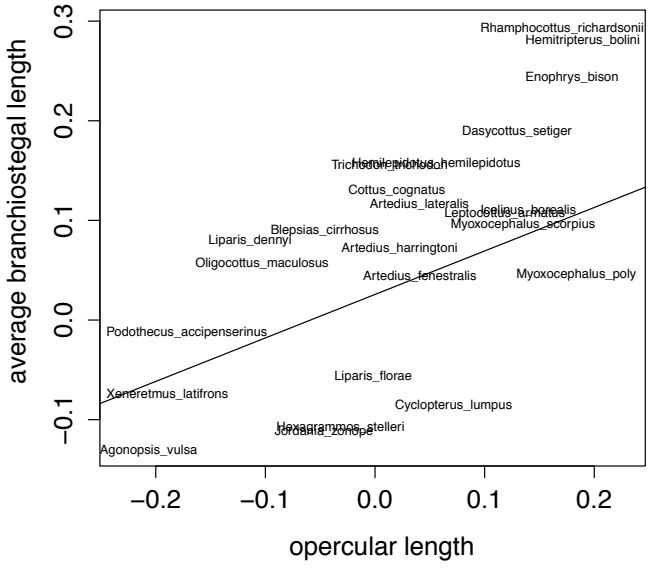

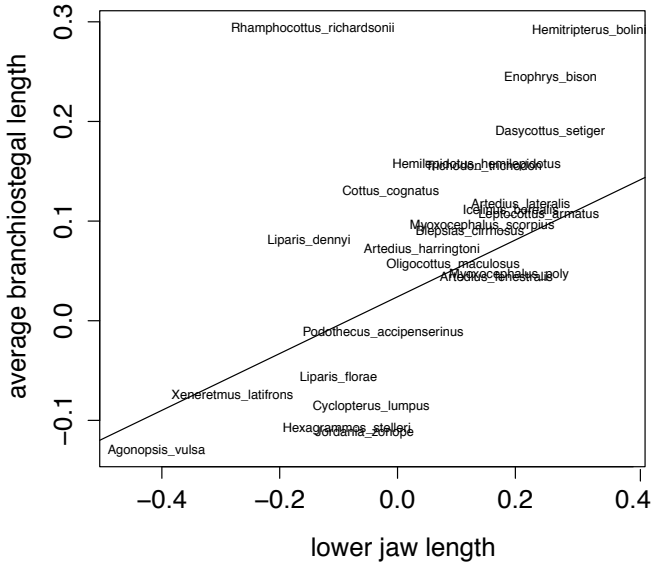

Figure 3. Bivariate plots of Phylogenetic Generalized Least Squares models. There is a strong correlation between opercular length and lower jaw length (top; p = 0.0001), but the correlations between opercular length and branchiostegal length (middle; p = 0.024) and branchiostegal length and lower jaw length (bottom; p = 0.030) were considerably weaker.

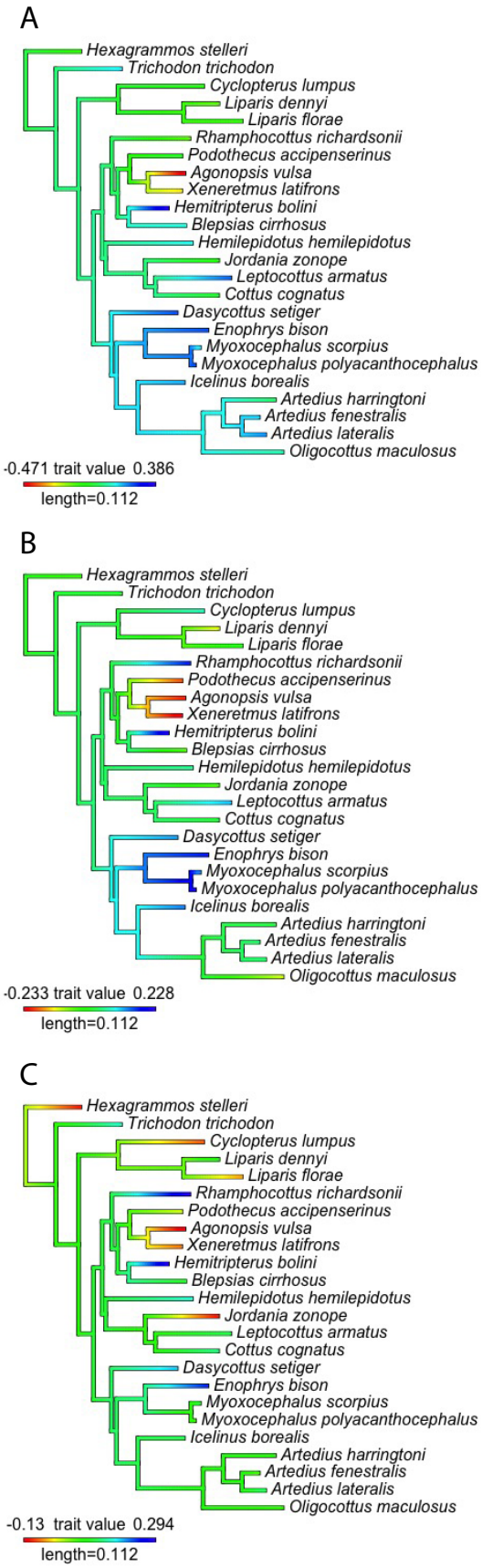

Figure 4. Color maps of continuous characters. Three continuous characters are shown visually to demonstrate the patterns of character evolution across the cottoid phylogeny. Lower jaw length (A) and opercular length (B) share a similar pattern, while average branchiostegal length (C) shows more instances of reduction**.**

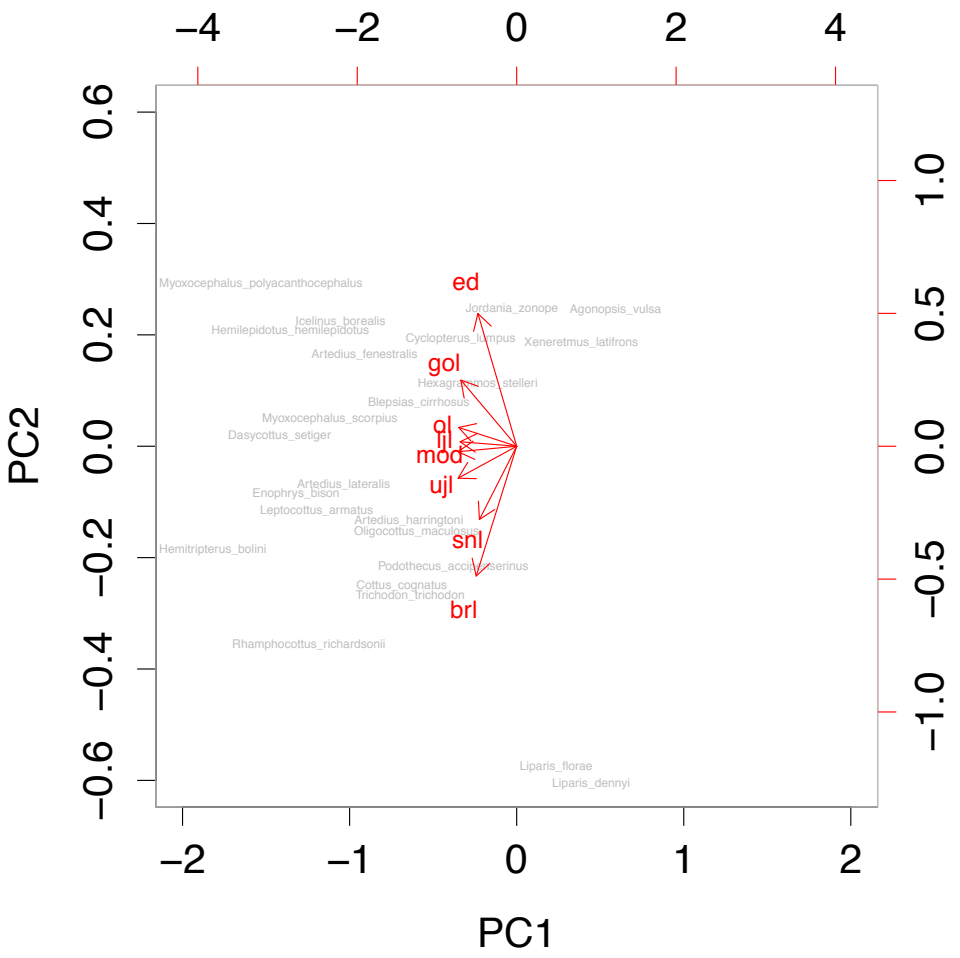

Figure 5. Phylogenetically corrected Principal Component Analysis. Upper jaw length, lower jaw length, mouth opening diameter, and opercular length are all closely correlated. This forms a suite of feeding-associated, co-evolving traits. Average length of branchiostegals is not closely correlated with these feeding traits.

Discussion

Phylogenetic Reconstruction

Our maximum clade credibility tree generally agrees with previous studies of phylogenetic relationships among cottoids, particularly in that we recovered Cottoidei, Cottoidea (*sensu* Smith and Busby, 2014), and a large monophyletic group of marine sculpins (Knope, 2013 (unnamed clade); Smith and Busby, 2014 (Psychrolutidae); Buser and Andrés López, 2015

(unnamed clade)). The placement of the monotypic genera *Rhamphocottus*, *Jordania*, and *Leptocottus* within Cottoidea conflicts with previous studies (Knope, 2013; Smith and Busby, 2014). These are problematic taxa, typically recovered at various positions among the non-psychrolutid cottoids with low node support (Knope, 2013; Smith and Busby, 2014).

Character Analysis – Suction Feeding

There is tight evolutionary integration among structures associated with suction feeding (opercle, lower jaw, and upper jaw) within the cottoids studied. This is supported by our phylogenetic generalized least squares bivariate comparisons (Table 2, Figure 3) as well as our observation that these characters co-evolve as a suite of evolutionarily correlated traits (Figure 5). The opercular bones (opercle, subopercle, and interopercle), via a ligamentous connection between the interopercle and the jaw joint, form a critical linkage in the rapid expansion that characterizes suction feeding (Anker, 1974). During this expansion, the opercular bones rotate dorsally by contraction of the levator operculi, contributing to lower jaw depression (Liem, 1970; Lauder, 1982a; Camp and Brainerd, 2015). While the evolutionary integration of suction feeding components is considered to be common knowledge among those that study the evolutionary morphology of fishes, it has rarely been demonstrated empirically (Holzman et al., 2008; Collar et al., 2014). We demonstrate this relationship here within a clade of diverse suction feeding fishes.

The gill chamber also expands during suction feeding (Lauder, 1980). The opercular bones, in addition to their role in depressing the lower jaw, form part of the lateral wall of the gill chamber and contribute to expansion of the gill chamber. The branchiostegals form part of the lateral and ventral wall of the gill chamber, and they also contribute to gill chamber expansion during suction feeding (Liem, 1978). However, gill chamber expansion has been shown to have

little influence on suction feeding pressures (Lauder, 1980; Lauder, 1982b) and has not been demonstrated to impact suction feeding performance other than potentially limiting backflow of water into the buccal chamber (Liem, 1978). Therefore, the tight correlation of opercular length with the length of the jaws is likely due to its role in depression of the lower jaw and not its role in gill chamber expansion during suction feeding. The lack of strong evolutionary correlation among the branchiostegals and other suction-feeding associated structures is likely explained by the lack of a strong role of the branchiostegals in suction feeding performance.

Character Analysis – Gill Ventilation

We predicted that opercular length would show a high degree of evolutionary integration with average branchiostegal length due to the shared role of these structures in expanding and contracting the gill chamber during ventilation (Hughes, 1960). However, these two characters showed only a weak evolutionary correlation (Table 2). We propose that the operculum evolves in response to strong selective pressures on the feeding system, while the branchiostegals evolve in response to selective pressure on ventilation. This is supported by the observation that the size of the branchiostegal apparatus is often an indication of gill ventilatory ecology, with slow breathing and bottom-dwelling fishes having considerably larger branchiostegal rays (Baglioni, 1907; Hughes, 1960; Farina, unpublished manuscript). Therefore, the gill ventilatory system is likely evolutionarily modular, with the branchiostegal apparatus as one of its primary modular components.

Functional Coupling

The overlap in structures associated with suction feeding and gill ventilation offers an unprecedented opportunity to examine co-evolving structures and coupled functions. There are distinct differences in the kinematics and pressure profiles observed during gill ventilation and

suction feeding, including substantial differences in the relative magnitudes of pressures between the buccal and gill chambers (Hughes, 1960; Lauder, 1980). Also, suction feeding often involves extreme protrusion of the upper jaw, while movement of the upper jaw is absent in typical gill ventilation. Suction feeding is therefore not simply an amplified gill ventilatory cycle but is instead a distinct suite of behaviors, and there are likely different selective pressures acting upon suction feeding and gill ventilation mechanics. The relatively weak evolutionary correlation of the branchiostegals with structures associated with suction-feeding indicates that the branchiostegals are possibly the modular component most susceptible to selective pressures that acting specifically on active gill ventilatory mechanics.

The coupling of functions is a topic that is typically addressed in the context of the evolutionary consequences of decoupling. Functional decoupling occurs when two functions that were previously performed by one anatomical system evolve to be performed by multiple anatomical systems (Wainwright, 2007). For example, prey capture and prey processing are typically both performed by the oral jaws of fishes, but in many species, the gill arches have developed into pharyngeal jaws with specializations for prey processing (e.g., Liem, 1973; Liem, 1986; Sibbing et al., 1986). Such functional decoupling is a major theme in the evolution of vertebrates, and it has been demonstrated to produce rapid phenotypic evolution (Lauder, 1981). Similarly, functional coupling can constrain morphological evolution (Tsuboi et al., 2015), because a set of anatomical characters performing multiple functions will be limited by the constraints all of the functions. However, if one of those functions requires a high degree of evolutionary integration, as in suction feeding, the constraint from both coupling and integration may severely limit potential for morphological evolution. Other suction-feeding vertebrates, including lungfishes and some elasmobranchs, have limited this problem by decreasing the level

of coupling between feeding and ventilatory structures through anatomical specializations of the suction feeding system (Bemis and Lauder, 1986; Bemis, 1987a,b; Motta et al., 2002). However, suction-feeding ray-finned fishes have maintained an extremely close anatomical coupling between the two functions. Our study suggests that the presence of modularity in gill ventilation provides partial decoupling. The branchiostegal apparatus may be a source of modularity within the gill ventilatory system that releases some of the constraint imposed by the close coupling of feeding and ventilation.

Acknowledgements

This chapter was written in collaboration with Matthew Knope, Katherine Corn, Adam Summers, and William E. Bemis. We would like to thank Amy McCune and Harry Greene for their feedback on the conceptual findings of this study. We would also like to thank the faculty and students of Cornell University's ENTOM 4610 Model-Based Phylogenetics 2015 course, especially Elizabeth Murray. For assistance with specimen collection and curation, we thank Charles Dardia, David Duggins, Kristy Kull, Petra Ditsche, Stephanie Crofts, Nicholas Gidmark, John Friel, Friday Harbor Laboratories, and the Cornell University Museum of Vertebrates. This research was supported by an NSF Doctoral Dissertation Improvement Grant (DEB-1310812) awarded to Stacy C. Farina and William E. Bemis and a Graduate Research Award from the Stephen and Ruth Wainwright Endowment from Friday Harbor Laboratories.

REFERENCES

Anker G. C. 1974. Morphology and kinetics of the head of the stickleback, *Gasterosteus aculeatus*. The Transactions of the Zoological Society of London 32:311-416.

Baglioni, S. 1907. Der Atmungsmechanismus der Fische. Ein Beitrag zur vergleichenden Physiologie des Atemrhythmus. Zeitschrift für allgemeine Physiologie 7:177-282.

Bels, V. L., M. Chardon, and K. V. Kardong. 1994. Biomechanics of the hyolingual system in squamata. Pages 197-240 *in* Bels V. L., M. Chardon, and P. Vandewalle, eds. Biomechanics of Feeding in Vertebrates. Springer Berlin Heidelberg.

Bemis, W. E., and G. V. Lauder. 1986. Morphology and function of the feeding apparatus of the lungfish, *Lepidosiren paradoxa* (Dipnoi). Journal of Morphology 187:81-108.

Bemis, W. E. 1987a. Feeding systems of living Dipnoi: Anatomy and function. IN: *The Biology and Evolution of Lungfishes*. W. E. Bemis, W.W. Burggren, and N.E. Kemp, eds. Alan Liss, N. Y. pp. 249-275.

Bemis, W. E. 1987b. Convergent evolution of jaw opening muscles in lungfishes and tetrapods. Canadian Journal of Zoology 65:2814-2817.

Benson, D. A., M. Cavanaugh, K. Clark, I. Karsch-Mizrachi, D. J. Lipman, J. Ostell, and E. W. Sayers. 2013. GenBank. Nucleic acids research 41(D1):D36-D42.

Buser, T.J., and J. Andrés López. 2015. Molecular phylogenetics of sculpins of the subfamily Oligocottinae (Cottidae). Molecular Phylogenetics and Evolution 86:64-74.

Camp, A. L., and E. L. Brainerd. 2015. Reevaluating musculoskeletal linkages in suction-feeding fishes with x-ray reconstruction of moving morphology (XROMM). Integrative and Comparative Biology doi: 10.1093/icb/icv034.

Cheverud, J.M. 1982. Phenotypic, genetic, and environmental morphological integration in the cranium. Evolution 36:499-516.

Cheverud, J. M. 1996. Developmental integration and the evolution of pleiotropy. American Zoologist 36:44-50.

Claverie, T., and S. N. Patek. 2013. Modularity and rates of evolutionary change in a power-amplified prey capture system. Evolution 67(11):3191-3207.

Collar, D. C., P. C. Wainwright, M. E. Alfaro, L. J. Revell, and R. S. Mehta. 2014. A novel feeding mode disrupts evolutionary integration of the skull in eels. Nature Communications 5:5505.

Darriba, D., G. L. Taboada, R. Doallo, and D. Posada. 2012. jModelTest 2: more models, new heuristics and parallel computing. Nature Methods 9(8):772.

Guindon S., and O. Gascuel. 2003. A simple, fast and accurate method to estimate large phylogenies by maximum-likelihood. Systematic Biology 52:696-704.

Edgar, R. C. 2004. MUSCLE: multiple sequence alignment with high accuracy and high throughput. Nucleic acids research 32(5):1792-1797.

Felsenstein, J. 1981. Evolutionary trees from DNA sequences: a maximum likelihood approach. Journal of Molecular Evolution 17:368-376.

Gould, S. J., and R. C. Lewontin. 1979. The spandrels of San Marco and the Panglossian paradigm: a critique of the adaptationist programme. Proceedings of the Royal Society of London B 205:581-598.

Holzman, R., S. W. Day, R. S. Mehta, and P. C. Wainwright. 2008. Integrating the determinants of suction feeding performance in centrarchid fishes. Journal of Experimental Biology 211:3296-3305.

Hughes, G. M. 1960. A comparative study of gill ventilation in marine teleosts. Journal of Experimental Biology 37:28-45.

Kane, E. A., and T. E. Higham. 2015. Complex systems are more than the sum of their parts: using integration to understand performance, biomechanics, and diversity. Integrative and Comparative Biology doi: 10.1093/icb/icv033.

Klingenberg, C. P. 2008. Morphological integration and developmental modularity. Annual review of ecology, evolution, and systematics 39:115-132.

Knope, M. L. 2013. Phylogenetics of the marine sculpins (Teleostei: Cottidae) of the North American Pacific Coast. Molecular Phylogenetics and Evolution 66:341-349.

Lauder, G. V. 1980. The suction feeding mechanism in sunfishes (Lepomis): an experimental analysis. Journal of Experimental Biology 88:49-72.

Lauder G. V. 1981. Form and function: structural analysis in evolutionary morphology. Paleobiology 7:430-442.

Lauder, G. V. 1982a. Patterns of evolution in the feeding mechanism of actinopterygian fishes. American Zoologist 22:275-285.

Lauder, G. V. 1982b. Prey capture hydrodynamics in fishes: experimental tests of two models. Journal of Experimental Biology 104:1-13.

Li , W., A. Cowley, M. Uludag, T. Gur, H. McWilliam, S. Squizzato, Y. M. Park, N. Buso, and R. Lopez. 2015. The EMBL-EBI bioinformatics and programmatic tools framework. Nucleic Acids Research doi:10.1093/nar/gkv279

Liem, K. F. 1970. Comparative functional anatomy of the Nandidae (Pisces: Teleostei). Fieldiana 56:1-166.

Liem, K. F. 1973. Evolutionary strategies and morphological innovations: cichlid pharyngeal jaws. Systematic Zoology 22:425-41

Liem, K. F. 1978. Modularity multiplicity in the functional repertoire of the feeding mechanism in chichlid fishes. I. Piscivores. Journal of Morphology 158:323-360.

Liem, K. F. 1986. The pharyngeal jaw apparatus of the Embiotocidae (Teleostei): a functional and evolutionary perspective Copeia 2:311-323.

Motta, P. J., R. E. Hueter, T. C. Tricas, and A. P. Summers. 2002. Kinematic analysis of suction feeding in the nurse shark, *Ginglymostoma cirratum* (Orectolobiformes, Ginglymostomatidae). Copeia 2002:24-38.

Norton, S. F. 1995. A functional approach to ecomorphological patterns of feeding in cottid fishes. Environmental Biology of Fishes 44:61-78.

Olson, E. C., and R. L. Miller. 1958. Morphological Integration. University of Chicago Press.

Paradis, E., J. Claude, and K. Strimmer. 2004. APE: analyses of phylogenetics and evolution in R language. Bioinformatics 20:289-290.

Pinheiro, J., D. Bates, S. DebRoy, D. Sarkar, and R Core Team. 2014. nlme: Linear and Nonlinear Mixed Effects Models. R package version 3.1-115.

Rambaut, A., M. A. Suchard, D. Xie, and A. J. Drummond. 2014. Tracer v1.6. Available from http://beast.bio.ed.ac.uk/Tracer.

Ramon, M. L., and M. L. Knope. 2008. Molecular support for marine sculpin (Cottidae; Oligocottinae) diversification during the transition from the subtidal to intertidal habitat in the Northeastern Pacific Ocean. Molecular Phylogenetics and Evolution 46:475-483.

Revell, L. J. 2009. Size-correction and principal components for interspecific comparative studies. Evolution 63:3258-3268.

Revell, L. J. 2012. phytools: An R package for phylogenetic comparative biology (and other things). Methods in Ecology and Evolution 3:217-223.

Ronquist, F., M. Teslenko, P. van der Mark, D. L. Ayres, A. Darling, S. Höhna, B. Larget, L. Liu, M. A. Suchard, and J. P. Huelsenbeck. 2012. MrBayes 3.2: efficient Bayesian phylogenetic inference and model choice across a large model space. Systematic Biology 61(3): 539-542.

Sibbing, F. A., J. W. M. Osse, and A. Terlouw. 1986. Food handling in the carp (Cyprinus carpio): its movement patterns, mechanisms, and limitations. Journal of Zoology 210:161-203.

Smith, W. L., and M. S. Busby. 2014. Phylogeny and taxonomy of sculpins, sandfishes, and snailfishes (Perciformes: Cottoidei) with comments on the phylogenetic significance of their early-life-history specializations. Molecular Phylogenetics and Evolution 79:332-352.

Smith, W. L., and W. C. Wheeler. 2004. Polyphyly of the mail-cheeked fishes (Teleostei: Scorpaeniformes): Evidence from mitochondrial and nuclear sequence data. Molecular Phylogenetics and Evolution 32:627-646.

Stamatakis, A. 2014. RAxML Version 8: A tool for Phylogenetic Analysis and Post-Analysis of Large Phylogenies. Bioinformatics 10.1093/bioinformatics/btu033

Tavaré, S. 1986. Some probabilistic and statistical problems in the analysis of DNA sequences. Lectures on mathematics in the life sciences 17:57-86.

Tsuboi, M., A. Gonzalez-Voyer, and N. Kolm. 2015. Functional coupling constrains craniofacial diversification in Lake Tanganyika cichlids. Biology Letters doi: 10.1098/rsbl.2014.1053.

Wainwright, P. C. 2007. Functional versus morphological diversity in macroevolution. Annual Review of Ecology, Evolution, and Systematics 38:381-401.

Wainwright, P. C., M. D. McGee, S. J. Longo, and L. P. Hernandez. 2015. Origins, innovations, and diversification of suction feeding in vertebrates. Integrative and Comparative Biology doi: 10.1093/icb/icv026.

Yabe, M. 1985. Comparative osteology and myology of the superfamily Cottoidea (Pisces: Scorpaeniformes) and its phylogenetic classification. Memoirs of the Faculty of Fisheries-Hokkaido University (Japan).

APPENDIX 1

Order	Family	RGO	Morphological Survey Taxa	Catalogue Number	Taxa Used for Phylogenetics
Polypteriformes	Polypteridae		*Polypterus palmas*	CUMV89480	*Polypterus ornatipinnis* *Erpetoichthys calabaricus*
Acipenseriformes	Acipenseridae	9%	*Acipenser fulvescens*	CUMV28111	*Scaphirhynchus platorynchus*
	Polyodontidae		*Polyodon spathula*	CUMV7927	*Polyodon spathula*
Lepisosteiformes	Lepisosteidae		*Lepisosteus osseus*	CUMV4639	*Atractosteus spatula*
Amiiformes	Amiidae		*Amia calva*	CUMV18959	*Amia calva*
Hiodontiformes	Hiodontidae		*Hiodon tergisus*	CUMV24090	*Hiodon tergisus*
Osteoglossiformes	Osteoglossidae		*Arapaima gigas*	CUMV78428	*Arapaima gigas*
	Notopteridae		*Papyrocranus afer*	CUMV71629	*Chitala chitala*
	Mormyridae	17%	*Mormyrops caballus*	CUMV93220	*Gnathonemus petersii*
	Gymnarchidae		*Gymnarchus niloticus*	CUMV80334	*Gymnarchus niloticus*
Elopiformes	Elopidae		*Elops lacerta*	CUMV64172	*Elops saurus*
	Megalopidae		*Megalops atlanticus*	CUMV13248	*Megalops atlanticus*
Albuliformes	Albulidae		*Albula vulpes*	CUMV56032	*Albula vulpes*
	Halosauridae		*Halosaurus ovenii*	CUMV48227	*Aldrovandia affinis*
	Notacanthidae		*Notacanthus chemnitzii*	ANSP109419	
Anguilliformes	Anguillidae	26%	*Anguilla rostrata*	CUMV92992	*Anguilla rostrata*
	Heterenchelyidae	14%	*Pythonichthys macrurus*	ANSP112261	
	Moringuidae	24%	*Moringua edwardsi*	CUMV44221	
	Chlopsidae	26%	*Chilorhinus platyrhynchus*	CUMV71610	
	Myrocongridae[1]				
	Muraenidae	50%	*Gymnothorax miliaris*	CUMV78439	*Echidna rhodochilus*
	Synaphobranchidae	10%	*Simenchelys parasitica*	CUMV53525	
	Ophichthidae	13%	*Myrichthys maculosus*	MCZ100513	*Myrichthys maculosus*
	Colocongridae	23%	*Coloconger meadi*	ANSP114943	
	Derichthyidae	19%	*Derichthys serpentinus*	ANSP130811	
	Muraenesocidae	9%	*Muraenesox bagio*	ANSP90504	
	Nemichthyidae	10%	*Nemichthys scolopaceus*	ANSP158360	
	Congridae	79%	*Conger oceanicus*	CUMV17048	*Conger oceanicus*

	Nettastomatidae	25%	*Nettastoma melanurum*	MCZ49338	
	Serrivomeridae	8%	*Serrivomer sector*	CUMV53534	*Serrivomer beanii*
Saccopharyngiformes	Cyematidae	11%	*Cyema atrum*	ANSP152121	
	Saccopharyngidae	15%	*Saccopharynx ampullaceus*	MCZ161545	*Saccopharynx ampullaceus*
	Eurypharyngidae	4%	*Eurypharynx pelecanoides*	UW110912	*Eurypharynx pelecanoides*
	Monognathidae	26%	*Monognathus jesperseni*	MCZ164702	
Clupeiformes	Denticipitidae		*Denticeps clupeoides*	MCZ56428	*Denticeps clupeoides*
	Pristigasteridae		*Pristigaster cayana*	CUMV81229	
	Engraulidae		*Anchoa hepsetus*	CUMV6943	
	Chirocentridae		*Chirocentrus dorab*	ANSP63417	
	Clupeidae		*Alosa mediocris*	CUMV43116	*Alosa pseudoharengus*
Gonorynchiformes	Chanidae		*Chanos chanos*	CUMV13313	*Chanos chanos*
	Gonorynchidae	9%	*Gonorynchus gonorynchus*	ANSP37748	*Gonorynchus greyi*
	Kneriidae	39%	*Parakneria abbreviata*	CUMV95146	*Cromeria nilotica*
	Phractolaemidae	19%	*Phractolaemus ansorgii*	ANSP141230	*Phractolaemus ansorgii*
Cypriniformes	Cyprinidae[2]	4%	*Carassius auratus*	CUMV27637	*Danio rerio*
	Psilorhynchidae[3]				
	Gyrinocheilidae	16%	*Gyrinocheilus aymonieri*	ANSP76836	
	Catostomidae	9%	*Catostomus commersonii*	CUMV84513	*Hypentelium nigricans*
	Cobitidae	24%	*Misgurnus fossilis*	CUMV131	
	Balitoridae	22%	*Balitora brucei*	CUMV46756	
Characiformes	Distichodontidae	6%	*Distichodus hypostomatus*	CUMV92198	*Distichodus maculatus*
	Citharinidae	< 1%	*Citharinus citharus*	CUMV86448	
	Parodontidae	< 1%	*Parodon apolinari*	CUMV78546	
	Curimatidae	1%	*Curimata mivartii*	CUMV47932	
	Prochilodontidae	6%	*Prochilodus magdalenae*	CUMV47931	
	Anostomidae	10%	*Leporellus sp.*	CUMV89289	*Leporinus copelandii*
	Chilodontidae	10%	*Caenotropus labyrinthicus*	CUMV3239	
	Crenuchidae		*Characidium boavistae*	CUMV78672	
	Hemiodontidae		*Hemiodus unimaculatus*	CUMV3254	
	Alestiidae		*Hydrocynus forskahlii*	CUMV81265	*Phenacogrammus interruptus*
	Gasteropelecidae		*Thoracocharax stellatus*	CUMV2820	
	Characidae		*Serrasalmus irritans*	CUMV3276	*Brycon pesu*
	Acestrorhynchidae		*Acestrorhynchus falcatus*	ANSP189374	
	Cynodontidae		*Rhaphiodon vulpinus*	CUMV3232	

	Erythrinidae		*Hoplerythrinus unitaeniatus*	CUMV84682	
	Lebiasinidae		*Lebiasina erythrinoides*	CUMV90158	
	Ctenoluciidae		*Ctenolucius hujeta*	CUMV46360	
	Hepsetidae		*Hepsetus odoe*	CUMV89981	
Siluriformes	Diplomystidae	< 1%	*Diplomystes nahuelbutaensis*	ANSP180476	
	Cetopsidae	22%	*Cetopsis coecutiens*	CUMV81302	
	Amphiliidae		*Amphilius cryptobullatus*	CUMV91058	
	Trichomycteridae	4%	*Trichomycterus sp.*	CUMV78771	
	Nematogenyidae	4%	*Nematogenys inermis*	ANSP177934	*Nematogenys inermis*
	Callichthyidae	19%	*Callichthys callicthys*	CUMV2739	*Corydoras aurofrenatus*
	Scoloplacidae	29%	*Scoloplax distolothrix*	ANSP181058	
	Astroblepidae	23%	*Astroblepus sp.*	CUMV78780	
	Loricariidae	30%	*Chaetostoma milesi*	CUMV83743	
	Amblycipitidae		*Amblyceps mangois*	ANSP59374	
	Akysidae	14%	*Akysis sp.*	CUMV46783	
	Sisoridae	8%	*Glyptothorax major*	ANSP178713	
	Erethistidae	23%	*Hara horai*	CUMV46782	
	Aspredinidae	32%	*Aspredo aspredo*	CUMV80324	
	Pseudopimelodidae	2%	*Pseudopimelodus pulcher*	CUMV94045	
	Heptapteridae		*Rhamdia quelen*	ANSP85118	
	Cranoglanididae		*Cranoglanis bouderius*	CUMV82701	*Cranoglanis bouderius*
	Ictaluridae		*Ameiurus natalis*	CUMV95041	*Ameiurus natalis*
	Mochokidae	34%	*Synodontis haugi*	CUMV92370	
	Doradidae	21%	*Oxydoras niger*	CUMV80953	
	Auchenipteridae[2]	44%	*Trachelyopterus galeatus*	CUMV76235	
	Siluridae		*Silurus asotus*	CUMV22749	
	Malapteruridae	32%	*Malapterurus beninensis*	CUMV90006	
	Auchenoglanididae		*Auchenoglanis occidentalis*	CUMV88150	
	Chacidae	39%	*Chaca sp.*	CUMV81201	
	Plotosidae		*Tandanus tandanus*	CUMV72818	
	Clariidae		*Clarias gariepinus*	CUMV93817	
	Heteropneustidae		*Heteropneustes fossilis*	CUMV46784	
	Austroglanidae		*Austroglanis sclateri*	CUMV90981	
	Claroteidae[4]				
	Ariidae	17%	*Ariopsis felis*	CUMV6814	

	Schilbeidae		*Schilbe mystus*	CUMV89969	
	Pangasiidae	< 1%	*Pangasius pangasius*	ANSP85769	
	Bagridae		*Bagrus docmak*	CUMV89952	
	Pimelodidae		*Hemisorubim platyrhynchos*	CUMV80959	
Gymnotiformes	Gymnotidae	13%	*Gymnotus carapo*	CUMV72147	*Electrophorus electricus*
	Rhamphichthyidae	25%	*Rhamphichthys marmoratus*	CUMV72371	*Gymnorhamphichthys petiti*
	Hypopomidae	24%	*Brachyhypopomus beebei*	CUMV83833	
	Sternopygidae	17%	*Rhabdolichops sp.*	CUMV82348	*Eigenmannia macrops*
	Apteronotidae	36%	*Apteronotus bonapartii*	CUMV72176	*Apteronotus albifrons*
Argentiniformes	Argentinidae		*Argentina silus*	CUMV17041	*Argentina silus*
	Opisthoproctidae	17%	*Opisthoproctus soleatus*	MCZ41536	*Macropinna microstoma*
	Microstomatidae		*Leuroglossus stilbius*	CUMV94349	*Bathylagus euryops*
	Platytroctidae		*Persparsia kopua*	CUMV95105	*Searsia koefoedi*
	Bathylaconidae		*Bathylaco nigricans*	MCZ140994	*Bathylaco nigricans*
	Alepocephalidae		*Alepocephalus agassizii*	ANSP69950	*Alepocephalus agassizii*
Osmeriformes	Osmeridae		*Osmerus mordax*	CUMV68457	*Osmerus mordax*
	Retropinnidae		*Retropinna semoni*	CUMV72817	*Retropinna semoni*
	Galaxiidae		*Galaxias sp.*	CUMV51998	*Galaxias maculatus*
Salmoniformes	Salmonidae		*Oncorhynchus kisutch*	CUMV23367	*Salvelinus alpinus*
Escociformes	Escoidae		*Esox americanus*	CUMV94915	*Esox americanus*
	Umbridae		*Umbra limi*	CUMV33447	*Umbra limi*
Stomiiformes	Diplophidae		*Diplophos taenia*	CUMV53441	
	Gonostomatidae		*Gonostoma elongatum*	CUMV53512	*Gonostoma elongatum*
	Sternoptychidae		*Argyropelecus gigas*	CUMV46913	*Argyropelecus gigas*
	Phosichthyidae		*Phosichthys argenteus*	CUMV95103	*Polymetme sp.*
	Stomiidae		*Stomias atriventer*	CUMV91948	*Neonesthes capensis*
Ateleopodiformes	Ateleopodidae		*Ijimaia antillarum*	MCZ148518	*Ijimaia loppei*
Aulopiformes	Paraulopidae[5]				
	Aulopidae		*Aulopus filamentosus*	CUMV48228	
	Pseudotrichonotidae[6]				
	Synodontidae		*Saurida undosquamis*	CUMV79717	*Synodus foetens*
	Bathysauroididae[6]				
	Chlorophthalmidae		*Parasudis fraserbrunneri*	CUMV48222	
	Bathysauropsidae		*Bathysauropsis gracilis*	MCZ130274	
	Notosudidae		*Scopelosaurus adleri*	UW117154	

	Ipnopidae		*Bathypterois bigelowi*	MCZ40536	*Bathypterois atricolor*
	Scopelarchidae		*Scopelarchoides nicholsi*	CUMV53511	*Benthalbella infans*
	Evermannellidae		*Evermannella indica*	CUMV54066	
	Alepisauridae		*Alepisaurus ferox*	MCZ40540	*Alepisaurus ferox*
	Paralepididae		*Stemonosudis gracilis*	CUMV55838	*Anotopterus pharao*
	Bathysauridae		*Bathysaurus ferox*	MCZ138024	
	Giganturidae	26%	*Gigantura chuni*	MCZ164306	
Myctophiformes	Neoscopelidae		*Neoscopelus macrolepidotus*	CUMV44185	*Neoscopelus macrolepidotus*
	Myctophidae		*Lampanyctus australis*	CUMV95108	*Krefftichthys anderssoni*
Lampriformes	Veliferidae[7]				
	Lampridae		*Lampris guttatus*	MCZ36628	*Lampris guttatus*
	Stylephoridae	4%	*Stylephorus chordatus*	CUMV46907	*Stylephorus chordatus*
	Lophotidae		*Eumecichthys fiski*	UW041480	
	Radiicephalidae				
	Trachipteridae	< 1%	*Trachipterus fukuzakii*	CUMV69222	*Trachipterus arcticus*
	Regalecidae		*Regalecus glesne*	CUMV73847	*Regalecus glesne*
Polymixiiformes	Polymixiidae		*Polymixia japonica*	CUMV56045	*Polymixia japonica*
Percopsiformes	Percopsidae	2%	*Percopsis omiscomaycus*	CUMV2109	*Percopsis omiscomaycus*
	Aphredoderidae	3%	*Aphredoderus sayanus*	CUMV94993	*Aphredoderus sayanus*
	Amblyopsidae	4%	*Amblyopsis spelaea*	CUMV64871	*Chologaster cornuta*
Gadiformes	Muraenolepididae		*Muraenolepis microps*	MCZ52359	*Muraenolepis microps*
	Bregmacerotidae		*Bregmaceros arabicus*	MCZ109216	
	Euclichthyidae[8]				
	Macrouridae	4%	*Coelorinchus caelorhincus*	CUMV43865	*Coryphaenoides rupestris*
	Moridae	< 1%	*Mora moro*	CUMV51289	
	Melanonidae		*Melanonus gracilis*	CUMV95099	
	Merlucciidae		*Merluccius albidus*	CUMV44071	
	Phycidae		*Urophycis tenuis*	CUMV43925	
	Gadidae		*Gadus morhua*	CUMV90895	*Gadus morhua*
Ophidiiformes	Carapidae		*Carapus sp.*	CUMV81861	*Onuxodon parvibrachium*
	Ophidiidae	3%	*Lepophidium profundorum*	CUMV46266	*Brotula multibarbata*
	Bythitidae		*Ogilbia cayorum*	CUMV43422	*Brosmophycis marginata*
	Aphyonidae		*Barathronus bicolor*	MCZ45999	*Barathronus maculatus*
	Parabrotulidae		*Parabrotula plagiophthalma*	MCZ149551	
Batrachoidiformes	Batrachoididae[2]	29%	*Opsanus tau*	CUMV12890	*Porichthys notatus*

Lophiiformes	Lophiidae	46%	*Lophius americanus*	CUMV51214	*Lophius americanus*
	Antennariidae	26%	*Histrio histrio*	CUMV79649	*Histiophryne cryptacanthus*
	Tetrabrachiidae	55%	*Tetrabrachium ocellatum*	UW021021	
	Lophichthyidae[9]				
	Brachionichthyidae	55%	*Brachiopsilus ziebelli*	UW021018	
	Chaunacidae	54%	*Chaunax pictus*	CUMV43879	*Chaunax suttkusi*
	Ogcocephalidae	32%	*Ogcocephalus radiatus*	CUMV78416	*Ogcocephalus nasutus*
	Caulophrynidae	36%	*Caulophryne jordani*	UW113763	
	Neoceratiidae	20%	*Neoceratias spinifer*	MCZ61075	
	Melanocetidae	68%	*Melanocetus johnsonii*	UW113789	
	Himantolophidae	48%	*Himantolophus appelii*	UW025871	*Himantolophus sagamius*
	Diceratiidae	18%	*Diceratias pileatus*	UW046525	
	Oneirodidae	55%	*Oneirodes thompsoni*	UW041787	
	Thaumatichthyidae	43%	*Thaumatichthys binghami*	UW047537	
	Centrophrynidae	35%	*Centrophryne spinulosa*	UW117074	
	Ceratiidae	35%	*Cryptopsaras couesii*	ANSP179567	*Cryptopsaras couesii*
	Gigantactinidae	37%	*Gigantactis microdontis*	UW046320	*Gigantactis vanhoeffeni*
	Linophrynidae	31%	*Linophryne arborifera*	MCZ49822	
Mugiliformes	Mugilidae		*Mugil curema*	CUMV15984	*Mugil curema*
Atheriniformes	Atherinopsidae		*Menidia menidia*	ANSP82962	*Labidesthes sicculus*
	Notocheiridae		*Iso natalensis*	ANSP134255	*Iso sp.*
	Melanotaeniidae		*Melanotaenia nigrans*	CUMV94345	*Rheocles wrightae*
	Atherionidae		*Atherion sp.*	ANSP114270	
	Phallostethidae		*Gulaphallus mirabilis*	ANSP91045	*Phenacostethus smithi*
	Atherinidae		*Atherina hepsetus*	CUMV47424	*Atherinomorus lacunosus*
Beloniformes	Adrianichthyidae		*Oryzias sp.*	ANSP179954	*Oryzias latipes*
	Exocoetidae		*Cheilopogon pinnatibarbatus*	CUMV33693	*Cheilopogon pinnatibarbatus*
	Hemiramphidae		*Hyporhamphus roberti*	CUMV6829	*Dermogenys collettei*
	Belonidae		*Potamorrhaphis eigenmanni*	CUMV77951	*Xenentodon cancila*
	Scomberesocidae		*Scomberesox saurus*	CUMV66124	*Scomberesox saurus*
Cyprinodontiformes	Aplocheilidae		*Aplocheilus panchax*	CUMV46733	*Pachypanchax playfairii*
	Nothobranchiidae		*Nothobranchius neumanni*	CUMV47913	
	Rivulidae		*Austrolebias elongatus*	CUMV47346	
	Profundulidae		*Profundulus scapularis*	ANSP64642	
	Goodeidae		*Goodea atripinnis*	CUMV71396	

	Fundulidae		*Fundulus catenatus*	CUMV89723	*Fundulus heteroclitus*
	Valenciidae		*Valencia hispanica*	ANSP53949	
	Cyprinodontidae		*Cyprinodon variegatus*	CUMV46022	*Cyprinodon variegatus*
	Anablepidae		*Anableps anableps*	CUMV1569	
	Poeciliidae		*Heterandria bimaculata*	CUMV71348	*Gambusia affinis*
Stephanoberyciformes	Melamphaidae		*Scopelogadus mizolepis*	CUMV53462	*Scopelogadus beanii*
	Stephanoberycidae		*Stephanoberyx sp.*	ANSP88789	*Acanthochaenus luetkenii*
	Hispidoberycidae				
	Gibberichthyidae		*Gibberichthys pumilus*	ANSP96777	
	Rondeletiidae		*Rondeletia loricata*	UW046800	*Rondeletia loricata*
	Barbourisiidae		*Barbourisia rufa*	UW021483	*Barbourisia rufa*
	Cetomimidae		*Cetomimus sp.*	MCZ162903	*Cetostoma regani*
	Mirapinnidae		*Eutaeniophorus festivus*	MCZ59200	
	Megalomycteridae		*Ataxolepis apus*	MCZ162902	
Beryciformes	Anoplogastridae		*Anoplogaster cornuta*	CUMV78502	*Anoplogaster cornuta*
	Diretmidae		*Diretmus argenteus*	CUMV95110	*Diretmus argenteus*
	Anomalopidae		*Anomalops katoptron*	CUMV75778	*Anomalops katoptron*
	Monocentridae		*Monocentris japonica*	CUMV22599	*Monocentris japonica*
	Trachichthyidae		*Hoplostethus mediterraneus*	CUMV95101	*Gephyroberyx darwini*
	Berycidae		*Centroberyx sp.*	ANSP63879	*Centroberyx druzhinini*
	Holocentridae		*Holocentrus rufus*	CUMV20073	*Sargocentron cornutum*
Zeiformes	Cyttidae		*Cyttus australis*	ANSP122808	
	Oreosomatidae		*Allocyttus folletti*	UW020831	
	Parazenidae		*Cyttopsis rosea*	CUMV43875	*Cyttopsis rosea*
	Zeniontidae		*Zenion hololepis*	CUMV43867	*Cyttomimus affinis*
	Grammicolepididae		*Xenolepidichthys sp.*	CUMV43871	
	Zeidae		*Zenopsis conchifer*	CUMV49611	*Zenopsis conchifer*
Gasterosteiformes	Hypoptychidae		*Hypoptychus dybowskii*	UW029655	*Hypoptychus dybowskii*
	Aulorhynchidae		*Aulorhynchus flavidus*	CUMV78826	*Aulorhynchus flavidus*
	Gasterosteidae	6%	*Gasterosteus aculeatus*	CUMV78823	*Gasterosteus aculeatus*
	Indostomidae		*Indostomus paradoxus*	MCZ46204	*Indostomus paradoxus*
	Pegasidae	62%	*Pegasus volitans*	CUMV53513	*Eurypegasus draconis*
	Solenostomidae	2%	*Solenostomus paradoxus*	MCZ30459	
	Syngnathidae	73%	*Syngnathus floridae*	CUMV22663	*Syngnathus fuscus*
	Aulostomidae		*Aulostomus chinensis*	ANSP88572	*Aulostomus chinensis*

	Fistulariidae		*Fistularia petimba*	CUMV22751	*Fistularia petimba*
	Macroramphosidae	8%	*Notopogon fernandezianus*	CUMV51290	*Macroramphosus scolopax*
	Centriscidae		*Aeoliscus strigatus*	CUMV75760	*Aeoliscus strigatus*
Synbranchiformes	Synbranchidae		*Synbranchus marmoratus*	CUMV54954	*Monopterus albus*
	Chaudhuriidae		*Chaudhuria caudata*	MCZ47058	
	Mastacembelidae		*Mastacembelus congicus*	CUMV88587	*Macrognathus siamensis*
Scorpaeniformes	Dactylopteridae	20%	*Dactylopterus volitans*	CUMV8489	*Dactyloptena peterseni*
	Scorpaenidae		*Sebastes norvegicus*	CUMV51204	*Sebastes fasciatus*
	Caracanthidae	7%	*Caracanthus sp.*	ANSP52932	
	Aploactinidae[10]		*Paraploactis trachyderma*	ANSP98678	
	Pataecidae[11]				
	Gnathanacanthidae		*Gnathanacanthus goetzeei*	MCZ51992	
	Congiopodidae	50%	*Congiopodus spinifer*	ANSP174849	
	Triglidae		*Prionotus evolans*	CUMV22574	*Prionotus evolans*
	Peristediidae	5%	*Peristedion miniatum*	CUMV46263	
	Bembridae		*Parabembras curtus*	MCZ47754	*Parabembras curtus*
	Platycephalidae		*Platycephalus indicus*	CUMV79736	*Platycephalus indicus*
	Hoplichthyidae	6%	*Hoplichthys citrinus*	MCZ148760	*Hoplichthys gilberti*
	Anoplopomatidae	5%	*Anoplopoma fimbria*	CUMV53581	*Anoplopoma fimbria*
	Hexagrammidae		*Hexagrammos lagocephalus*	CUMV55941	*Hexagrammos otakii*
	Normanichthyidae[12]				
	Rhamphocottidae	45%	*Rhamphocottus richardsonii*	CUMV54050	
	Ereuniidae[13]				
	Cottidae	5%	*Myoxocephalus scorpius*	CUMV48699	*Cottus carolinae*
	Comephoridae		*Comephorus baikalensis*	MCZ3014	
	Abyssocottidae	10%	*Procottus jeittelesii*	MCZ3011	
	Hemitripteridae		*Hemitripterus americanus*	CUMV95841	
	Agonidae[2]	7%	*Podothecus accipenserinus*	CUMV55946	*Stellerina xyosterna*
	Psychrolutidae	4%	*Dasycottus setiger*	CUMV55943	
	Bathylutichthyidae[14]				
	Cyclopteridae	40%	*Cyclopterus lumpus*	CUMV22666	*Cyclopterus lumpus*
	Liparidae	46%	*Liparis florae*	CUMV78469	*Paraliparis meganchus*
Perciformes	Centropomidae		*Centropomus undecimalis*	CUMV5090	*Centropomus undecimalis*
	Ambassidae		*Chanda nama*	CUMV77151	*Ambassis urotaenia*
	Latidae		*Lates niloticus*	CUMV93500	*Lates niloticus*

Moronidae		*Morone americana*	CUMV93717	*Morone chrysops*
Percichthyidae		*Bostockia porosa*	CUMV72843	*Maccullochella peelii*
Perciliidae		*Percilia gillissi*	ANSP71081	*Percilia irwini*
Acropomatidae		*Synagrops bellus*	ANSP101291	*Acropoma japonicum*
Symphysanodontidae		*Symphysanodon berryi*	ANSP112724	
Polyprionidae		*Polyprion americanus*	ANSP122479	*Stereolepis gigas*
Serranidae		*Epinephelus striatus*	CUMV12891	*Pseudanthias pascalus*
Centrogeniidae		*Centrogenys vaigiensis*	ANSP13443	*Centrogenys vaigiensis*
Ostracoberycidae		*Ostracoberyx sp.*	ANSP171319	*Ostracoberyx dorygenys*
Callanthiidae		*Callanthias platei*	CUMV51293	*Grammatonotus surugaensis*
Pseudochromidae		*Labracinus cyclophthalmus*	ANSP163506	*Labracinus cyclophthalmus*
Grammatidae		*Gramma loreto*	ANSP189950	*Gramma loreto*
Plesiopidae		*Plesiops corallicola*	CUMV76959	*Plesiops coeruleolineatus*
Notograptidae	3%	*Notograptus guttatus*	ANSP109653	
Opistognathidae		*Opistognathus aurifrons*	CUMV68567	*Opistognathus aurifrons*
Dinopercidae		*Dinoperca petersi*	ANSP53434	
Banjosidae		*Banjos banjos*	CUMV86566	*Banjos banjos*
Centrarchidae		*Ambloplites rupestris*	CUMV43204	*Ambloplites rupestris*
Percidae		*Perca flavescens*	CUMV35556	*Perca flavescens*
Priacanthidae		*Priacanthus arenatus*	CUMV7972	*Priacanthus arenatus*
Apogonidae		*Apogonichthyoides melas*	CUMV86595	*Ostorhinchus lateralis*
Epigonidae		*Epigonus sp.*	CUMV44184	
Sillaginidae		*Sillago sihama*	CUMV79720	*Sillago sihama*
Malacanthidae		*Malacanthus plumieri*	CUMV79616	*Malacanthus plumieri*
Lactariidae		*Lactarius lactarius*	ANSP63653	
Dinolestidae		*Dinolestes lewini*	MCZ8740	
Scombropidae		*Scombrops boops*	MCZ29011	
Pomatomidae		*Pomatomus saltatrix*	CUMV26852	*Pomatomus saltatrix*
Nematistiidae		*Nematistius pectoralis*	ANSP170436	*Nematistius pectoralis*
Coryphaenidae		*Coryphaena equiselis*	CUMV53979	*Coryphaena hippurus*
Rachycentridae		*Rachycentron canadum*	CUMV4988	*Rachycentron canadum*
Echeneidae		*Remora osteochir*	CUMV34858	*Echeneis naucrates*
Carangidae		*Caranx fusus*	CUMV96198	*Caranx crysos*
Menidae		*Mene maculata*	ANSP97856	*Mene maculata*
Leiognathidae	5%	*Leiognathus sp.*	CUMV73214	*Leiognathus equulus*
Bramidae		*Brama sp.*	CUMV86449	*Brama japonica*

Caristiidae		*Caristius macropus*	UW020920	*Caristius macropus*
Emmelichthyidae		*Erythrocles scintillans*	ANSP104593	*Erythrocles scintillans*
Lutjanidae		*Lutjanus apodus*	CUMV79020	*Lutjanus biguttatus*
Caesionidae		*Caesio cuning*	ANSP59954	*Caesio cuning*
Lobotidae		*Lobotes surinamensis*	CUMV20075	*Lobotes surinamensis*
Gerreidae		*Eucinostomus jonesii*	CUMV23924	*Eugerres plumieri*
Haemulidae		*Haemulon plumierii*	CUMV78978	*Haemulon plumierii*
Inermiidae		*Haemulon vittatum*	ANSP145059	*Haemulon vittatum*
Nemipteridae		*Pentapodus caninus*	CUMV54900	*Pentapodus caninus*
Lethrinidae		*Lethrinus erythracanthus*	CUMV54893	*Lethrinus erythracanthus*
Sparidae		*Archosargus probatocephalus*	CUMV73795	*Lagodon rhomboides*
Centracanthidae		*Spicara smaris*	ANSP100004	
Polynemidae		*Galeoides decadactylus*	CUMV53911	*Eleutheronema rhadinum*
Sciaenidae		*Pogonias cromis*	CUMV79693	*Aplodinotus grunniens*
Mullidae	3%	*Upeneus parvus*	CUMV43914	*Upeneus parvus*
Pempheridae		*Pempheris sp.*	CUMV86599	*Pempheris schomburgkii*
Glaucosomatidae[6]				
Leptobramidae		*Leptobrama muelleri*	ANSP122539	
Bathyclupeidae		*Bathyclupea argentea*	ANSP136707	
Monodactylidae		*Monodactylus sebae*	CUMV71384	*Monodactylus sebae*
Toxotidae		*Toxotes chatareus*	ANSP178868	*Toxotes jaculatrix*
Arripidae		*Arripis georgianus*	ANSP178918	
Dichistiidae		*Dichistius capensis*	ANSP53019	
Kyphosidae		*Kyphosus sectatrix*	CUMV46708	*Kyphosus elegans*
Drepaneidae		*Drepane punctata*	CUMV52107	*Drepane punctata*
Chaetodontidae	5%	*Chaetodon blackburnii*	CUMV73256	*Chaetodon ornatissimus*
Pomacanthidae		*Pomacanthus imperator*	CUMV68573	*Pomacanthus zonipectus*
Enoplosidae		*Enoplosus armatus*	ANSP33163	*Enoplosus armatus*
Pentacerotidae		*Pentaceros capensis*	ANSP63799	*Pentaceros japonicus*
Nandidae		*Nandus nandus*	MCZ4262	*Nandus nandus*
Polycentridae		*Monocirrhus polyacanthus*	CUMV46724	*Monocirrhus polyacanthus*
Terapontidae		*Terapon puta*	CUMV79739	*Hephaestus fuliginosus*
Kuhliidae		*Kuhlia marginata*	ANSP87044	*Kuhlia marginata*
Oplegnathidae		*Oplegnathus punctatus*	ANSP29609	*Oplegnathus punctatus*
Cirrhitidae		*Paracirrhites forsteri*	CUMV54072	*Paracirrhites arcatus*
Chironemidae		*Chironemus marmoratus*	ANSP135442	

Aplodactylidae		*Aplodactylus punctatus*	ANSP122521	
Cheilodactylidae		*Chirodactylus brachydactylus*	ANSP90070	*Chirodactylus brachydactylus*
Latridae		*Latris hecateia*	MCZ6646	
Cepolidae		*Cepola australis*	ANSP165125	*Cepola schlegelii*
Elassomatidae		*Elassoma zonatum*	CUMV33220	*Elassoma zonatum*
Cichlidae		*Astronotus ocellatus*	CUMV1639	*Paratilapia polleni*
Embiotocidae		*Cymatogaster aggregata*	CUMV22501	*Cymatogaster aggregata*
Pomacentridae		*Stegastes fuscus*	CUMV71590	*Stegastes leucostictus*
Labridae		*Labroides phthirophagus*	CUMV36868	*Halichoeres bivittatus*
Odacidae		*Haletta semifasciata*	ANSP49341	*Haletta semifasciata*
Scaridae		*Scarus coelestinus*	CUMV23982	*Scarus niger*
Bathymasteridae		*Bathymaster signatus*	CUMV55980	*Bathymaster signatus*
Zoarcidae	12%	*Zoarces americanus*	CUMV18374	*Lycodes diapterus*
Stichaeidae[15]		*Xiphister atropurpureus*	CUMV91369	*Cebidichthys violaceus*
Cryptacanthodidae	10%	*Cryptacanthodes maculatus*	CUMV47699	*Cryptacanthodes maculatus*
Pholidae		*Pholis gunnellus*	CUMV66705	*Pholis ornata*
Anarhichadidae	18%	*Anarhichas lupus*	CUMV17043	*Anarhichas lupus*
Ptilichthyidae		*Ptilichthys goodei*	UW048965	
Zaproridae		*Zaprora silenus*	CUMV55993	
Scytalinidae		*Scytalina cerdale*	UW019509	
Bovichtidae		*Bovichtus variegatus*	MCZ25558	*Bovichtus diacanthus*
Pseudaphritidae		*Pseudaphritis urvillii*	MCZ12836	
Eleginopidae	7%	*Eleginops maclovinus*	MCZ12910	*Eleginops maclovinus*
Nototheniidae		*Pagothenia borchgrevinki*	CUMV73371	*Dissostichus eleginoides*
Harpagiferidae	15%	*Harpagifer bispinis*	ANSP97927	
Artedidraconidae	16%	*Pogonophryne barsukovi*	MCZ126463	
Bathydraconidae		*Cygnodraco mawsoni*	MCZ152944	
Channichthyidae	4%	*Channichthys sp.*	CUMV71587	*Chionobathyscus dewitti*
Chiasmodontidae		*Chiasmodon niger*	ANSP51251	*Chiasmodon sp.*
Champsodontidae		*Champsodon vorax*	ANSP24739	*Champsodon snyderi*
Trichodontidae		*Trichodon trichodon*	CUMV78471	*Trichodon trichodon*
Pinguipedidae		*Pinguipes chilensis*	MCZ12876	*Parapercis clathrata*
Cheimarrhichthyidae		*Cheimarrichthys fosteri*	MCZ46212	*Cheimarrichthys fosteri*
Trichonotidae		*Trichonotus sp.*	ANSP151603	
Creediidae		*Tewara cranwellae*	ANSP122762	*Limnichthys sp.*
Percophidae		*Bembrops greyi*	CUMV48217	*Bembrops gobioides*

Leptoscopidae[16]				
Ammodytidae		*Ammodytes hexapterus*	CUMV55989	*Ammodytes hexapterus*
Trachinidae		*Trachinus draco*	ANSP11626	
Uranoscopidae		*Uranoscopus japonicus*	CUMV22750	*Astroscopus y-graecum*
Pholidichthyidae		*Pholidichthys anguis*	ANSP173800	*Pholidichthys leucotaenia*
Tripterygiidae		*Enneanectes carminalis*	CUMV54038	*Enneanectes boehlkei*
Dactyloscopidae		*Dactylagnus parvus*	CUMV53559	*Gillellus semicinctus*
Blenniidae[17]		*Scartella cristata*	CUMV79205	*Meiacanthus grammistes*
Clinidae		*Heterostichus rostratus*	CUMV18540	*Gibbonsia metzi*
Labrisomidae		*Labrisomus nuchipinnis*	CUMV3615	*Labrisomus multiporosus*
Chaenopsidae		*Neoclinus blanchardi*	CUMV53509	*Chaenopsis alepidota*
Icosteidae		*Icosteus aenigmaticus*	UW016251	*Icosteus aenigmaticus*
Gobiesocidae		*Gobiesox strumosus*	CUMV42644	*Gobiesox maeandricus*
Callionymidae	91%	*Synchiropus goodenbeani*	CUMV97547	*Callionymus bairdi*
Draconettidae	38%	*Centrodraco acanthopoma*	ANSP83825	
Rhyacichthyidae	22%	*Rhyacichthys aspro*	CUMV70991	
Odontobutidae		*Odontobutis sp.*	ANSP24751	*Odontobutis potamophila*
Eleotridae	18%	*Eleotris vittata*	CUMV93519	*Eleotris pisonis*
Xenisthmidae[18]				
Kraemeriidae		*Kraemeria samoensis*	ANSP134979	
Gobiidae[2]	12%	*Periophthalmus barbarus*	CUMV51544	*Lepidogobius lepidus*
Microdesmidae	27%	*Gunnellichthys pleurotaenia*	ANSP109663	
Ptereleotridae	4%	*Ptereleotris splendidus*	CUMV73257	*Ptereleotris evides*
Schindleriidae				
Kurtidae		*Kurtus indicus*	MCZ33039	*Kurtus gulliveri*
Ephippidae	14%	*Chaetodipterus faber*	CUMV73439	*Chaetodipterus faber*
Scatophagidae		*Scatophagus argus*	ANSP12333	*Scatophagus argus*
Siganidae	5%	*Siganus guttatus*	MCZ30815	*Siganus vulpinus*
Luvaridae	6%	*Luvarus imperialis*	ANSP11053	*Luvarus imperialis*
Zanclidae	32%	*Zanclus cornutus*	CUMV64760	*Zanclus cornutus*
Acanthuridae	9%	*Acanthurus monroviae*	CUMV53956	*Acanthurus nigricans*
Scombrolabracidae		*Scombrolabrax heterolepis*	MCZ41144	
Sphyraenidae		*Sphyraena sphyraena*	CUMV1525	*Sphyraena barracuda*
Gempylidae		*Gempylus serpens*	CUMV53520	*Ruvettus pretiosus*
Trichiuridae		*Trichiurus lepturus*	CUMV33622	*Trichiurus lepturus*
Scombridae		*Scomber scombrus*	CUMV18613	*Scomber scombrus*

	Xiphiidae		*Xiphias gladius*	ANSP11065	*Xiphias gladius*
	Istiophoridae		*Istiophorus platypterus*	CUMV53496	*Tetrapturus angustirostris*
	Amarsipidae		*Amarsipus carlsbergi*	MCZ46370	
	Centrolophidae		*Hyperoglyphe perciformis*	CUMV17051	*Icichthys lockingtoni*
	Nomeidae		*Nomeus gronovii*	CUMV78450	*Cubiceps baxteri*
	Ariommatidae		*Ariomma luridum*	ANSP88254	
	Tetragonuridae		*Tetragonurus cuvieri*	ANSP95481	
	Stromateidae		*Peprilus paru*	CUMV72512	*Peprilus triacanthus*
	Anabantidae		*Ctenopoma acutirostre*	CUMV88528	*Ctenopoma kingsleyae*
	Helostomatidae		*Helostoma temminkii*	MCZ25756	*Helostoma temminkii*
	Osphronemidae		*Parasphaerichthys ocellatus*	CUMV71785	*Betta splendens*
	Channidae		*Channa striata*	CUMV71626	*Channa striata*
	Caproidae		*Antigonia eos*	CUMV56164	*Antigonia rubescens*
Pleuronectiformes	Psettodidae		*Psettodes belcheri*	CUMV71389	*Psettodes erumei*
	Citharidae		*Citharoides macrolepis*	ANSP95013	*Citharoides macrolepis*
	Scophthalmidae		*Scophthalmus aquosus*	CUMV47689	*Scophthalmus aquosus*
	Paralichthyidae		*Paralichthys albigutta*	CUMV48348	*Paralichthys dentatus*
	Pleuronectidae		*Pseudopleuronectes americanus*	CUMV46026	*Pseudopleuronectes americanus*
	Bothidae		*Bothus ocellatus*	CUMV76654	*Bothus lunatus*
	Paralichthodidae		*Paralichthodes algoensis*	ANSP171677	
	Poecilopsettidae		*Poecilopsetta hawaiiensis*	ANSP176064	
	Rhombosoleidae		*Rhombosolea plebeia*	ANSP122857	
	Achiropsettidae[1]				
	Samaridae		*Samariscus triocellatus*	ANSP113542	*Samariscus latus*
	Achiridae		*Trinectes maculatus*	CUMV76656	*Gymnachirus melas*
	Soleidae		*Synapturichthys kleinii*	CUMV64161	*Heteromycteris japonicus*
	Cynoglossidae		*Symphurus atricaudus*	CUMV72908	*Symphurus atricaudus*
Tetraodontiformes	Triacanthodidae	31%	*Parahollardia lineata*	CUMV77157	*Triacanthodes anomalus*
	Triacanthidae	40%	*Triacanthus biaculeatus*	CUMV64765	*Triacanthus biaculeatus*
	Balistidae	44%	*Rhinecanthus aculeatus*	CUMV76867	*Rhinecanthus verrucosus*
	Monacanthidae	32%	*Aluterus schoepfii*	CUMV6832	*Cantherhines pullus*
	Ostraciidae	31%	*Acanthostracion quadricornis*	CUMV43979	*Aracana aurita*
	Triodontidae	38%	*Triodon macropterus*	MCZ5909	*Triodon macropterus*
	Tetraodontidae	45%	*Tetraodon lineatus*	CUMV94482	*Tetraodon miurus*
	Diodontidae	47%	*Diodon holocanthus*	CUMV78406	*Diodon holocanthus*

Molidae	49%	*Mola mola*	ANSP177882	*Mola mola*	

Supplemental Table 1. A list of families from Nelson, 2006, which includes branchiostegal membrane morphology and species examined in the survey and used in the phylogenetic analysis. Colors indicate membranes that are "separate and free from the isthmus" (green), "united and free from the isthmus" (blue), "joined to the isthmus" (yellow), and "joined to the isthmus, gill openings restricted" (red).

[1]Nelson JS. 2006. Fishes of the World, 4th Edition. New York: John Wiley & Sons. 601p.
[2]Membranes joined to the isthmus, some with restricted gill openings
[3]Rainboth WJ. 1983. *Psilorhynchus gracilis*, a new cyprinoid fish from the Gangetic lowlands. Proc Calif Acad Sci 43: 67–76.
[4]Günther ACLG. 1864. Catalogue of the fishes of the British Museum. British Museum, London. 5:1-455.
[5]Sato T, Nakabo T. 2002. Paraulopidae and *Paraulopus*, a new family and genus of aulopiform fishes with revised relationships within the order. Ichthyol Res 49:25-46.
[6]McAllister DE. 1968. Evolution of branchiostegals and classification of teleostome fishes. Bull Natl Mus Canada 221:1-237.
[7]Regan CT. 1907. Descriptions of the teleost fish *Velifer hypselopterus* and of a new genus *Velifer*. Proc. Zool. Soc. London 2:633-634.
[8]McCann C. 1972. Additions to the deep-sea fishes of New Zealand. New Zeal J Mar Fresh 6(4):619-640.
[9]Boeseman M. 1964. Notes on the fishes of western New Guinea II. *Lophichthys boschmai*, a new genus and species from the Arafoera Sea. Zool Meded (Leiden) 39:12-18.
[10]Membranes united and free from the isthmus or gill openings restricted
[11]Scott EOG. 1986. Observations on some Tasmanian fishes: Part XXXI - Review of Gnathanacanthidae. Pap Proc R Soc Tasmania 120:51-75.
[12]Norman JR. 1938. On The Affinities of The Chilean Fish, *Normanichthys crockery* Clark. Copeia 1938(1):29-32.
[13]Jordan DS, Starks EC. 1904. A review of the Cottidae or sculpins found in the waters of Japan. Proc U S Nat Mus 27:231-335.
[14]Balushkin AV, Voskoboinikova OS. 1990. A new cottoid family, Bathylutichthyidae fam. n. (Cottoidei, Scorpaeniformes) for a deepsea fish Bathylutichthyes taranetzi gen. et sp. n. from South Georgia Island (Antarctic). J Ichthyol 30(2):67-75.
[15]Membranes united and free from the isthmus or joined to the isthmus
[16]Regan CT. 1913. XVII.—The classification of the Percoid fishes. Ann Mag Nat Hist 8(12):111-145.
[17]Membranes united and free from the isthmus or joined to the isthmus, some with restricted gill openings
[18]Gill AC, Randall JE. 1994. *Xenisthmus balius*, a new species of fish from the Persian Gulf (Gobioidei: Xenisthmidae). Proc Biol Soc Wash 107(3):445-450.

APPENDIX 2

Table A2.1. Molecular data from Chapter 4. A list of species and associated molecular data used for phylogenetic reconstruction.

Species	COI	cytb	S7
Agonopsis vulsa	JQ353955	FJ264384	-
Alcichthys elongatus	-	Knope, 2013	Knope, 2013
Archaulus biseriatus	-	Knope, 2013	Knope, 2013
Artediellus fuscimentus	-	Knope, 2013	Knope, 2013
Artediellus pacificus	-	Knope, 2013	Knope, 2013
Artediellus scaber	HQ712291	Knope, 2013	Knope, 2013
Artedius corallinus	GU440235	Knope, 2013	Knope, 2013
Artedius fenestralis	JQ353989	Knope, 2013	Knope, 2013
Artedius harringtoni	JQ353991	Knope, 2013	Knope, 2013
Artedius lateralis	JQ353992	Knope, 2013	Knope, 2013
Artedius notospilotus	GU440239	Knope, 2013	Knope, 2013
Atopocottus tribranchius	-	Knope, 2013	Knope, 2013
Bero elegans	-	Knope, 2013	Knope, 2013
Blepsias bilobus	HQ712320	Knope, 2013	Knope, 2013
Blepsias cirrhosus	GU440252	Knope, 2013	Knope, 2013
Chitonotus pugetensis	JQ354043	Knope, 2013	Knope, 2013
Clinocottus acuticeps	GU440285	Knope, 2013	Knope, 2013
Clinocottus analis	GU440286	Knope, 2013	Knope, 2013
Clinocottus embryum	GU440287	Knope, 2013	Knope, 2013
Clinocottus globiceps	GU440288	Knope, 2013	Knope, 2013
Clinocottus recalvus	GU440289	Knope, 2013	Knope, 2013
Cottiusculus gonez	-	Knope, 2013	Knope, 2013
Cottus amblystomopsis	-	Knope, 2013	Knope, 2013
Cottus cognatus	EU524507	Knope, 2013	Knope, 2013
Cottus kazika	-	Knope, 2013	Knope, 2013
Cottus pollux	-	Knope, 2013	Knope, 2013
Cyclopterus lumpus	KC015308	EU492269	-
Dasycottus setiger	HQ712348	Knope, 2013	Knope, 2013
Enophrys bison	GU440313	Knope, 2013	Knope, 2013
Enophrys diceraus	HQ712362	Knope, 2013	Knope, 2013
Enophrys lucasi	HQ712365	Knope, 2013	Knope, 2013
Enophrys taurina	GU440315	Knope, 2013	Knope, 2013
Furcina osimae	-	Knope, 2013	Knope, 2013
Gymnocanthus galeatus	HQ712423	Knope, 2013	Knope, 2013
Gymnocanthus pistilliger	-	Knope, 2013	Knope, 2013
Gymnocanthus tricuspis	HQ712427	Knope, 2013	Knope, 2013
Hemilepidotus gilberti	-	Knope, 2013	Knope, 2013
Hemilepidotus hemilepidotus	JQ354115	Knope, 2013	Knope, 2013

Hemilepidotus jordani	KF929962	Knope, 2013	Knope, 2013
Hemilepidotus papilio	HQ712444	Knope, 2013	Knope, 2013
Hemilepidotus spinosus	JQ354117	Knope, 2013	Knope, 2013
Hemilepidotus zapus	HQ712450	Knope, 2013	Knope, 2013
Hemitripterus bolini	KJ450885	Knope, 2013	Knope, 2013
Hexagrammos decagrammus	GU440339	FJ264357	AY583194
Hexagrammos stelleri	GU440341	FJ264320	AY583193
Icelinus borealis	JQ354140	Knope, 2013	Knope, 2013
Icelinus burchami	GU440352	Knope, 2013	Knope, 2013
Icelinus filamentosus	FJ164692	Knope, 2013	Knope, 2013
Icelinus fimbriatus	GU440354	Knope, 2013	Knope, 2013
Icelinus tenuis	GU440357	Knope, 2013	Knope, 2013
Icelus canaliculatus	-	Knope, 2013	Knope, 2013
Icelus euryops	-	Knope, 2013	Knope, 2013
Icelus ochotensis	-	Knope, 2013	Knope, 2013
Icelus spatula	KC015493	Knope, 2013	Knope, 2013
Icelus spiniger	HQ712508	Knope, 2013	Knope, 2013
Icelus toyamensis	-	Knope, 2013	Knope, 2013
Icelus uncinalis	-	Knope, 2013	Knope, 2013
Jordania zonope	-	Knope, 2013	Knope, 2013
Leiocottus hirundo	HQ010066	Knope, 2013	Knope, 2013
Leptocottus armatus	GU440370	Knope, 2013	Knope, 2013
Liparis dennyi	FJ164720	FJ264371	-
Liparis florae	GU440375	FJ264400	-
Megalocottus platycephalus	JF278613	Knope, 2013	Knope, 2013
Microcottus sellaris	-	Knope, 2013	Knope, 2013
Myoxocephalus brandtii	KC351874	Knope, 2013	Knope, 2013
Myoxocephalus cf.scorpioides	-	Knope, 2013	Knope, 2013
Myoxocephalus jaok	KC351879	Knope, 2013	Knope, 2013
Myoxocephalus polyacanthocephalus	HQ712660	Knope, 2013	Knope, 2013
Myoxocephalus scorpius	HQ712668	Knope, 2013	Knope, 2013
Myoxocephalus stelleri	JF278624	Knope, 2013	Knope, 2013
Myoxocephalus verrucosus	-	Knope, 2013	Knope, 2013
Nautichthys oculofasciatus	GU440420	Knope, 2013	Knope, 2013
Nautichthys pribilovius	HQ712690	Knope, 2013	Knope, 2013
Oligocottus maculosus	FJ164917	Knope, 2013	Knope, 2013
Oligocottus rimensis	GU440428	Knope, 2013	Knope, 2013
Oligocottus rubellio	GU440429	Knope, 2013	Knope, 2013
Oligocottus snyderi	GU440430	Knope, 2013	Knope, 2013
Orthonopias triacis	GU440439	Knope, 2013	Knope, 2013
Podothecus accipenserinus	GU440470	FJ264262	-
Porocottus allisi	-	Knope, 2013	Knope, 2013
Porocottus camtschaticus	-	Knope, 2013	Knope, 2013

Pseudoblennius percoides	-	Knope, 2013	Knope, 2013
Pseudoblennius sp3	-	Knope, 2013	Knope, 2013
Psychrolutes phrictus	GU440485	Knope, 2013	Knope, 2013
Radulinus asprellus	GU440488	Knope, 2013	Knope, 2013
Rastrinus scutiger	-	Knope, 2013	Knope, 2013
Rhamphocottus richardsonii	GU440501	Knope, 2013	Knope, 2013
Ricuzenius pinetorum	-	Knope, 2013	Knope, 2013
Ruscarius creaseri	GU440508	Knope, 2013	Knope, 2013
Ruscarius meanyi	-	Knope, 2013	Knope, 2013
Scorpaenichthys marmoratus	JQ354334	Knope, 2013	Knope, 2013
Stellerina xyosterna	GU440532	Knope, 2013	Knope, 2013
Stlengis misakia	-	Knope, 2013	Knope, 2013
Synchirus gilli	GU440542	Knope, 2013	Knope, 2013
Thyriscus anoplus	-	Knope, 2013	Knope, 2013
Trichocottus brashnikovi	HQ712651	Knope, 2013	Knope, 2013
Trichodon trichodon	GU440560	FJ264405	-
Triglops forficatus	-	Knope, 2013	Knope, 2013
Triglops macellus	JQ354525	Knope, 2013	Knope, 2013
Triglops metopias	-	Knope, 2013	Knope, 2013
Triglops murrayi	KC015974	Knope, 2013	Knope, 2013
Triglops nybelini	KC015977	Knope, 2013	Knope, 2013
Triglops pingelii	KC016006	Knope, 2013	Knope, 2013
Triglops quadricornis	-	Knope, 2013	Knope, 2013
Triglops scepticus	-	Knope, 2013	Knope, 2013
Triglops xenostethus	-	Knope, 2013	Knope, 2013
Xeneretmus latifrons	FJ165462	KM057911	-
Zesticelus profundorum	HM481476	Knope, 2013	Knope, 2014

APPENDIX 3

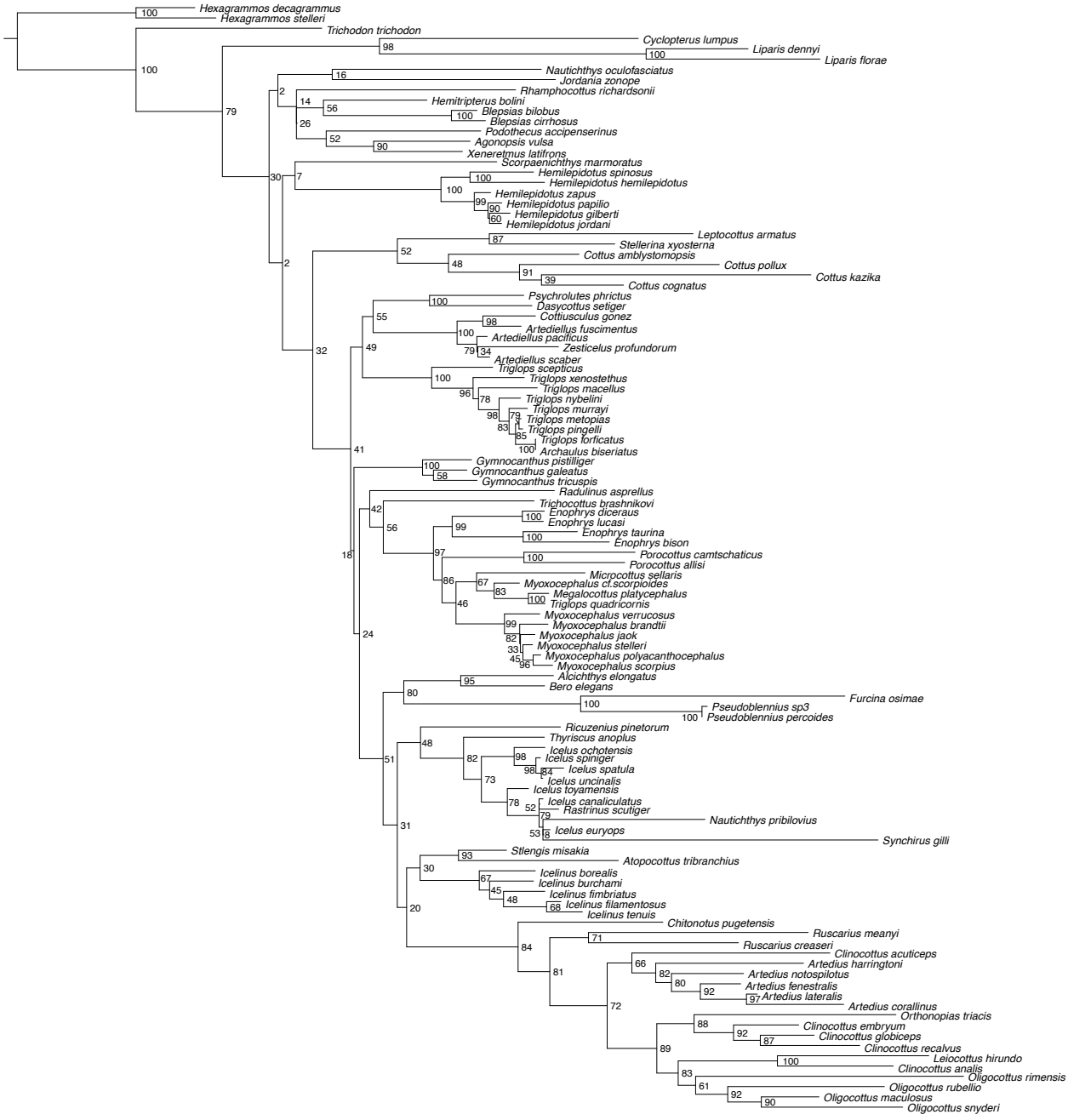

Figure A3.1. RAxML tree. This maximum likelihood tree constructed using RAxML recovers Cottoidei (*sensu* Smith and Busby, 2014) and Cottoidea (*sensu* Yabe, 1985) but shows low bootstrap support for interfamilial relationships.

Figure A3.2. Maximum clade credibility tree. Maximum clade credibility tree from the best MrBayes runis the best fit to our molecular dataset. It recovers Cottoidei (*sensu* Smith and Busby, 2014) and Cottoidea (*sensu* Yabe, 1985) and generally shows high posterior probabilities at the family level.